The Dissertation Committee for Ni Yan Certifies that this is the approved version of the following dissertation:

Ion Transport in Crosslinked AMPS/PEGDA Hydrogel Membranes

Committee:

Benny D. Freeman, Supervisor

Donald R. Paul, Co-Supervisor

Isaac C. Sanchez

Christopher J. Ellison

Wei Li

Ion Transport in Crosslinked AMPS/PEGDA Hydrogel Membranes

by

Ni Yan

Dissertation

Presented to the Faculty of the Graduate School of

The University of Texas at Austin

in Partial Fulfillment

of the Requirements

for the Degree of

Doctor of Philosophy

The University of Texas at Austin

December 2017

Dedication

To my family, friends, and mentors

Acknowledgements

Approaching the end of my time at the University of Texas at Austin, I gradually realized how grateful I am for the invaluable time I spent here. I benefited greatly from all the challenges in my Ph.D. work, which drove me to reach beyond my limits and better prepared me for my future professional career. I am thankful to all the failures and dead-ends I hit, from which I learnt to never give up. I also appreciate all the people who have inspired me, encouraged me, and helped me, as well as the people who have doubted me. Without them, I wouldn't be as motivated to endlessly improve myself and become who I am today with such a strong mind.

I am deeply indebted to my thesis advisers, Profs. Benny Freeman and Donald Paul. I would like to extend greatest gratitude to the incredible opportunity they provided me to study under their guidance, whom I had never dreamed of to work with before I left China six years ago. Their trust in me is a constant source of motivation for me over the course of my Ph.D. When I look back, there are countless inspiring and influential moments. I remember how Dr. Freeman taught me to persevere when I kept failing my experiments, how he spurred me to bravely explore the unknowns, and how excited I was when I first successfully synthesized my free-standing films and Dr. Freeman said to me 'I know you can do it!'. His exceptional patience in listening to my conference talk countlessly and teaching me how to deliver an effective scientific talk slide by slide is always unforgettable. I also remember the long caring and encouraging email after my poster presentation did not go as desired. Dr. Freeman has not only taught me how to be extremely meticulous

in fundamental understanding through tireless discussions and conversations, but also served as an exemplar of extraordinary kindness, generosity, and leadership.

I am beyond fortunate to be co-advised by Dr. Paul, who inspired me and impacted my work ethic through his exceptional dedication to the field of polymer science and engineering. He was instrumental in guiding us finding out the most fundamental roots for experimental observations no matter how complicated and confusing the results would be. He taught us to be always curious to the science behind our findings and showed us how to pull the thread out a mess from a standpoint of the simplest scenario. I owe my special thanks to his generosity and hospitability gathering us every Thanksgiving, which I attended every year and will continue to attend in the future. Many laughs, warmness, and, sweet memories Dr. Paul and his families made us, especially foreign students, not lonely any more.

I would also like to acknowledge my committee members Prof. Isaac Sanchez, Prof. Christopher Ellison, and Prof. Wei Li, who have contributed their time and efforts to help and guide me through my studies.

I have had great mentorship and friendship from all the past and current graduate students in the Freeman and Paul group. I would like to thank Geoff Geise, who taught me lab techniques, presentation skills, and patiently answered all my research and English questions helping me to adapt to my first year Ph.D. life smoothly. Dr. Tom Murphy was the first group member I met, and I appreciate his kindness in introducing me to this group. I would also like to thank Dr. Daniel (DanDan) Miller who offered help to my presentation skill after my first (rough) group meeting talk. Dr. Grant (Granty) Offord taught me a number of English slangs and emphasized to me the value of networking. Drs. Kevin

Tung and David Sanders have been good friends and I had pleasure playing basketball with them in my early PhD years. Dr. Katrina Czenkusch spent hours re-organizing my first conference talk was very encouraging and I enjoyed practicing yoga with her. Dr. Kevin Stevens mentored me to be a responsible safety officer with great professions. I have had many memorable Korean food nights with Dr. Sirirat (Peachy) Kasemset, Dr. HeeJung Oh, and Dr. Joe Cook (JoJo Cookie) with inspiring conversations about Ph.D. life. Prof. Michele Galizia has not only helped me tremendously with my research but also become a lifelong friend as my wedding witness.

I am grateful to the companionship of my office mates: Jaesung Park and Alon Kirschner, who have shared wisdom and laughs (though with sarcastic jokes) with me every day. Other current and past group members including Lu Wang, Michelle Does, Amanda Paine, Melanie Merrick, Zhengwang He, Josh Moon, Yu-heng Cheng, Euisoung Jang, Jovan Kamcev, and Rahul Sujanani have made this group like a family with endless support and delicious food/cake.

Last but not least, I need to thank my best friend, my past and future co-worker, and now my husband, Qiang Liu. Thank you for always offering me a strong shoulder I can lean on when I feel hopeless, for showing me the magic in turning my frustrations into motivations, for sharing with me all my sorrows and happiness. Without your support, I will never reach today and be a better myself. Thank you for your constant motivation, and I am also very lucky to have you in my life and can't wait for our new life together in Dow Chemical.

Finally, I owe my heartfelt gratitude to my parents who brought me to this world and always unconditionally support me to follow my dream. I will always be a kind, grateful, humble, generous, and diligent person as you taught me to be.

Ion Transport in Crosslinked AMPS/PEGDA Hydrogel Membranes

Ni Yan, Ph.D.

The University of Texas at Austin, 2017

Supervisors: Benny D. Freeman and Donald R. Paul

Ion exchange membranes (IEMs) are key components to water purification [e.g., electrodialysis (ED)] and energy generation [e.g., fuel cells, reverse electrodialysis (RED)] applications. IEMs are also being explored for other membrane-based techniques, such as reverse osmosis (RO), pressure-retarded osmosis (PRO) [12, 13], and membrane-assisted capacitive deionization (CDI). Membrane performance (e.g., conductivity and permeability) in these applications is sensitive to membrane transport (water/ion sorption and diffusion) characteristics. However, much remains unknown about the influence of polymer membrane architecture on water and ion transport properties critical to high performance membranes.

In this study, a series of homogeneous cross-linked uncharged and sulfonated hydrogel membranes with various IEC values were prepared. Equilibrium water uptake, ion sorption, and ion diffusion coefficients in the membranes were determined as a function of external salt concentration. Co-ion sorption decreased markedly as IEC increased slightly, suggesting that even low levels of fixed charges exclude co-ions significantly.

However, co-ion sorption became independent of charge density at higher IEC values due to non-idealities in the solution and membrane phases. Counter-ion and co-ion diffusion coefficients are mainly governed by water content in the membrane. Meares' model predictions for counter-ion and co-ion diffusion coefficients agree reasonably with the experimental values. Minor deviations for co-ion diffusion coefficients were evident in more highly charged membranes. These discrepancies might be a result of the interactions omitted by Meares' model (e.g., fixed charges-ion, ion-ion, etc.).

The effects of water content and charge density on ion sorption were also isolated. Membranes with similar water content but different charge densities and similar charge density but different water uptake values were synthesized and characterized. At constant charge density, the sorbed mobile salt concentration increases as membrane water content increases. At fixed water content, mobile salt sorption decreases as charge density increases due to stronger Donnan exclusion effect. Salt sorption in the membranes with the highest water content or charge density could be predicted after accounting for the non-idealities in solution and in the membrane. However, this approach fails for less hydrated or weakly charged membranes due to more pronounced thermodynamic non-idealities introduced by the uncharged polymer segments.

Table of Contents

List of Tables

List of Figures

Chapter 1: Introduction

Water and energy are highly interrelated resources. In the 21st century, water and energy supply will be two of the largest problems facing the world [1]. About 97% of water on earth is sea water, and another 2% is locked in glaciers and icecaps. Only 0.5% of the overall water resources is fresh water that can be used directly by human beings [1, 2]. About 41% of the world's population has limited access to clean drinking water. With the rapid growth in the world's population, the average fresh water supply per person will drop by 1/3 in about 20 years [1]. Many countries suffer from a scarcity of fresh water, and problems, including environmental pollution, food shortages, and energy crisis, will arise as a consequence of water scarcity [1]. Supplying clean water is one of the greatest challenges the world is facing in this century [1].

Industrial processes and agricultural irrigation consume almost 90% of all usable fresh water. With only 10% fresh water left for domestic use, approximately 1.2 billion people don't have access to safe drinking water according to the World Health Organization. Currently, there are 2.6 billion people living in water-stressed areas, and this number will increase to 3.5 billion by 2035 [3, 4]. The demand for fresh water is increasing twice as fast as the increase in population [1]; thus, the water crisis will get worse as population increases.

Many global problems are also associated with the lack of fresh water, such as environmental quality, economic development and most importantly, energy generation [4]. Fresh water and energy are highly interrelated: water purification consumes energy, while the production of energy requires large amounts of water [5]. Therefore, there is a

great need to replace the conventional energy used in the water purification with renewable energy and develop more energy-efficient techniques to produce fresh water.

To satisfy this intensively growing water demand, various desalination techniques have been introduced and developed during the last century. Membrane-based reverse osmosis (RO) has been a widely used desalination method to provide purified water at a lower energy cost than other techniques, such as multi-stage flash (MSF) and multi-effect distillation (MED). RO technique has successfully achieved a 32-fold increase in capacity over the past 3 decades [6-8]. However, with the increased growth of industrial and agricultural activities, the established world desalination capacity can only account for 7.5% of the world fresh water demand [9]. Therefore, alternative renewable energy generation and low-cost water purification techniques need to be developed to solve these issues. In addition to RO, other membrane-based techniques for water treatment and energy generation, such as forward osmosis (FO) [10, 11], pressure-retarded osmosis (PRO) [12-14], electrodialysis (ED) [15-20], reverse electrodialysis (RED) [21-23], and membrane-assisted capacitive deionization (CDI) [24-30], have recently received a great deal of attention since they could provide new solutions to the water and energy crisis [31, 32]. All of these techniques rely on controlling water/ion transport characteristics of polymeric membranes. To enhance membrane performance, we need a better understanding of how the fundamental water and ion transport properties relate to membrane structure. Such information will facilitate the design and engineering of new generations of membranes with desired energy efficiency and separation properties.

1.1 DISSERTATION GOALS AND OUTLINE

The ultimate goal of this project is to broaden our fundamental water and ion transport knowledge in polymeric membranes for various water treatment and energy generation applications. This knowledge base will include an understanding of how membrane's physical and chemical structure correlates with ion transport properties.

This dissertation consists of 8 chapters. Chapter 1 gives a brief introduction to the importance of this project and chapter organization. Then, fundamental concepts and theoretical models regarding water/ion sorption, diffusion, and permeation are introduced in Chapter 2. Subsequently, Chapter 3 provides information about polymer synthesis and preparation procedures. In addition, experimental techniques to characterize membrane physical and transport properties are also included in Chapter 3.

Chapter 4 systematically investigates the influence of adding fixed charges to the polymer backbone on polymer water and ion sorption properties. Equilibrium water uptake and ion content (Na^+, Cl^-) in the membranes were determined as a function of external NaCl concentration (0.01-1.0 mol/L). Interestingly, co-ion (Cl^-) sorption decreased significantly as IEC increased slightly. However, at IEC values of 0.97 meq/g and higher, Cl^- sorption became independent of charge density. Such behavior is qualitatively consistent with ideal Donnan theory. Quantitative agreement between experimental and theoretical values is not achieved in almost all the membranes considered, suggesting highly non-ideal ion behavior in the membrane and solution phases that is not captured by Donnan theory.

Chapter 5 seeks to elucidate the individual influence of water content and fixed charge concentration on ion sorption properties. Water content and charge density were controlled independently by varying the AMPS content in the pre-polymerization mixture

and PEGDA chain length. Membranes with similar water content but different charge densities and similar charge density but different water uptake values were synthesized and characterized. Ion sorption (e.g., Na^+, Cl^-) in these materials was measured using aqueous NaCl solutions at concentrations ranging from 0.01 to 1.0 M. Theoretical ion sorption values predicted using the Donnan/Manning approach agrees remarkably well with the experimental data for the most highly charged and hydrated membranes. For weakly charged and less hydrated membranes, the experimental values cannot be described by model predictions, likely due to more pronounced thermodynamic non-idealities contributed by interactions between polymer segments and ions, which are not considered in Manning's model.

Chapter 6 explores ion diffusion coefficients in a series of uncharged and negatively charged membranes. To accomplish this goal, membrane salt permeability and ionic conductivity properties were measured in a consistent manner. Individual ion diffusion coefficients are mainly governed by water content in the membrane, in accordance with the Mackie and Meares tortuosity model. Salt permeability coefficients and ionic conductivity data are interpreted using the solution-diffusion model and the Nernst-Plank equation. Finally, conclusions and recommendations for future research are provided in Chapter 7.

1.2 REFERENCES

[1] G.M. Geise, H.S. Lee, D.J. Miller, B.D. Freeman, J.E. McGrath, D.R. Paul, Water purification by membranes: The role of polymer science, Journal of Polymer Science Part B: Polymer Physics, 48 (2010) 1685-1718.

[2] A.D. Khawaji, I. Kutubkhanah, J.M. Wie, Advances in seawater desalination technologies, Desalination, 221 (2008) 47-69.

[3] R.F. Service, Desalination freshens up, Science(Washington, D. C.), 313 (2006) 1088-1090.

[4] M.A. Shannon, P.W. Bohn, M. Elimelech, J.G. Georgiadis, B.J. Marinas, A.M. Mayes, Science and technology for water purification in the coming decades, Nature, 452 (2008) 301-310.

[5] M.E. Webber, Energy versus water: solving both crises together, Scientific American, 18 (2008) 1-5.

[6] C. Fritzmann, J. Löwenberg, T. Wintgens, T. Melin, State-of-the-art of reverse osmosis desalination, Desalination, 216 (2007) 1-76.

[7] G. Raluy, L. Serra, J. Uche, Life cycle assessment of MSF, MED and RO desalination technologies, Energy, 31 (2006) 2361-2372.

[8] T. Pancratz, Membranes Provide Emergency Relief, Water Desalination Report, 43 (2007) 3-5.

[9] V.G. Gude, N. Nirmalakhandan, S. Deng, Renewable and sustainable approaches for desalination, Renewable and Sustainable Energy Reviews, 14 (2010) 2641-2654.

[10] T.Y. Cath, A.E. Childress, M. Elimelech, Forward Osmosis: Principles, Applications, and Recent Development, Journal of Membrane Science, 281 (2006) 70-87.

[11] J.E. Miller, L.R. Evans, Forward osmosis: a new approach to water purification and desalination, Sandia Report, 2006.

[12] I.L. Alsvik, M.B. Hägg, Pressure Retarded Osmosis and Forward Osmosis Membranes: Materials and Methods, Polymers, 5 (2013) 303-327.

[13] C. Klaysom, T.Y. Cath, T. Depuydt, I.F.J. Vankelecom, Forward and pressure retarded osmosis: potential solutions for global challenges in energy and water supply, Chemical Society Reviews, 42 (2013) 6959-6989.

[14] J.R. McCutcheon, M. Elimelech, Influence of concentrative and dilutive internal concentration polarization on flux behavior in forward osmosis, Journal of Membrane Science, 284 (2006) 237-247.

[15] G.M. Geise, A.J. Curtis, M.C. Hatzell, M.A. Hickner, B.E. Logan, Salt concentration differences alter membrane resistance in reverse electrodialysis stacks, Environmental Science & Technology Letters, 1 (2013) 36-39.

[16] R. Ghalloussi, W. Garcia-Vasquez, N. Bellakhal, C. Larchet, L. Dammak, P. Huguet, D. Grande, Ageing of ion-exchange membranes used in electrodialysis: Investigation of static parameters, electrolyte permeability and tensile strength, Separation and Purification Technology, 80 (2011) 270-275.

[17] J. Wiśniewski, A. Różańska, Donnan dialysis with anion-exchange membranes as a pretreatment step before electrodialytic desalination, Desalination, 191 (2006) 210-218.

[18] S.D. Alexandratos, Ion-Exchange Resins: A Retrospective from Industrial and Engineering Chemistry Research, Industrial & Engineering Chemistry Research, 48 (2009) 388-398.

[19] T.Sata, Ion exchange membranes: Preparation, characterization, modification and application, Tokuyama Research, Tokuyama City, Japan, 2002.

[20] T. Xu, Ion Exchange Membranes: State of Their Development and Perspective, Journal of Membrane Science, 263 (2005) 1-29.

[21] P. Długołęcki, A. Gambier, K. Nijmeijer, M. Wessling, Practical potential of reverse electrodialysis as process for sustainable energy generation, Environmental Science & Technology, 43 (2009) 6888-6894.

[22] J. Veerman, R.M. De Jong, M. Saakes, S.J. Metz, G.J. Harmsen, Reverse electrodialysis: Comparison of six commercial membrane pairs on the thermodynamic efficiency and power density, Journal of Membrane Science, 343 (2009) 7-15.

[23] P. Długołęcki, B. Anet, S.J. Metz, K. Nijmeijer, M. Wessling, Transport limitations in ion exchange membranes at low salt concentrations, Journal of Membrane Science, 346 (2010) 163-171.

[24] P.M. Biesheuvel, A. Van der Wal, Membrane capacitive deionization, Journal of Membrane Science, 346 (2010) 256-262.

[25] P.M. Biesheuvel, B. Van Limpt, A. Van der Wal, Dynamic adsorption/desorption process model for capacitive deionization, The Journal of Physical Chemistry C, 113 (2009) 5636-5640.

[26] J.C. Farmer, D.V. Fix, G.V. Mack, R.W. Pekala, J.F. Poco, Capacitive deionization of NaCl and NaNO3 solutions with carbon aerogel electrodes, Journal of the Electrochemical Society, 143 (1996) 159-169.

[27] H.H. Jung, S.W. Hwang, S.H. Hyun, K.H. Lee, G.T. Kim, Capacitive deionization characteristics of nanostructured carbon aerogel electrodes synthesized via ambient drying, Desalination, 216 (2007) 377-385.

[28] J.B. Lee, K.K. Park, H.M. Eum, C.W. Lee, Desalination of a thermal power plant wastewater by membrane capacitive deionization, Desalination, 196 (2006) 125-134.

[29] S. Porada, R. Zhao, A. Van Der Wal, V. Presser, P.M. Biesheuvel, Review on the Science and Technology of Water Desalination by Capacitive Deionization, Progress in Materials Science, 58 (2013) 1388-1442.

[30] T.J. Welgemoed, C.F. Schutte, Capacitive deionization technology™: an alternative desalination solution, Desalination, 183 (2005) 327-340.

[31] G.M. Geise, L.P. Falcon, B.D. Freeman, D.R. Paul, Sodium chloride sorption in sulfonated polymers for membrane applications, Journal of Membrane Science, 423-424 (2012) 195-208.

[32] G.T. Gray, J.R. McCutcheon, M. Elimelech, Internal Concentration Polarization in Forward Osmosis: Role of Membrane Orientation, Desalination, 197 (2006) 8.

Chapter 2: Background

2.1 Ion Exchange Membranes

Ion exchange membranes (IEMs) are widely used commercially in various fields, such as desalination, electrodialysis (ED), diffusion dialysis, and solid polymer electrolytes for batteries, medication, sensors, etc. [21]. IEMs often consist of a cross-linked hydrocarbon matrix to which charged functional groups are attached [1]. These charged functional groups can be introduced to the polymer backbone by, for example, copolymerizing functionalized monomers [1]. Ion exchange membranes may contain acidic functional groups (e.g., sulfonate groups), basic functional groups (e.g., quaternary-ammonium groups), or both. Strong acidic or basic groups (e.g., $-SO_3H$, $-R_3NH$) can solvate and ionize completely in contact with aqueous solutions [1]. To maintain electroneutrality, the charge on the functional groups (e.g., $-SO_3^-$, $-R_3N^+$) must be balanced by ions bearing an opposite charge, which are termed counter-ions. Thus, the ion exchange membrane is usually specified according to its counter-ion form. For example, a cation exchange membrane, which means the functional group is negatively charged, can be referred to as in the 'acid form' or 'salt form' depending on whether the counter-ion is a proton (H^+) or other cations (e.g., Na^+, K^+, and Ca^{2+}). Ions bearing the same charge as the functional group are called co-ions. Negatively charged membranes are cation exchange membranes (CEMs), and positively charged membranes are anion exchange membranes (AEMs).

To quantify charge density in IEMs, ion exchange capacity (IEC), defined as milliequivalents (mmol) of fixed charges based on dry polymer weight [meq/g (dry polymer)], can be readily computed from polymer composition [17]. However, the molar

concentration of fixed charges or ions based on the volume of sorbed water [molarity, mol/L (water sorbed)] is the relevant charge density experienced by ions sorbing into IEMs [16-18]. In this study, IEC is used to label samples, and charge molarity (i.e., charge density) is used to interpret ion sorption results.

2.2 Membrane Water Content

Water uptake equilibrium depends on the polymer's intrinsic properties (e.g., matrix hydrophilicity, number of charged groups, degree of cross-linking) and external electrolyte solution concentration, with all other conditions held constant (e.g., the type of charged groups and external electrolytes, and the interaction between ions and charged groups, etc.) [1-3]. When a dry polymer is placed in DI water, polar (e.g., ether oxygen) groups and hydrophilic charged (e.g., sulfonate) groups bound to the polymer backbone tend to surround themselves with water molecules from the external solution [4]. As the charged groups ionize, more water sorbs into the membrane and dilutes the fixed charge concentration. Therefore, water uptake generally increases as more ionogenic groups are added to the polymer backbone [1, 5-7].

2.3 Donnan Theory

The charges in ion exchange membranes have a great influence on salt transport characteristics, such as salt sorption and salt diffusion [21, 55-57]. In uncharged membranes, ions are sorbed through a partitioning mechanism. However, in charged membranes, ions are sorbed as a result of both partitioning and ion exchange with the fixed charge groups [37]. For example, when a membrane with fixed sulfonate groups in the acid form is immersed in a NaCl solution, the counter-ion sodium (Na^+) will not only associate with the chloride co-ion (Cl-), but also replace protons associated with the

sulfonate groups if the external solution has a large enough number of available sodium ions [21, 22, 33, 54, 58-60]. The fact that more counter-ions (Na^+) are sorbed into the polymer matrix than co-ions (Cl^-) will induce the migration of counter-ions back to the solutions and co-ions into the membranes. This migration causes the membrane to have more anions, in this case, while the solution has more cations. Thus, an electric field between the membrane and the solution is formed, and this potential is usually referred to as Donnan potential [54, 61]. The Donnan potential then favors the transport of cations into the membrane, and anions into the solution. But eventually, equilibrium is achieved when the tendency of migration in the two directions cancels out. Hence, ion exchange membranes, in general, attempt to exclude ions of the same charges, and this feature is typically referred to as Donnan exclusion [21, 54].

When ion sorption equilibrium is established, the product of ion activities, a, for every ionic species ($+$ for cation, $-$ for anion), that can partition between an IEM and a strong 1:1 electrolyte solution should be the same [1, 8-11] in the two phases, i.e.:

$$a_+^m a_-^m = a_-^s a_-^s \tag{2.1}$$

where the superscripts m and s represent the membrane phase and the solution phase, respectively. Writing the ion activity as the product of the ion activity coefficient, γ, and the concentration, C (i.e., $a_i^j \equiv \gamma_i^j C_i^j$), Eqn. (2.1) can be rewritten as follows:

$$(\gamma_+^m C_+^{m,w})(\gamma_-^m C_-^{m,w}) = (\gamma_+^s C_+^s)(\gamma_-^s C_-^s) \tag{2.2}$$

where γ_+^m and γ_-^m are the cation and anion activity coefficients in the membrane, respectively. C_+^m and C_-^m are the concentrations of cations and anions in the membrane

(moles of ions per liter of water sorbed in the membrane). The concentration of a 1:1 electrolyte in solution, C_s^s, is equal to its cation or anion concentration ($C_s^s = C_+^s = C_-^s$). The mean activity coefficient, $\gamma_\pm^s$, in the solution phase, defined as $(\gamma_\pm^s)^2 = \gamma_+^s \gamma_-^s$, is typically used [12]. Thus, Eqn. (2.2) can be rearranged to:

$$\gamma_+^m \gamma_-^m = \frac{\left(\gamma_\pm^s\right)^2 (C_s^s)^2}{C_+^{m,w} C_-^{m,w}} \tag{2.3}$$

The product of membrane ion activity coefficients, $\gamma_+^m \gamma_-^m$, can be computed from the external electrolyte solution concentration, C_s^s, the measured membrane ion concentrations, $C_+^{m,w}$ and $C_-^{m,w}$, and the mean ion activity coefficient in solution, $\gamma_\pm^s$, which can be taken from data tabulated in literature or computed by theory such as the Pitzer model [13]. For a CEM (e.g., sulfonated polymer) equilibrated in a NaCl solution, a charge balance in the membrane for a CEM is given by [11]:

$$C_+^{m,w} = C_-^{m,w} + C_A^{m,w} \tag{2.4}$$

where $C_+^{m,w}$, $C_-^{m,w}$, and $C_A^{m,w}$ are the molar concentrations of Na^+, Cl^-, and fixed charges in the swollen membrane [mol/L (water sorbed)]. Combining Eqn. (2.3) and (2.4), one can express the co-ion (-) concentration in a swollen CEM as follows [14]:

$$C_-^{m,w} = \left[\frac{(C_A^{m,w})^2}{4} + \frac{(C_s^s)^2 \left(\gamma_\pm^s\right)^2}{\gamma_+^m \gamma_-^m}\right]^{\frac{1}{2}} - \frac{C_A^{m,w}}{2} \tag{2.5}$$

where $\frac{\left(\gamma_\pm^s\right)^2}{\gamma_+^m \gamma_-^m}$ is defined as Γ:

$$\Gamma \equiv \frac{\left(\gamma_{\pm}^{s}\right)^{2}}{\gamma_{+}^{m}\gamma_{-}^{m}} \tag{2.6}$$

Γ is set to 1 in ideal Donnan theory [1, 14]. Recently, highly non-ideal ion behavior was demonstrated in charged membranes due to electrostatic interactions between ions and fixed charges, leading to values of this ratio far from unity; in this study, $\gamma_{+}^{m}\gamma_{-}^{m}$ was described by Manning's model [11].

Thus, $C_{-}^{m,w}$ can be computed based on knowledge of the basic membrane property, $C_{A}^{m,w}$, and the external electrolyte concentration, C_{s}^{s}. The counter-ion concentration, $C_{+}^{m,w}$, can then be calculated using Eqn. (2.4). In a CEM, the mobile salt concentration, $C_{s}^{m,w}$, is equivalent to the sorbed co-ion concentration, $C_{-}^{m,w}$, therefore, the salt sorption (or partition) coefficient, K_{s}^{w}, in a CEM is defined as follows [14]:

$$K_{s}^{w} = \frac{C_{s}^{m,w}}{C_{s}^{s}} \tag{2.7}$$

where $C_{s}^{m,w}$ is the mobile salt concentration (e.g., $C_{s}^{m,w} = C_{-}^{m,w}$ for CEMs) in the membrane. $C_{s}^{m,w}$ has units of mol/L (swollen membrane) when considering transport phenomena and units of mol/L (sorbed water) when used for sorption model [15]. Combining Eqn. (2.6) and (2.7) yields:

$$K_{s}^{w} = \left[\frac{1}{4}\left(\frac{C_{A}^{m,w}}{C_{s}^{s}}\right)^{2} + \Gamma\right]^{\frac{1}{2}} - \frac{1}{2}\left(\frac{C_{A}^{m,w}}{C_{s}^{s}}\right) \tag{2.8}$$

For an uncharged membrane ($C_{A}^{m,w}$ = 0):

$$C_-^{m,w} = C_+^{m,w} = C_s^{m,w} = (\Gamma)^{\frac{1}{2}} C_s^s \tag{2.9}$$

so $C_-^{m,w}$ and $C_+^{m,w}$ in uncharged membranes are equal to the mobile salt concentration and proportional to the external electrolyte solution concentration, provided Γ is a constant. The salt sorption coefficient in an uncharged membrane is defined as follows [14]:

$$K_s^w = \frac{C_s^{m,w}}{C_s^s} = \Gamma^{\frac{1}{2}} \tag{2.10}$$

Combining Eqn. (2.4)-(2.5), the ion concentration ratio in CEMs, $C_+^{m,w}/C_-^{m,w}$, is given by:

$$C_+^{m,w}/C_-^{m,w} = 1 + \frac{2}{[1 + 4\Gamma\left(\frac{C_s^s}{C_A^{m,w}}\right)^2]^{\frac{1}{2}} - 1} \tag{2.11}$$

For uncharged membrane, $C_+^{m,w}/C_-^{m,w}$ is 1 based on Eqn. (2.9).

2.4 MANNING'S MODEL

Manning's model was originally developed to compute colligative properties of aqueous polyelectrolyte solutions with added salt [16]. The model assumes the polyelectrolyte chain is fully extended with dense, uniformly distributed charges on it [16]. Electrostatic interactions between charged groups on distant chains and between distant segments on the same chain are neglected [16, 17]. Interactions between neutral molecules and ions (e.g., uncharged polymer segments and ions) are neglected, and interactions between fixed charges and mobile ions are the major contributors to the free energy [16, 18, 19]. Recently, Manning's model was extended to estimate ion activity coefficients in IEMs [11, 20]. The only parameter in this model, ξ, is given by [16]:

$$\xi = \frac{\lambda_B}{b} = \frac{e^2}{4\pi\varepsilon_0\varepsilon kTb} \tag{2.12}$$

where ξ is referred to as the Manning parameter [16, 21]. b is the average distance between successive fixed charges on the polymer chain. λ_B is the Bjerrum length, which characterizes the distance within which ions strongly "associate" with fixed charges [11]. λ_B is determined by the unit electrostatic charge, e, the vacuum permittivity, ε_0, the media dielectric constant, ε, the absolute temperature, T, and Boltzmann's constant, k [16]. Thus, λ_B is constant if the dielectric constant and temperature of a system are invariant (e.g., $\lambda_B = 7.135$ Å in water at ambient conditions). Then ξ is essentially a measure of charge density, since higher ξ values (i.e., smaller b) denote more densely distributed fixed charges on the polymer chain [16]. For IEMs with univalent fixed charges in a 1:1 electrolyte solution, when $\xi > 1$, some counter-ions "condense" onto the fixed charges on the polymer chain (i.e., counter-ion condensation) [16]. When $\xi < 1$, counter-ions do not undergo condensation [16]. To determine ξ in IEMs, in some cases, ε can be estimated as the volume fraction averaged dielectric constants of dry polymer and water, and b can be estimated based on polymer chemistry [11, 20, 22]. Detailed calculations of ε are b are included in the Supporting Information. b values vary between 23 and 206 Å ($\xi < 1$) for the polymers considered. This study focuses mainly on cases where $\xi < 1$, and $\gamma_+^m\gamma_-^m$ is given by [16]:

$$\gamma_+^m\gamma_-^m = exp\left[-\frac{\xi}{1 + 2\frac{C_-^{m,w}}{C_A^{m,w}}}\right] = exp\left[-\frac{\xi}{1 + 2K_s^w\frac{C_s^s}{C_A^{m,w}}}\right] \tag{2.13}$$

Combining Eqn. (2.7) and (2.13) yields:

$$K_s^w \left(\frac{C_A^{m,w}}{C_s^s} + K_s \right) exp\left[- \frac{\xi}{1 + 2K_s^w \frac{C_s^s}{C_A^{m,w}}} \right] = \left(\gamma_\pm^s \right)^2 \tag{2.14}$$

Thus, K_s^w depends on membrane properties (i.e., $C_A^{m,w}$ and ξ), the electrolyte solution concentration (i.e., C_s^s) surrounding the membrane, and the mean activity coefficient of the ions in the external solution (i.e., $\gamma_\pm^s$). For common aqueous electrolytes, values of $\gamma_\pm^s$ are tabulated in the literature or may be estimated by, for example, the Pitzer model [23]. Then, $\gamma_+^m \gamma_-^m$, can be computed from Eqn. (2.13).

Since the swollen membrane volume (i.e., volume of polymer, water, and ions) is often considered for transport phenomena [15], ion concentrations based on the volume of sorbed water were converted to concentrations based on the volume of swollen membrane as follows [15]:

$$C_i^{m,p} = C_i^{m,w} \phi_w \tag{2.15}$$

where $C_i^{m,p}$ is expressed as mol of ions ($i = +$ for counter-ion, $i = -$ for co-ion) per liter of swollen membrane. The salt sorption coefficient, K_s^p, is defined as follow [14]:

$$K_s^p = \frac{C_s^{m,p}}{C_s^s} \tag{2.16}$$

where $C_s^{m,p}$ is the mobile salt concentration (i.e., co-ion for a CEM) in the membrane. That is, $C_s^{m,p}$ is equal to $C_-^{m,p}$ in a CEM.

2.5 MEARES' MODEL

Salt and ion diffusion in membranes can be described by a simple tortuosity model, which was developed based on a rigid lattice-type matrix [24]. This model assumes water present in highly swollen polymers connects and constitutes a liquid-like pathway [25, 26], in which penetrants move freely. This pathway is often tortuous because bulky polymer chains hinder the penetrant's diffusion path. Therefore, the penetrants must travel extra distance to traverse the membrane rather than the direct distance between the two sides of the membrane [24]. Consequently, ions or salt appear to diffuse slower in the membrane than in aqueous electrolyte solution. The ratio of diffusion coefficient in the membrane, D_i^m, to that in aqueous solution, D_i^s, can be related to polymer water volume fraction, ϕ_w [24]:

$$\frac{D_i^m}{D_i^s} = \left(\frac{\phi_w}{2-\phi_w}\right)^2 \tag{2.17}$$

where $\left(\frac{\phi_w}{2-\phi_w}\right)^2$ is referred to as the tortuosity factor and ϕ_w is expressed as L (sorbed water)/L (swollen membrane). Thus, D_i^m can be predicted based on polymer water volume fraction and penetrant diffusion coefficients in external solution (e.g., $D_{Na^+}^s$ = 13.3 cm^2/s, $D_{Cl^-}^s$ = 20.3 cm^2/s, and D_{NaCl}^s = 16.1 cm^2/s), which are tabulated in literature [15, 27].

2.6 SOLUTION-DIFFUSION MODEL

At steady state, the integral salt permeability coefficient, $\langle P_s \rangle$, is given by [28, 29]:

$$\langle P_s \rangle = \langle \overline{D}_s^{m*} \rangle K_s^p \tag{2.18}$$

where $\langle \bar{D}_s^{m*} \rangle$ is the concentration averaged (i.e., apparent) salt diffusion coefficient, which can be computed from experimental salt permeability and salt sorption coefficients via Eqn. (2.18). However, salt diffusion coefficients determined in this manner neglect frame of reference and nonideal thermodynamic effects [28]. Frame of reference effects can be corrected by accounting for convection using Fick's law [28]. Correcting for nonideal effects uses ion activity coefficient gradients in the membrane, which can be obtained from experimental ion sorption results [28, 30]. After these corrections, local salt diffusion coefficient, D_s^m, was obtained [28]. In this study, frame of reference and nonideal thermodynamic effects almost cancel each other for highly charged samples considered ($D_s^m \approx \langle \bar{D}_s^{m*} \rangle$, cf. Supporting Information), similar to prior studies [28]. In contrast, D_s^m values for the uncharged sample are slightly higher (< 5%) than $\langle \bar{D}_s^{m*} \rangle$ values, since both effects increased salt diffusion coefficients (cf. Supporting Information). However, this difference between D_s^m and $\langle \bar{D}_s^{m*} \rangle$ is within the experimental uncertainty. Thus, for the materials considered in this study, apparent salt diffusion coefficient was used to a first approximation as the local salt diffusion coefficient for data interpretations.

2.7 NERNST-PLANK EQUATION

When a concentration gradient is present in a CEM, D_s^m can be expressed as [28]:

$$D_s^m = \frac{D_+^m D_-^m (C_-^{m,p} + C_+^{m,p})}{D_+^m C_+^m + D_-^m C_-^m} \tag{2.19}$$

where D_+^m and D_-^m are the counter-ion and co-ion diffusion coefficients in the membrane.

When an electric field is applied to a CEM, the ionic conductivity, κ, is given by [31]:

$$\kappa = \frac{F^2}{RT}(D_+^m C_+^{m,p} + D_-^m C_-^{m,p}) \tag{2.20}$$

where F is Faraday's constant, R is the gas constant, and T is absolute temperature. Typically, ion diffusion coefficients are presumed to be independent of driving force [26]. Combining Eqn. (2.19)-(2.20) yields:

$$D_-^m = \frac{\frac{\kappa RT}{F^2} \pm \sqrt{\left(\frac{\kappa RT}{F^2}\right)^2 - 4\frac{\kappa RT}{F^2}\frac{C_-^{m,p} C_+^{m,p} D_s^m}{C_-^{m,p} + C_+^{m,p}}}}{2C_-^m} \tag{2.21}$$

Thus, D_-^m can be calculated using the experimental ionic conductivity, ion concentrations in the membrane, and local salt diffusion coefficients. Then, D_+^m can be obtained using Eqn. (2.19) or (2.20).

2.8 REFERENCES

[1] F. Helfferich, Ion Exchange, McGraw-Hill Book Co., Inc., New York, 1962.

[2] C. Calmon, Application of volume characteristics of sulfonated polystyrene resins as a tool in analytical chemistry, Analytical Chemistry, 25 (1953) 490-492.

[3] G.M. Geise, M.A. Hickner, B.E. Logan, Ionic resistance and permselectivity tradeoffs in anion exchange membranes, ACS Applied Materials & Interfaces, 5 (2013) 10294-10301.

[4] A.A. Zagorodni, Ion exchange materials: properties and applications, Elsevier, 2006.

[5] G.M. Geise, B.D. Freeman, D.R. Paul, Characterization of a novel sulfonated pentablock copolymer for desalination applications, Journal of Membrane Science, 24 (2010) 5815-5822.

[6] H.B. Park, B.D. Freeman, Z.B. Zhang, M. Sankir, J.E. McGrath, Highly chlorine-tolerant polymers for desalination, Angewandte Chemie, 120 (2008) 6108-6113.

[7] S. Lindenbaum, C. Jumper, G. Boyd, Selectivity coefficient measurements with variable capacity cation and anion exchangers, The Journal of Physical Chemistry, 63 (1959) 1924-1929.

[8] F.G. Donnan, Theory of membrane equilibria and membrane potentials in the presence of non-dialysing electrolytes. A contribution to physical-chemical physiology, Journal of Membrane Science, 100 (1995) 11.

[9] J.W. Gibbs, On the equilibrium of heterogeneous substances, American Journal of Science, (1878) 441-458.

[10] J. Duncan, A theoretical treatment of cation exchangers. II. Equilibria between an ion exchanger and an aqueous solution with a common cation, in: Proceedings of the Royal Society of London A: Mathematical, Physical and Engineering Sciences, The Royal Society, 1952, pp. 344-355.

[11] J. Kamcev, D.R. Paul, B.D. Freeman, Ion activity coefficients in ion exchange polymers: Applicability of Manning's counterion condensation theory, Macromolecules, 48 (2015) 8011-8024.

[12] N. Lakshminarayanaisah, Transport phenomena in membranes, Academic Press, New York and London, 1969.

[13] K.S. Pitzer, G. Mayorga, Thermodynamics of electrolytes. II. Activity and osmotic coefficients for strong electrolytes with one or both ions univalent, The Journal of Physical Chemistry, 77 (1973) 2300-2308.

[14] G.M. Geise, L.P. Falcon, B.D. Freeman, D.R. Paul, Sodium chloride sorption in sulfonated polymers for membrane applications, Journal of Membrane Science, 423-424 (2012) 195-208.

[15] J. Kamcev, D.R. Paul, G.S. Manning, B.D. Freeman, Predicting salt permeability coefficients in highly swollen, highly charged ion exchange membranes, ACS Applied Materials & Interfaces, 9 (2017) 4044-4056.

[16] G.S. Manning, Limiting laws and counterion condensation in polyelectrolyte solutions I. Colligative properties, The Journal of Chemical Physics, 51 (1969) 924-933.

[17] R.A. Robinson, R.H. Stokes, Electrolyte solutions, Courier Corporation, 2002.

[18] S. Lammertz, T. Grünfelder, L. Ninni, G. Maurer, A model for the Gibbs energy of aqueous solutions of polyelectrolytes, Fluid Phase Equilibria, 280 (2009) 132-143.

[19] M. Nagvekar, F. Tihminlioglu, R.P. Danner, Colligative properties of polyelectrolyte solutions, Fluid Phase Equilibria, 145 (1998) 15-41.

[20] J. Kamcev, M. Galizia, F.M. Benedetti, E.-S. Jang, D.R. Paul, B.D. Freeman, G.S. Manning, Partitioning of mobile ions between ion exchange polymers and aqueous salt solutions: importance of counter-ion condensation, Physical Chemistry Chemical Physics, 18 (2016) 6021-6031.

[21] G.S. Manning, Limiting laws and counterion condensation in polyelectrolyte solutions: IV. The approach to the limit and the extraordinary stability of the charge fraction, Biophysical Chemistry, 7 (1977) 95-102.

[22] J. Kamcev, D.R. Paul, B.D. Freeman, Effect of fixed charge group concentration on equilibrium ion sorption in ion exchange membranes, Journal of Materials Chemistry A, 5 (2017) 4638-4650.

[23] K.S. Pitzer, Thermodynamics of electrolytes. I. Theoretical basis and general equations, The Journal of Physical Chemistry, 77 (1973) 268-277.

[24] J.S. Mackie, P. Meares, The diffusion of electrolytes in a cation-exchange resin membrane. I. Theoretical, Proceedings of the Royal Society of London A: Mathematical, Physical and Engineering Sciences, 232 (1955) 498-509.

[25] P. Meares, Ion exchange membranes: Principles, production and processes, in: Ion Exchange: Science and Technology, Springer, 1986, pp. 529-558.

[26] J. Mackie, P. Meares, The diffusion of electrolytes in a cation-exchange resin membrane. II. Experimental, in: Proceedings of the Royal Society of London A: Mathematical, Physical and Engineering Sciences, The Royal Society, 1955, pp. 510-518.

[27] J.H. Wang, S. Miller, Tracer-diffusion in Liquids. II. The Self-diffusion as Sodium Ion in Aqueous Sodium Chloride Solutions1, Journal of the American Chemical Society, 74 (1952) 1611-1612.

[28] J. Kamcev, D.R. Paul, B.D. Freeman, Accounting for Frame of Reference and Thermodynamic Non-Idealities When Calculating Ion Diffusion Coefficients in Ion Exchange Membranes, Journal of Membrane Science, 537 (2017) 396-406.

[29] J.G. Wijmans, R.W. Baker, The solution-diffusion model: a review, Journal of Membrane Science, 107 (1995) 1-21.

[30] N. Yan, D.R. Paul, B.D. Freeman, Water and ion sorption in a series of cross-linked AMPS/PEGDA hydrogel membranes, In preparation, (2017).

[31] A.J. Bard, L.R. Faulkner, J. Leddy, C.G. Zoski, Electrochemical methods: fundamentals and applications, Wiley New York, 1980.

Chapter 3: Materials and Methods

3.1 Materials and Film Preparation

The ionic monomer, 2-acrylamido-2-methyl-1-propanesulfonic acid (AMPS), a neutral cross-linker, poly(ethylene glycol) diacrylate [PEGDA with n = 13, n = 10, and n = 4, where n represents the average number of ethylene oxide (EO) groups per cross-linker molecule], a photoinitiator, 2,2-dimethoxy-2-phenylacetophenone (DMPA), sodium chloride (NaCl), and sodium bicarbonate ($NaHCO_3$) were purchased from Sigma-Aldrich (Milwaukee, WI). De-ionized (DI) water (18.2 MΩ cm, 1.2 ppb total organic carbon) was produced by a Millipore Milli-Q Advantage A10 water purification system (Millipore Corporation, Bedford, MA). All chemicals were used as received.

Free-standing XL(AMPS-PEGDA) films were prepared from a pre-polymerization mixture by free radical UV-photopolymerization as shown in Figure 3.1 (a) [1-4]. The pre-polymerization mixture contained PEGDA, AMPS, DMPA, and solvent [water, and in some cases, methanol (MeOH)]. Table 3.1 summarizes various polymer composition information. The DMPA content was 0.1 wt% (based on the total weight of PEGDA and AMPS), consistent with our prior studies [5, 6]. The solvent content was set to 25 wt% (based on the total solution weight), which allowed AMPS to dissolve in all pre-polymerization solutions considered. Samples were named based on n and the IEC values of the samples. For example, sample 13-0 denotes an uncharged membrane (IEC = 0 meq/g) cross-linked with PEGDA of n = 13. Sample 10-0.44 represents a membrane cross-linked with PEGDA of n = 10 having an IEC of 0.44 meq/g. At a given n value, by adjusting the ratio of PEGDA to AMPS, theoretical IEC values ranging from 0 to 2.18 were obtained. The same conditions were used to synthesize polymers with n = 13 and n = 10

[7]. Before polymerization, AMPS was dissolved in water after stirring for 10 min in a glass jar. Then, PEGDA and DMPA were added to the mixture. All reagents were mixed using a stirrer (Isotemp® S88854200, Fisher Scientific, Hampton, NH) at 1000 rpm for about 30 min, after which the solution was transparent and visually homogeneous. Then, the mixture was stirred at 150 rpm for about one hr to eliminate air bubbles. During this process, the glass jar was wrapped with aluminum foil to minimize photoinitiation due to exposure to ambient light.

Table 3.1 also shows the polymer composition for homopolymers XLPEGDA (film) and PAMPS (liquid). They were prepared using the same procedure discussed above via the scheme shown in Figure 3.1 (b) and (c). Preparation of the pre-polymerization mixtures prepared with n = 4 is described below.

For polymers having IEC values of 0.97 to 2.18 meq/g at n = 4, AMPS was first dissolved in water while stirring for 30 min. PEGDA and DMPA were then added to the solution and stirred at 1000 rpm for 3.5 hrs to fully dissolve the DMPA. The mixture was stirred at 150 rpm for another hour to become homogeneous. At IEC values of 0 to 0.44 meq/g for n = 4, water/methanol (60/40, v/v) mixtures were used as the pre-polymerization solvent, since PEGDA of n = 4 barely dissolves in water.

A plastic pipette was used to transfer a fixed volume (2-3 ml) of the pre-polymerization mixture to a leveled square quartz plate [CGQ-0620-14, 4 in × 4 in × 1/8 in thick (10 cm × 10 cm × 0.3 cm thick), Chemglass, Vineland, NJ] in the center of a microprocessor-controlled UV cross-linker (Spectroline™, Spectronics Corporation, Westbury, NY). Then, a round quartz plate [4 in diameter × 1/8 in thick (10 cm diameter × 0.3 cm thick), Chemglass] was carefully placed on top of the mixture. Four

feeler gauges (Precision Brand 19740, Downers Grove, IL) were placed at the edges between the plates to control membrane thickness (e.g., 203 or 508 μm). This assembly was then irradiated with UV-light (312 nm wavelength) for three mins at 3.0 mW/cm^2. The liquid mixture was converted to a transparent solid hydrogel film for the homopolymer XLPEGDA and copolymer XL(AMPS-PEGDA). Afterwards, the film was removed from the quartz plate and cut into circular coupons with diameters ranging from 1.6 to 5 cm. All films from each batch were then soaked in DI water (750 ml) for one day. The water was changed three times to extract any residual components not bound to the network. Wet films were first dried at ambient conditions overnight to minimize film cracking as water naturally evaporates out of the films. Then, films were dried under full vacuum at 50 ℃ for three days prior to FTIR, thermal, density, and mechanical analysis. After polymerization, the homopolymer PAMPS dissolved in water maintained a clear, transparent liquid form. Following the same drying process discussed above, the PAMPS liquid turned into a white powder.

Polymer gel fraction was nearly 100% after the water extraction process [7, 8]. All pre-polymerization solutions were transparent, as were most of the dry and hydrated polymers, suggesting that the materials are homogeneous. One exception is the XLPEGDA sample prepared from n = 4, which exhibits cloudiness following the UV treatment, likely due to polymerization induced phase separation (PIPS) [9]

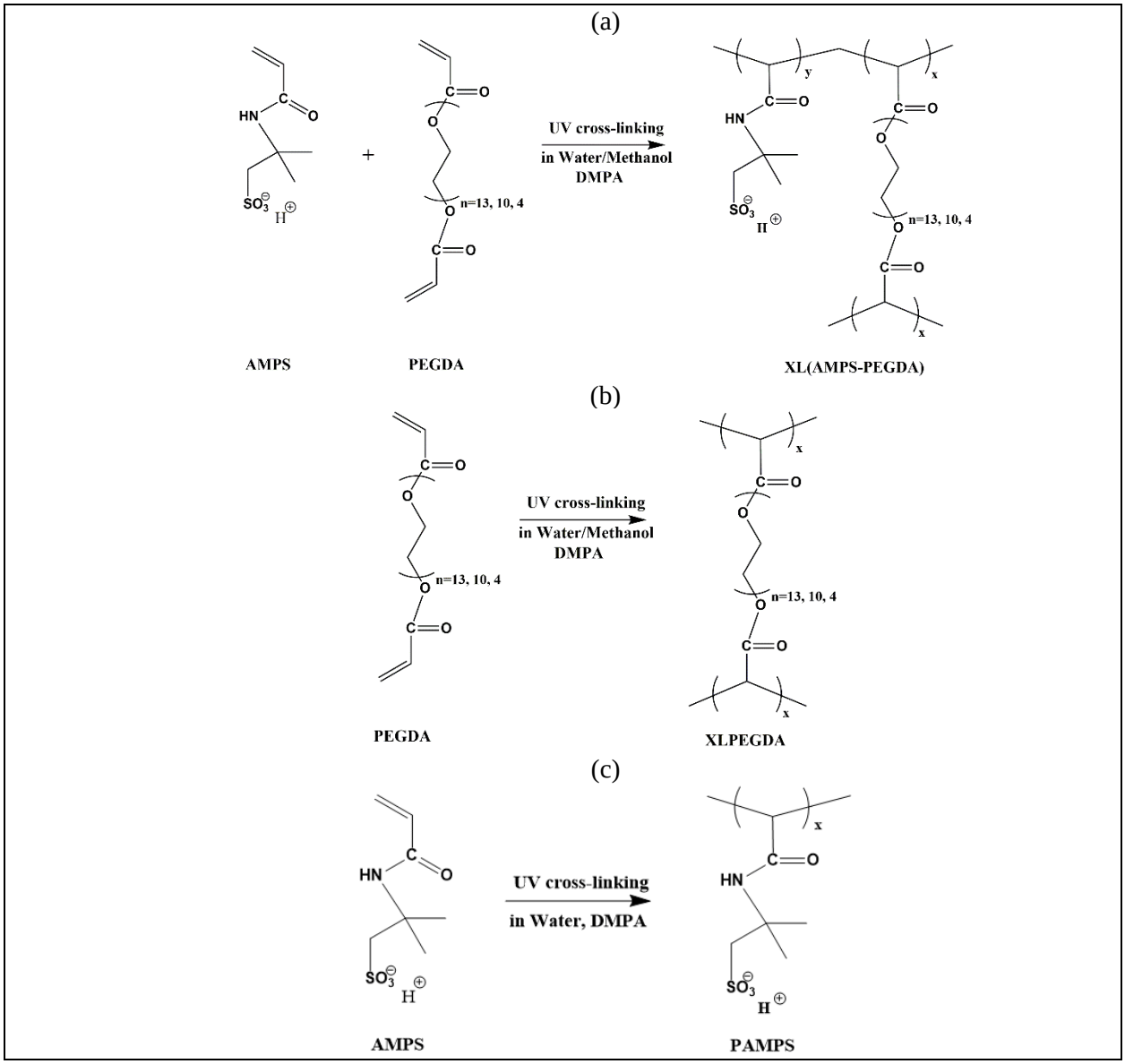

Figure 3.1 Preparation of UV cross-linked: (a) XL(AMPS-PEGDA) membranes, (b) XLPEGDA membranes, and (c) PAMPS.

Table 3.1 Composition of pre-polymerization mixtures.

Sample	IEC [a] [meq/g (dry polymer)]	AMPS [b] content [wt%]	Cross-linker (PEGDA) [g]	Ionic monomer (AMPS) [g]	Initiator (DMPA) [g]	DI water [g]	Methanol [g]
13-0	0	0	15.0	-	0.0200	5.00	-
13-0.33	0.33	7	17.0	1.0	0.0180	6.00	-
13-0.44	0.44	9	15.0	1.5	0.0165	5.50	-
13-0.97	0.97	20	12.0	3.0	0.0150	5.00	-
13-1.40	1.40	29	12.3	5.0	0.0173	5.77	-
13-1.46	1.46	30	11.5	5.0	0.0165	5.50	-
13-1.93	1.93	40	9.00	6.0	0.0150	5.00	-
10-0	0	0	15.0	-	0.0200	5.00	-
10-0.44	0.44	9	15.0	1.5	0.0165	5.50	-
10-0.97	0.97	20	12.0	3.0	0.0150	5.00	-
10-1.46	1.46	30	11.5	5.0	0.0165	5.50	-
10-1.93	1.93	40	9.00	6.0	0.0150	5.00	-
4-0	0	0	15.0	-	0.0200	3.00	2.00
4-0.44	0.44	9	15.0	1.5	0.0165	3.30	2.20
4-0.97	0.97	20	12.0	3.0	0.0150	5.00	-
4-1.46	1.46	30	11.5	5.0	0.0165	5.50	-
4-1.93	1.93	40	9.00	6.0	0.0150	5.00	-
4-2.18	2.18	45	9.76	8.0	0.0178	5.92	-
PAMPS	-	100	-	15.0	0.0200	5.00	

[a] Theoretical IEC values of the acid form (H^+) XL(AMPS-PEGDA) films were determined as milliequivalents of AMPS/(wt of AMPS + wt of PEGDA) [meq/g (dry polymer)] [7].
[b] wt% AMPS = wt of AMPS/(wt of AMPS + wt of PEGDA)

XL(AMPS-PEGDA) films were converted to their salt form prior to water and ion sorption measurements. The films were initially immersed in a 5 M NaCl solution (1 L) for two days. The solution was changed three times daily, and the films were then transferred to a 1 M $NaHCO_3$ solution (1 L, prepared from $NaHCO_3$ powder and DI water) for 1-2 days to completely convert the acid form polymers to their sodium form [10].

During this process, sodium ions exchange with the protons initially associated with the fixed sulfonate groups on the polymer backbone [11]. Protons released by the films combined with bicarbonate groups in the solution and formed CO_2 bubbles accumulating on the surface of the films [12]. $NaHCO_3$ solution was changed three times a day until effervescence ceased. Then the films were rinsed in DI water (1 L) for 2-3 hrs to extract any residual salt solution (i.e., mobile salt) in the film. This rinsing process continued until the conductivity of the rinsing solution remained constant at ~ 0.75 μS/cm, which is the conductivity of DI water equilibrated with the carbon dioxide in ambient air [13]. The conductivity was measured using a conductivity meter (InoLab Cond 730, WTW, Germany). Basic membrane properties are summarized in Table 3.2.

Table 3.2 Polymer theoretical cross-linking density, density, water uptake, water volume fraction, and volumetric fixed charge concentration.

Sample	ρ_p [a] [g/cm^3]	v_t x 10^3 [b] [mol/cm^3 (dry polymer)]	w_u [c] [g (water)/g (dry polymer)]	ϕ_w [d] [L (water)/L (swollen polymer)]	$C_A^{m,w}$ [e] [mol/L (water sorbed)]
13-0	1.186	3.39	0.787 ± 0.014	0.483 ± 0.002	0
13-0.33	1.210 [f]	3.27	0.946 ± 0.007	0.534 ± 0.002	0.349 ± 0.002
13-0.44	1.223	3.18	0.989 ± 0.012	0.547 ± 0.003	0.444 ± 0.005
13-0.97	1.257	2.87	1.179 ± 0.009	0.597 ± 0.002	0.818 ± 0.006
13-1.40	1.287	2.61	1.346 ± 0.006	0.634 ± 0.002	1.036 ± 0.005
13-1.46	1.292	2.57	1.385 ± 0.014	0.641 ± 0.002	1.056 ± 0.011
13-1.93	1.320	2.26	1.577 ± 0.012	0.676 ± 0.002	1.224 ± 0.009
10-0	1.205	4.19	0.581 ± 0.006	0.411 ± 0.004	0
10-0.01	1.210	4.19	0.593 ± 0.014	0.418 ± 0.006	(1.69 ± 0.04)×10^{-2}
10-0.05	1.213	4.18	0.619 ± 0.003	0.429 ± 0.003	(8.40 ± 0.05)×10^{-2}
10-0.13	1.218	4.12	0.645 ± 0.004	0.440 ± 0.002	0.208 ± 0.005
10-0.44	1.242	3.93	0.764 ± 0.009	0.487 ± 0.003	0.575 ± 0.007
10-0.97	1.284	3.57	0.936 ± 0.014	0.546 ± 0.004	1.031 ± 0.015
10-1.46	1.307	3.17	1.110 ± 0.024	0.593 ± 0.005	1.318 ± 0.029
10-1.93	1.329	2.77	1.300 ± 0.018	0.633 ± 0.003	1.485 ± 0.021
4-0	1.264	8.37	0.230 ± 0.005	0.226 ± 0.004	0
4-0.44	1.288	7.75	0.423 ± 0.007	0.353 ± 0.004	1.037 ± 0.017
4-0.97	1.302	6.90	0.577 ± 0.008	0.429 ± 0.003	1.672 ± 0.023
4-1.46	1.326	6.12	0.713 ± 0.006	0.486 ± 0.002	2.051 ± 0.017
4-1.93	1.350	5.36	0.882 ± 0.010	0.544 ± 0.003	2.189 ± 0.025
4-2.18	1.362	4.96	0.934 ± 0.010	0.560 ± 0.003	2.329 ± 0.025

[a] The dry polymer density was determined using Eqn. (3.1).
[b] The theoretical cross-link density was estimated via Eqn. (3.3).
[c] The pure water uptake was measured gravimetrically [cf. Eqn. (3.4)].
[d] The volume fraction of water in the swollen membrane was calculated using theoretical IEC and dry polymer density via Eqn. (3.5).
[e] The fixed charge concentration was computed based on theoretical IEC and pure water uptake results using Eqn. (3.9).
[f] The measured XL(AMPS-PEGDA) films are in sodium form (Na^+).

3.2 ATR-FTIR

Attenuated total reflection Fourier transform infrared spectroscopy (ATR-FTIR, Thermo Nicolet Nexus 470, Madison, WI) was performed to characterize the chemical structure of the films. Spectra were acquired by accumulating 256 scans at a resolution of 4 cm^{-1}.

3.3 THERMAL ANALYSIS

Thermal analyses of the polymers were conducted using both thermogravimetric analysis (TGA, Q500, TA instruments, New Castle, DE) and differential scanning calorimetry (DSC, Q100, TA instruments, New Castle, DE). All XLPEGDA, PAMPS, and acid form XL(AMPS-PEGDA) samples were dried under vacuum at 50 ℃ for three days before the tests. The TGA instrument was purged with N_2 (UHP 99.999%, Air Gas, Austin, TX) over the balance at 40 mL/min and over the sample at 60 mL/min. A dry sample of 5 to 7 mg was initially kept at 60 ℃ isothermally for one hour to evaporate as much residual moisture as possible. Then the TGA scan was performed at 10 ℃/min between 60 ℃ and 800 ℃. The onset of the sample's degradation temperature was used to help set measurement conditions for DSC measurements.

DSC measurements were conducted with a N_2 (UHP 99.999%) purge flowrate of 50 mL/min. Approximately 4 to 6 mg of dry sample was sealed in an aluminum pan. Samples were initially heated to 160 ℃ and held at this temperature for 10 min to remove moisture and erase any thermal history. DSC scans were then performed between -90 ℃ and 160 ℃ at a heating rate of 20 ℃/min for two repeated cycles. At the end of each cycle, samples were held isothermally (at -90 ℃ or 160 ℃) for 10 min. The glass transition temperature, T_g, was assigned as the midpoint of the step change in heat capacity observed during the second heating cycle.

3.4 DENSITY AND MECHANICAL ANALYSIS

The dry polymer density was determined by hydrostatic weighing using a Mettler Toledo analytical balance (AG204, Switzerland) and a density determination kit (# 238490) at ambient temperature. The film density, ρ_p, was calculated as follows [4]:

$$\rho_p = \frac{m_d}{m_d - m_l}\rho_l \tag{3.1}$$

where m_d and m_l are the dry film weights in air and in an auxiliary liquid (i.e., non-solvent), respectively, and ρ_l is the density of the auxiliary liquid. Heptane was selected as the auxiliary liquid because the polymer samples show negligible uptake of it over the duration of the density measurements.

The dynamic mechanical analysis (DMA, Q800, TA instruments, New Castle, DE) of a dry rectangular sample (18 mm × 6 mm × 0.5 mm) was performed under a N_2 (UHP 99.999%) atmosphere. The sample was heated from -90 ℃ to 160 ℃ using a temperature sweep at 1 ℃/min with a test frequency of 1 Hz. Storage modulus (E'), loss modulus (E''), and loss tangent ($\tan\delta$) were recorded. The peak of the $\tan\delta$-temperature curve was considered as the T_g.

The crosslink density was estimated from the DMA scans. The storage modulus, E', reached a rubbery plateau at temperatures above the glass transition temperature (T_g + 30~60℃) [14, 15]. Based on Flory's rubber elasticity theory [16], the following equation was used to estimate the effective crosslink density [17]:

$$v_e = \frac{E_r}{3RT} \tag{3.2}$$

where E_r is the apparent rubbery modulus at 30℃ above T_g ($T = T_g + 30$℃), and R is the gas constant.

The cross-linking density was also estimated from the theoretical number of network junctions assuming every vinyl group in the cross-linker reacts and engages in

cross-linkages without self loops and free chain ends [18]. The following equation was used to determine the theoretical cross-linking density, v_t [5, 18]:

$$v_t = c = 2\frac{m_c/M_n}{m_d/\rho_p} \tag{3.3}$$

where c is the molar concentration of vinyl groups in the cross-linker per unit volume of the dry polymer (mol/cm^3), 2 indicates every cross-linker has two vinyl groups, m_c is the cross-linker weight, and M_n is the molecular weight of the cross-linker [18].

3.5 WATER SORPTION

Equilibrium water uptake was determined gravimetrically [4, 19]. The XLPEGDA and the sodium form XL(PEGDA-AMPS) films were soaked in DI water and aqueous NaCl solutions (100ml, 0.01-1 M) at ambient conditions. When a wet film was removed from the external solution, water on its surface was quickly and carefully wiped off using Kimwipes™ (Delicate Task Wipes, Kimberly-Clark, Roswell, GA). The wet mass of the film, m_{wet}, was measured using an analytical balance (PB503-S/FACT, Mettler Toledo, Columbus, OH). Generally, m_{wet} stabilized after no more than 24 hr of soaking in external solutions. The dry mass of the film, m_{dry}, was determined after drying under vacuum at 50 ℃. Generally, the dry mass reached a constant value after 24 hr of drying for samples having a diameter of 2.5 cm and a thickness of 500 um. The weight fraction of water based on the dry film mass, w_u, is defined as follows [19]:

$$w_u = \frac{m_{wet} - m_{dry}}{m_{dry}} \tag{3.4}$$

After equilibration in each solution, the swollen membrane thickness was measured at five positions across the film surface using a low force digital micrometer (LiteMatrix VL-50A, Mitutoyo Corporation, Japan), and the film area was determined by analyzing a scanned image of the film using ImageJ software. The water volume fraction in the hydrated film, ϕ_w, was calculated as follows [4, 20]:

$$\phi_w = \frac{(m_{wet} - m_{dry})/\rho_w}{V_p} \tag{3.5}$$

where ρ_w was taken as the density of water in aqueous solution (1.0 g/cm^3) [4, 5, 20]. The volume of the hydrated film, V_p, was determined from the measured membrane thickness and area. The volume of fully hydrated films used in this study ranged from 0.1 to 0.5 cm^3. Following each measurement, the film was immediately returned to its solution to minimize any contamination.

3.6 CHLORIDE ION SORPTION

Films of XLPEGDA and the sodium form XL(AMPS-PEGDA) were first immersed in NaCl solution (100 ml) for one day in a plastic bottle. The NaCl solution was changed three times to maintain its desired concentration, which ranged from 0.01 to 1.0 mol/L [19, 21]. The measured ion sorption results were independent of the soaking time after 24 hr of equilibration in the NaCl solution.

Sorbed chloride ion (Cl^-) concentration in XLPEGDA and XL(AMPS-PEGDA) films was determined using a desorption method [21-25]. Presumably, Cl^- desorbs in the form of NaCl. Following the sorption process, surface water on a film was carefully wiped off, and the film was immediately immersed in DI water in a plastic bottle. The volume (25-750 ml), V_d, of the DI water was selected to ensure that the chloride

concentration in the desorption solution, $C_{Cl^-}^{d}$, was above 0.06 mg (NaCl)/L to eliminate any impact of potential salt contamination from the laboratory environment. $C_{Cl^-}^{d}$ was controlled to be below 1 mg (NaCl)/L, to drive the desorption process to completion. All equipment contacting the film and/or desorption solution were thoroughly washed with DI water to be as free of ions as possible.

The Cl^- concentration in the membrane, $C_{Cl^-}^{m,p}$, was determined from the Cl^- concentration in the desorption solution, $C_{Cl^-}^{d}$, measured by an ion chromatograph (IC) (ICS-2100, Dinoex Corporation, Sunnyvale, CA), using the following equation [21]:

$$C_{Cl^-}^{m,p} = \frac{V_d C_{Cl^-}^{d}}{\phi_w V_p} \tag{3.6}$$

where $C_{Cl^-}^{m,p}$ has units of moles of Cl^- per unit volume of water sorbed in the swollen polymer [mol/L (water sorbed)], V_d is the volume of the desorption solution, and V_p is the volume of swollen polymer.

3.7 SODIUM ION SORPTION

The concentration of sodium ions (Na^+) in uncharged membranes was determined by the desorption method discussed above [21]. The Na^+ concentration was measured using flame atomic absorption (Flame AA) spectrophotometry (Varian AA240, Clayton South, Victoria, Australia) [21]. To perform accurate elemental analysis, the desorption solution for XLPEGDA was diluted with a 2% (v/v) nitric acid solution (HNO_3, $\geqslant$ 99.999% trace metals basis, Sigma-Aldrich) to a concentration of 0.5~1.0 mg (Na)/L. The Na^+ concentration in the diluted desorption solution, $C_{Na^+}^{d}$, was used to calculate the Na^+ concentration in hydrated uncharged XLPEGDA films, $C_{Na^+}^{m,p}$, as follows [21]:

$$C_{Na^+}^{m,p} = \frac{xV_d C_{Na^+}^d}{\phi_w V_p} \tag{3.7}$$

where $C_{Na^+}^{m,p}$ has units of mol (Na^+)/L (water sorbed), and x is the number of times the desorption solution was diluted. $C_{Na^+}^{m,p}$ was found to be essentially equal to $C_{Cl^-}^{m,p}$, as expected [21].

For a sulfonated polymer desorbed in water, H^+ dissociated from the carbonic acid present in water (due to uptake of CO_2 from the atmosphere) can ion exchange with Na^+ associated with the sulfonate groups on the polymer backbone [26]. Therefore, the sorbed Na^+ concentration in more highly charged membranes (i.e., IEC > 0.44 meq/g) was determined by an ashing method [21]. After the sorption process, XL(AMPS-PEGDA) films (i.e., diameter of 2.2 cm, thickness of 500 μm) were dried under vacuum at 50 ℃ for one day [21]. Each dry film was then immediately placed in a 30 ml porcelain crucible (wide-form, FB-965-K, Fisher Scientific) which was put in a furnace (Isotemp® 750-58, Fisher Scientific) to minimize any water sorption from the atmosphere. The crucible was rinsed with the 2% (v/v) nitric acid solution and DI water three times, respectively, and dried before adding the film to the crucible. To get a good ashing result, the crucible was positioned close to the furnace wall where the heating element was located. The ashing process was performed by heating the sample to 700 ℃ at 10 ℃/min [21, 27]. Air was blown into the furnace using a fan to ensure sufficient exposure of the samples to air. After the ashing process, the residual ash left in the crucible retained the circular shape of the dry films. This white ash contained essentially all of the sodium ions [26]. The ash was readily dissolved in a 2% (v/v) HNO_3 solution (15 ml). This solution was transferred to a clean vial (05-538-59A, Fisher Scientific) for further dilution after the dissolved ash

solution was fully mixed. The Na^+ concentration of the diluted ash solution was analyzed by Flame AA.

However, the residual white ash of less charged membranes (i.e., IEC < 0.44 meq/g) after the ashing process can barely maintain a circular shape. Some of them appeared to be fused to the crucible. Therefore, the sorbed Na^+ concentration in these membranes was determined by an ion exchange method using another electrolyte (i.e., CsCl) [28]. Following the sorption process, the films were soaked in a 0.01 M CsCl solution (100 ml) for one day. Cesium ion (Cs^+), which is more selective in a CEM than Na^+, presumably replaced all the Na^+ in the membrane and associated with the sulfonate groups on the polymer backbone [11]. The CsCl solution was then diluted with a 2% (v/v) HNO_3 solution and the desorbed Na^+ concentration was measured by Flame AA.

The sorbed Na^+ concentration in hydrated charged XL(AMPS-PEGDA) films, $C_{Na^+}^m$, can be calculated as follows [21]:

$$C_{Na^+}^{m,p} = \frac{xV_a C_{Na^+}^a}{\phi_w V_p} \tag{3.8}$$

where the units of $C_{Na^+}^{m,p}$ are mol/L (water sorbed), V_a is the volume of the dissolved ash solution or the CsCl solution, $C_{Na^+}^a$ is the sodium ion concentration in the dissolved ash solution or the CsCl solution. $C_{Na^+}^{m,p}$ and $C_{Cl^-}^{m,p}$ can be converted to $C_{Na^+}^{m,w}$ and $C_{Cl^-}^{m,w}$ via Eqn. (2.16). $C_{Na^+}^{m,w}$ is expected to be equal to the summation of the fixed charge concentration, $C_A^{m,w}$, and the chloride ion concentration, $C_{Cl^-}^{m,w}$, in hydrated sulfonated films [cf. Eqn. (2.4)] [29].

$C_A^{m,w}$, the sample charge density, was calculated from the membrane's theoretical IEC value and water uptake as follows:

$$C_A^{m,w} = 1000 \times \frac{IEC}{w_u/\rho_w} \tag{3.9}$$

where $C_A^{m,w}$ has units of [mol/L (water sorbed)], and ρ_w was taken as 1.0 g/cm^3. When a CEM is equilibrated with a 0.01 M NaCl solution, very little Cl^- can sorb into the membrane due to the strong Donnan exclusion of co-ions (Cl^-) ($C_{Cl^-}^{m,w}$ is often orders of magnitude smaller than $C_A^{m,w}$) [21, 28]. Thus, C_A^m can be estimated from the experimentally measured $C_{Na^+}^{m,w}$ [$C_{Na^+}^{m,w} \approx C_A^{m,w}$, cf. Eqn. (2.4)] [28]. As shown in Table 2, the calculated $C_A^{m,w}$ values via Eqn. (3.9) were found to be essentially equal to the measured $C_{Na^+}^{m,w}$ values at 0.01 M NaCl [i.e., Eqn. (3.7) and (3.8)] within experimental uncertainty. Therefore, $C_A^{m,w}$ estimated from Eqn. (3.9) was used throughout this study due to experimental simplicity.

3.8 SALT PERMEABILITY

Prior to salt permeaiblity test, films of XLPEGDA and Na^+ form XL(AMPS-PEGDA) were equilibrated with DI water for at least one day. Then, a film was clamped between a pair of jacketed glass diffusion cells (custom-made, PermeGear Side-bi-Side, Hellertown, PA) [4, 19]. The donor (upstream) and receiver (downstream) cells were filled with NaCl solution at desired concentrations (i.e., 0.01-1 M) and DI water of equal volumes, respectively. The solutions in both cells were vigorously stirred, and the temperature was maintained at 25 $\pm$ 0.1 ℃. Conductivity change in the downstream solution with respect to time was monitored by a conductivity meter (WTW inoLab Cond730, Woburn, MA). The downstream salt concentration was computed from conductivity data using a pre-determined calibration curve. At pseudo-steady state, the integral salt permeability can be determined using the following expression [4, 19]:

$$\ln\left[1-\frac{2C_{sl}^{s}[t]}{C_{s0}^{s}[0]}\right]=-\left(\frac{2A\langle P_S\rangle}{VL}\right)t \tag{3.10}$$

where $C_{s0}^{s}[0]$ is the initial upstream salt concentration, $C_{sl}^{s}[t]$ is the downstream salt concentration at time t. A is the active sample area exposed to solutions (1.77 cm^2), V is the liquid volume in both cells (35 mL), and L is the membrane thickness measured right after the experiment.

Recently, dissolution of CO_2 in solution was found to elevate the downstream conductivity and cause the measured salt permeability coefficient to be higher than the true value [26]. Such interference is more pronounced when salt permeation tests are performed with highly charged membranes at low upstream salt concentrations such as 0.01 M [26]. To address this issue for more highly charged membranes (e.g., IEC of 0.44-1.93 meq/g) used in this study, an ultra-high purity N_2 (Airgas, Austin, TX) was bubbled through the upstream (i.e., 0.01 M NaCl) and downstream solutions before and during the experiments. This strategy can mitigate the effect of CO_2 on salt permeability results measured at low upstream solution concentrations, as reported elsewhere [26].

3.9 Osmotic Water Permeability

Water flux, driven by an osmotic pressure difference across the membrane during the salt permeability test, was measured using a pair of plastic diffusion cells, as described elsewhere [30]. Following the water equilibration process, sample films were clamped between two cell chambers. The upstream and downstream solutions were NaCl solution (1 M) and DI water of equal volumes (200 mL), respectively. Care was taken to ensure no air bubbles were trapped between the solution and cell wall [30]. Then, two capillary tubes were screwed on top of each cell. The tubes were filled with the same solution as

their respective cell. At pseudo-steady state, the decrease of the solution level in the downstream tube (or the solution level increase in the upstream tube) was recorded as a function of time, $\Delta V/\Delta t$ (e.g., ml/10 min), and water permeability was calculated as follows:

$$P_w = \frac{|\Delta V|}{|\Delta t|}\frac{L}{A\rho_w(\Delta p - \Delta\pi)} \tag{3.11}$$

where L is the membrane thickness determined following the test, A is the effective membrane area in contact with solutions (1.767 cm^2), ρ_w is the density of water (1 g/mL), and Δp is the hydrostatic pressure difference applied on the membrane (= 0 in this experiment). $\Delta\pi$ is the osmotic pressure difference across the membrane, where the osmotic pressure on the water side is considered zero (due to its relatively low salt concentration during the experiment) and that of the 1 M NaCl side is estimated from the Pitzer model [31].

3.10 MEMBRANE RESISTANCE/IONIC CONDUCTIVITY

Membrane electrical resistance was measured using an Electrochemical Impedance Spectroscopy (EIS) system (1287A, 1260A, Solartron, Ameteck Scientific Instruments, Berwyn, PA), as described elsewhere [32]. Prior to the test, films of XLPEGDA and sodium form XL(AMPS-PEGDA) were equilibrated in NaCl solution (100ml, 0.01-1 M) for one day. Membrane resistance of the uncharged and weakly charged films (i.e., IEC of 0-0.13 meq/g) were determined using a difference method, as described elsewhere [32]. Films were sandwiched between two plastic half cells (kindly provided by Calera Corporation, Los Gatos, CA), which were equipped with electrodes made of platinum. The cells were connected to a jacketed beaker containing about 200 mL of feed solution

(i.e., NaCl solution having the same concentration with the equilibration solution), the temperature of which was kept at 25 ± 0.1 ℃. Then, feed solution was pumped through the cell chambers using a peristaltic pump (150 mL/min, Masterflex 7528-10, 77292-50). In the measurements conducted at high salt concentrations (0.1-1 M), DC current of 5 mA and AC current of 1 mA were used [32]. At lower salt concentrations (0.01-0.03 M), AC current of 0.3 mA was used [32]. The frequency sweep was between 40 and 0.5 kHz, and the step interval for frequency change was 10 Hz. The total resistance (i.e., membrane + solution resistance), R_{m+s}, and solution resistance (i.e., blank cell), R_s, were recorded, and the membrane resistance, R_m, is given by [32]:

$$R_m = R_{m+s} - R_s \tag{3.12}$$

In uncharged and weakly charged membranes, R_{m+s}, was 2-10 times higher than R_s over the entire range of salt concentrations considered. This large difference ensures the subtracted R_m value is less susceptible to the experimental errors (< 3%) involved in R_{m+s} and R_s values. The membrane ionic conductivity was then calculated as follows [32]:

$$\kappa = \frac{L}{R_m A} \tag{3.13}$$

where L is the membrane thickness measured after the experiment, and A is the area of the electrodes in contact with cell solutions (3.81 cm^2).

For more highly charged membranes (i.e., IEC of 0.44-1.93 meq/g), the difference between R_{m+s} and R_s is small, so a recently developed direct contact method was used to measure the resistance of these membranes [32]. Following the equilibration process

in NaCl solution, a sample was quickly dipped into 3 M NaCl solution (~1 sec) to rinse off the dilute equilibration solution (i.e., 0.01-1 M) left on membrane surface. The resistance results change little as the dipping concentration increases from 3 to 5 M (cf. Supporting Information). Above 3 M, the hydrogel films used in this study could easily break due to the sudden de-swelling caused by the elevated concentration of the solution surrounding the membrane. Then, the film was clamped between two electrodes. The frequency range was 40-1 kHz with a DC current of 5 mA and AC current of 1 mA [32]. Membrane ionic conductivity results for XLPEGDA measured using the difference method and direct contact method were equivalent within the experimental uncertainty (cf. Supporting Information).

3.11 REFERENCE

[1] H. Lin, B.D. Freeman, S. Kalakkunnath, D.S. Kalika, Effect of copolymer composition, temperature, and carbon dioxide fugacity on pure-and mixed-gas permeability in poly (ethylene glycol)-based materials: Free volume interpretation, Journal of Membrane Science, 291 (2007) 131-139.

[2] H. Lin, E.V. Wagner, J.S. Swinnea, B.D. Freeman, S.J. Pas, A.J. Hill, S. Kalakkunnath, D.S. Kalika, Transport and structural characteristics of crosslinked poly (ethylene oxide) rubbers, Journal of Membrane Science, 276 (2006) 145-161.

[3] A.C. Sagle, E.M. Van Wagner, H. Ju, B.D. McCloskey, B.D. Freeman, M.M. Sharma, PEG-coated reverse osmosis membranes: desalination properties and fouling resistance, Journal of Membrane Science, 340 (2009) 92-108.

[4] H. Ju, A.C. Sagle, B.D. Freeman, J.I. Mardel, A.J. Hill, Characterization of sodium chloride and water transport in crosslinked poly (ethylene oxide) hydrogels, Journal of Membrane Science, 358 (2010) 131-141.

[5] H. Lin, T. Kai, B.D. Freeman, S. Kalakkunnath, D.S. Kalika, The effect of cross-linking on gas permeability in cross-linked poly (ethylene glycol diacrylate), Macromolecules, 38 (2005) 8381-8393.

[6] H. Ju, B.D. McCloskey, A.C. Sagle, V.A. Kusuma, B.D. Freeman, Preparation and characterization of crosslinked poly (ethylene glycol) diacrylate hydrogels as fouling-resistant membrane coating materials, Journal of Membrane Science, 330 (2009) 180-188.

[7] N. Yan, D.R. Paul, B.D. Freeman, Water and ion sorption in a series of cross-linked AMPS/PEGDA hydrogel membranes, In preparation, (2017).

[8] E.V.W. Haiqing Lin, John S. Swinnea, Benny D. Freeman, Steven J. Pas, Anita J. Hill, Sumod Kalakkunnath, Douglass S. Kalika, Transport and structural characteristics of crosslinked poly(ethylene oxide) rubbers, Journal of Membrane Science, 276 (2006) 17.

[9] Y.-H. Wu, H.B. Park, T. Kai, B.D. Freeman, D.S. Kalika, Water uptake, transport and structure characterization in poly (ethylene glycol) diacrylate hydrogels, Journal of Membrane Science, 347 (2010) 197-208.

[10] C.S. Gudipati, R.J. MacDonald, Cation exchange materials prepared in aqueous media, in: Washington, DC: U.S. Patent and Trademark Office, U.S. Patent No. 9,156,933, 2015.

[11] F. Helfferich, Ion Exchange, McGraw-Hill Book Co., Inc., New York, 1962.

[12] W. Stumm, J.J. Morgan, Aquatic chemistry: chemical equilibria and rates in natural waters, John Wiley & Sons, 2012.

[13] R.A. Robinson, R.H. Stokes, Electrolyte solutions, Courier Corporation, 2002.

[14] H. Miyagawa, M. Misra, L.T. Drzal, A.K. Mohanty, Fracture toughness and impact strength of anhydride-cured biobased epoxy, Polymer Engineering & Science, 45 (2005) 487-495.

[15] J.D. Liu, H.-J. Sue, Z.J. Thompson, F.S. Bates, M. Dettloff, G. Jacob, N. Verghese, H. Pham, Effect of crosslink density on fracture behavior of model epoxies containing block copolymer nanoparticles, Polymer, 50 (2009) 4683-4689.

[16] J.D. Ferry, Viscoelastic properties of polymers, John Wiley & Sons, 1980.

[17] R. Parthasarathy, A. Misra, J. Park, Q. Ye, P. Spencer, Diffusion coefficients of water and leachables in methacrylate-based crosslinked polymers using absorption experiments, Journal of Materials Science: Materials in Medicine, 23 (2012) 1157-1172.

[18] P.J. Flory, Principles of polymer chemistry, Cornell University Press, 1953.

[19] G.M. Geise, B.D. Freeman, D.R. Paul, Characterization of a novel sulfonated pentablock copolymer for desalination applications, Journal of Membrane Science, 24 (2010) 5815-5822.

[20] A.C. Sagle, H. Ju, B.D. Freeman, M.M. Sharma, PEG-based hydrogel membrane coatings, Polymer, 50 (2009) 756-766.

[21] G.M. Geise, L.P. Falcon, B.D. Freeman, D.R. Paul, Sodium chloride sorption in sulfonated polymers for membrane applications, Journal of Membrane Science, 423-424 (2012) 195-208.

[22] H.K. Lonsdale, U. Merten, R.L. Riley, Transport properties of cellulose acetate osmotic membranes, Journal of Applied Polymer Science, 9 (1965) 1341-1362.

[23] H. Yasuda, C.E. Lamaze, L.D. Ikenberry, Permeability of solutes through hydrated polymer membranes. Part I. Diffusion of sodium chloride, Die Makromolekulare Chemie, 118 (1968) 19-35.

[24] W. Pusch, Measurement techniques of transport through membranes, Desalination, 59 (1986) 105-199.

[25] P.N. Pintauro, D.N. Bennion, Mass transport of electrolytes in membranes. 1. Development of mathematical transport model, Industrial & Engineering Chemistry Fundamentals, 23 (1984) 230-234.

[26] J. Kamcev, E.-S. Jang, N. Yan, D.R. Paul, B.D. Freeman, Effect of ambient carbon dioxide on salt permeability and sorption measurements in ion-exchange membranes, Journal of Membrane Science, 479 (2015) 55-56.

[27] ASTM, Standard test method for ash in the analysis sample of coal and coke from coal, D3174-11 (2011).

[28] J. Kamcev, D.R. Paul, B.D. Freeman, Ion activity coefficients in ion exchange polymers: Applicability of Manning's counterion condensation theory, Macromolecules, 48 (2015) 8011-8024.

[29] T. Sata, Ion exchange membranes: preparation, characterization, modification and application, Royal Society of Chemistry, 2004.

[30] J. Kamcev, D.R. Paul, B.D. Freeman, Accounting for Frame of Reference and Thermodynamic Non-Idealities When Calculating Ion Diffusion Coefficients in Ion Exchange Membranes, Journal of Membrane Science, 537 (2017) 396-406.

[31] K.S. Pitzer, Thermodynamics of electrolytes. I. Theoretical basis and general equations, The Journal of Physical Chemistry, 77 (1973) 268-277.

[32] J. Kamcev, R. Sujanani, E.-S. Jang, N. Yan, N. Moe, D. Paul, B. Freeman, Salt concentration dependence of ionic conductivity in ion exchange membranes, In preparation, (2017).

Chapter 4: Water and Ion Sorption in a Series of Cross-linked AMPS/PEGDA Hydrogel Membranes[1]

4.1 INTRODUCTION

Water and energy are highly interrelated resources [1]. There is a great need to develop energy-efficient techniques to produce fresh water and generate sustainable energy [2]. Polymeric ion exchange membranes (IEMs) are used in water purification [e.g., electrodialysis (ED)] [3, 4] and energy generation [e.g., fuel cells, reverse electrodialysis (RED)] applications [5-9]. IEMs are also being explored for other membrane-based techniques, such as reverse osmosis (RO) [1, 10, 11], pressure-retarded osmosis (PRO) [12, 13], and membrane-assisted capacitive deionization (CDI) [14, 15]. Membrane performance (e.g., conductivity and permeability) in these applications is sensitive to membrane transport (water/ion sorption and diffusion) characteristics. However, much remains unknown about the influence of polymer membrane architecture on water and ion transport properties critical to high performance membranes [1].

IEMs often consist of a cross-linked hydrocarbon matrix to which ionizable acidic or basic groups are attached [16]. These charged functional groups can be introduced to the polymer backbone by, for example, copolymerizing functionalized monomers [16]. Strong acidic or basic groups (e.g., $-SO_3H$, $-R_3NH$) can solvate and ionize completely in contact with aqueous solutions [16]. To maintain electroneutrality, the charge on the functional groups (e.g., $-SO_3^-$, $-R_3N^+$) must be balanced by ions bearing an opposite charge,

---

[1] This chapter has been adapted from: Yan, N., Paul, D.R., Freeman, B.D., Water and ion sorption in a series of cross-linked AMPS/PEGDA hydrogel membranes (in preparation). Yan, N. made the major contributions to this chapter.

which are termed counter-ions. Ions bearing the same charge as the functional group are called co-ions. Negatively charged membranes are cation exchange membranes (CEMs), and positively charged membranes are anion exchange membranes (AEMs).

To quantify charge density in IEMs, ion exchange capacity (IEC), defined as milliequivalents of fixed charges based on dry polymer weight [meq/g (dry polymer)], can be readily computed from polymer composition [17]. However, the molar concentration of fixed charges or ions based on the volume of sorbed water [mol/L (water sorbed)] is the relevant charge density experienced by ions sorbing into IEMs [16-18]. In this study, IEC is used to label samples, and charge density is used to interpret ion sorption results.

An important feature of IEMs is co-ion exclusion [19-34]. When a water-equilibrated CEM is immersed in a dilute electrolyte solution (e.g., NaCl), a so-called Donnan potential builds up at the membrane/solution boundary, and it acts to retain counter-ions in the membrane and exclude co-ions in the solution from entering the membrane [16, 18, 34]. The Donnan potential is dependent on the counter-ion concentration difference between the membrane and solution phases [16]. As the external electrolyte solution concentration decreases or the membrane charge density increases, the Donnan potential and the co-ion exclusion effect become stronger [16, 17].

Water sorption is another important characteristic of IEMs and is highly correlated with ion transport [16, 35]. Typically, ions sorb into and transport across a membrane together with some water [36]. Membranes with higher water content generally have higher ion sorption and diffusion rates [37, 38].

Systematic studies of the influence of polymer structure and external electrolyte solution concentration on water and ion sorption are not widely available. Earlier studies

often focused on highly charged membranes having IEC values of 1-10 meq/g [9], which inhibits developing a complete fundamental understanding of water and ion sorption in charged materials, due to limited data for weakly charged IEMs (IEC < 1 meq/g).

Quantitative experimental co-ion sorption results typically deviate from theoretical predictions due to thermodynamic non-idealities in the membrane and solution phases [18, 23, 39, 40]. Ion activity coefficients in aqueous electrolyte solutions are well documented [41]. However, there is a lack of experimental or fundamental theoretical values of ion activity coefficients in IEMs [42, 43]. Measuring the content of water and ions in a membrane as a function of external electrolyte solution concentration allows computation of membrane ion activity coefficients [16]. In this study, analysis of the influence of IEC and external electrolyte solution concentration on membrane water uptake, fixed charge concentration, ion sorption, and ion activity coefficients will be discussed.

4.2 Results and Discussion

4.2.1 Hydrogel Synthesis

Both pre-polymerization mixtures and their resulting hydrogel films, following UV irradiation, were transparent, suggesting that the films were relatively homogeneous. PEGDA and AMPS have similar reactivity ratios, which favors formation of a random cross-linked network [70]. The gel fraction provides an estimate of the percentage of monomers not attached to the network. After five days of soaking in DI water, which was changed periodically, the sample film was dried and weighed. The mass of the dry film was about 99% of the combined mass of PEGDA and AMPS added for polymerization, indicating essentially complete monomer incorporation into the network [50, 51].

After photopolymerization, there could be 'dangling' cross-linker units with one double bond end attached to the network, and the other unable to reach an appropriate position for attachment to the network [60]. Such unreacted corsslinker ends cannot be detected by gel fraction measurements. In the FTIR spectra of the copolymers, the disappearance of double bonds indicates essentially complete acrylate group conversion [cf. Figure A.1 (a) and (b)]. Polymer structure was confirmed by the FTIR spectra and is independent of membrane thickness [cf. Figure A.1 (c) and (d)]. The T_gs of the copolymers determined by DSC (cf. Figure A.3) and DMA (cf. Figure A.4) were found to depend on the polymer composition (cf. Table A.1), and the T_gs of the component homopolymers obeyed the rule of mixtures (cf. Figure A.5) [31]. The DMA tan δ-temperature curves (cf. Figure A.4) of the copolymers always show a single peak, consistent with the samples not having substantial blocking.

4.2.2 Water Uptake

As shown in Figure 4.1 (a), water uptake increases by roughly a factor of 2 over the entire range of IEC values. An increase in the mass fraction of ionogenic groups in the polymer is often accompanied by a reduction in the degree of cross-linking (fewer cross-linkers) [1, 5, 32-37]. Table 3.2 and Table 4.1 summarizes basic properties of the polymers considered in this study, including dry polymer density, theoretical cross-link density, pure water uptake, and fixed charge concentration. As IEC (meq/g) increases from 0 to 1.93, the theoretical cross-link density, v_t, decreases by about 34% and the effective cross-link density, v_e, decreases by about 13%. The reduced cross-link density and introduction of more highly hydrophilic ionogenic groups both may contributed to the observed increase in water uptake as IEC increases [60].

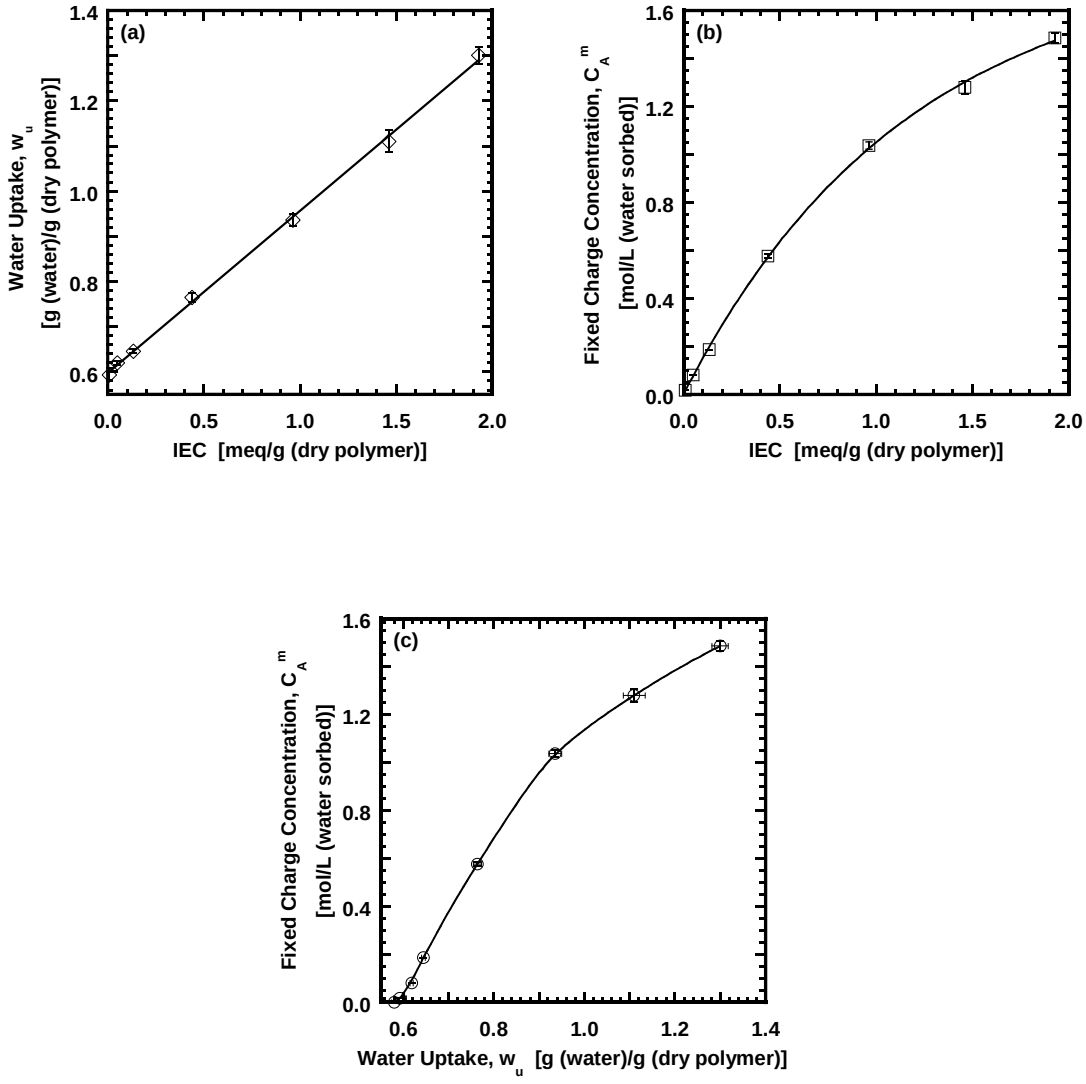

Figure 4.1 The dependence of: (a) water uptake on IEC, (b) fixed charge concentration on IEC, and (c) fixed charge concentration on water uptake.

Table 4.1 Properties of polymers prepared with PEGDA of n = 10.

IEC [a] [meq/g (dry polymer)]	ρ_p^H [b] [g/cm^3]	v_e [d] $\times 10^3$ [mol/cm^3]	w_u [e] [g (water)/g (dry polymer)]	$C_A^{m,w}$ [f] [mol/L (water sorbed)]	$C_{Na^+}^{m,w}$ [g] [mol/L (water sorbed)]
0	1.205 [c]	1.95 [c]	0.581 ± 0.006		
0.01	1.210	1.95	0.593 ± 0.014	(1.69 ± 0.04)×10^{-2}	(1.76 ± 0.05)×10^{-2}
0.05	1.212	1.95	0.619 ± 0.003	(8.40 ± 0.05)×10^{-2}	(8.49 ± 0.05)×10^{-2}
0.13	1.216	1.94	0.645 ± 0.004	0.208 ± 0.005	0.200 ± 0.020
0.44	1.229	1.93	0.764 ± 0.009	0.575 ± 0.007	0.578 ± 0.033
0.97	1.260	1.91	0.936 ± 0.014	1.031 ± 0.015	1.037 ± 0.017
1.46	1.282	1.89	1.110 ± 0.024	1.318 ± 0.029	1.281 ± 0.083
1.93	1.299	1.70	1.300 ± 0.018	1.485 ± 0.021	1.489 ± 0.029

[a] Theoretical IEC values are determined from polymer chemistry.
[b] The XL(AMPS-PEGDA) films are in acid form.
[c] The dry polymer density of the XLPEGDA film is consistent with literature values [38].
[d] The effective cross-linking density was estimated from DMA scans via Eqn. (3.2).
[e] The XL(AMPS-PEGDA) films are in sodium form.
[f] The fixed charge concentration was calculated from the theoretical IEC values and water uptake via Eqn. (2.9).
[g] The sorbed Na^+ concentration was measured in the hydrated films equilibrated in 0.01 M NaCl solution via Eqn. (3.7) and (3.8).

Fixed charge concentration, defined as the molar concentration of fixed charges per unit volume of sorbed water, depends on IEC and water uptake as shown in Eqn. (3.9). Figure 4.1 (b) and (c) show C_A^m increases as IEC and water uptake increase. However, the increase in C_A^m is non-linear especially in more highly charged samples, which can be ascribed to the water dilution effect discussed above.

Figure 4.2 shows the influence of external NaCl concentration on water uptake and fixed charge concentration. As shown in Figure 4.2 (a), the membranes sorb less water when equilibrated in solutions of higher external NaCl concentration, C_S^S, due to osmotic de-swelling [4, 5, 32, 34, 37, 39]. When a charged membrane is equilibrated in water,

the osmotic pressure inside it is higher than that in the solution due to the presence of fixed charges on the polymer backbone [40]. When C_S^s is 1 M, the osmotic pressure difference between the charged membrane and solution phases is lowered, resulting in less water uptake. Due to osmotic de-swelling, the fixed charge concentration, based on the volume of sorbed water, increases as C_S^s increases from 0 to 1 M [cf. Figure 4.2 (b)]. But this increase in C_A^m is not substantial until C_S^s reaches ~ 0.1 M and higher because the osmotic de-swelling effect is more significant when the external electrolyte solution is concentrated [8]. The extent of de-swelling increases as IEC increases. For instance, when a water-equilibriated uncharged membrane is immersed in 1 M NaCl solution, 5% of the water in the membrane desorbs into the solution. The high osmotic pressure outside the membrane (~ 47 bar) provides some indication of the decrease in water activity as shown in Figure 4.2 (c) [41]. This de-swelling effect is greater for more highly charged membranes (e.g., 20% for the IEC = 1.93 meq/g membrane). The increase in the extent of de-swelling with IEC is qualitatively consistent with the theoretical prediction (i.e., swelling model) for charged membranes [30, 40].

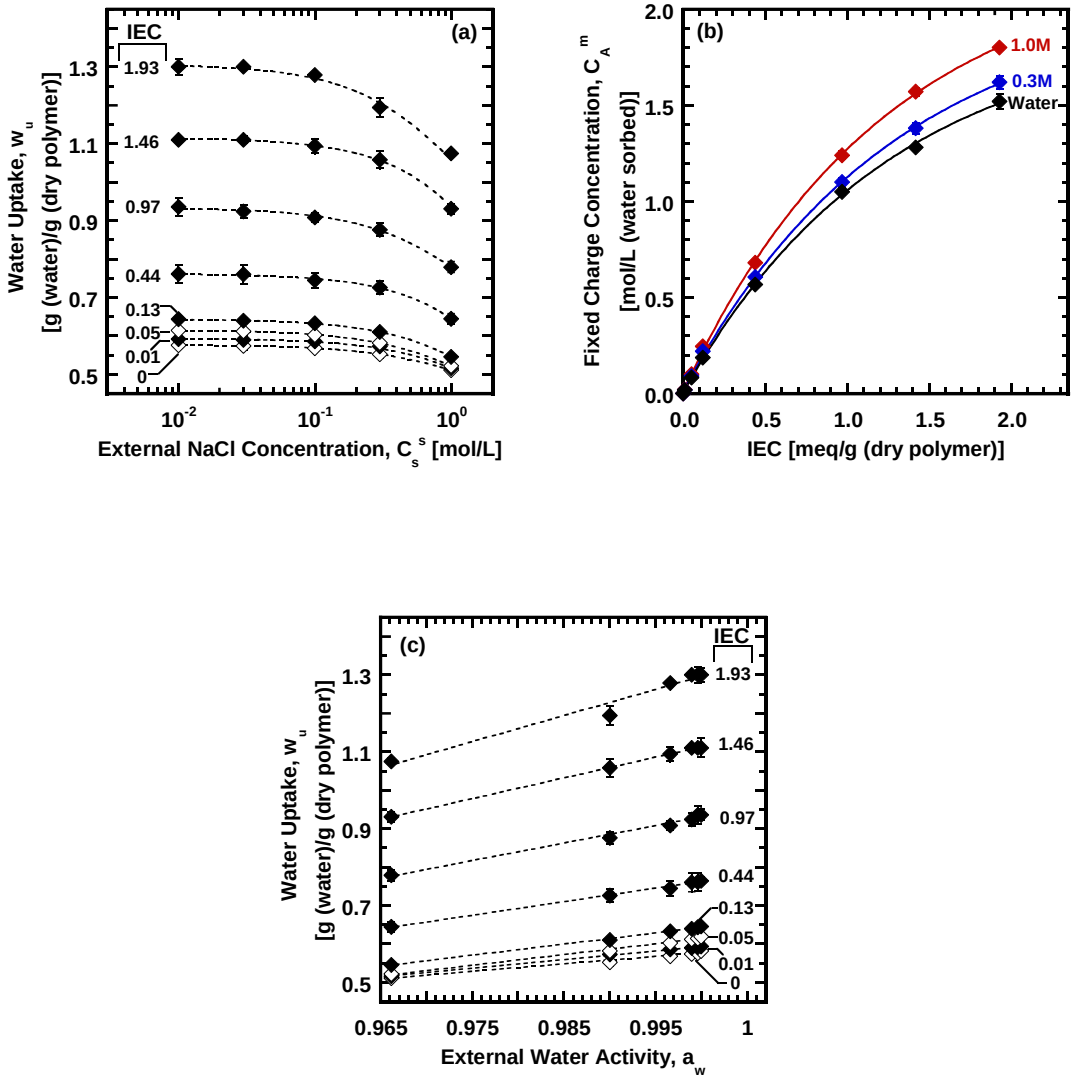

Figure 4.2 The influence of (a) external NaCl concentration on water uptake and (b) IEC on fixed charge concentration at fixed C_S^S (i.e., 1 M, 0.3 M, and water).

4.2.3 Ion Sorption

Figure 4.3 (a) presents the concentrations of sodium (Na^+) and chloride ions (Cl^-) in selected membranes as a function of external NaCl concentration, C_s^s. The dashed line labeled "0" represents ion concentrations in an uncharged XLPEGDA membrane. To maintain electroneutrality, there are equal numbers of Na^+ and Cl^- ions dissolved in the uncharged membrane, as expected [cf. Eqn. (2.9)]. As C_s^s increases from 0.01 to 1 M, concentrations of Na^+ and Cl^- increase by approximately two orders of magnitude in the uncharged membrane, as expected from Eqn. (8) [42]. The resulting salt sorption coefficients, K_s, determined via Eqn. (2.7) and (2.10) are shown in Figure 4 (b).

Ion sorption behavior in charged membranes is qualitatively different from that in neutral membranes [42]. As shown in Figure 4.3 (a), Cl^- (co-ion) concentrations in CEMs are lower than in the uncharged membrane, especially when C_s^s is low (e.g., 0.01 M). In contrast, more Na^+ (counter-ion) sorbs into CEMs than in the uncharged membrane. This distinction between Na^+ and Cl^- sorption stems primarily from the electrostatic interaction between ions and fixed charge groups on the polymer backbone. Fixed charges must be neutralized by Na^+, and they act to inhibit Cl^- sorption via Donnan exclusion [1]. To maintain electroneutrality, any Cl^- ions present in the membrane must be accompanied by an equal number of Na^+ ions. Therefore, the total concentration of Na^+ is larger than that of Cl^- by an amount equal to the fixed charge concentration [i.e., $C_{Na^+}^{m,w} = C_{\mathrm{A}}^{m,w} + C_{Cl^-}^{m,w}$ in Eqn. (2.4)] [1].

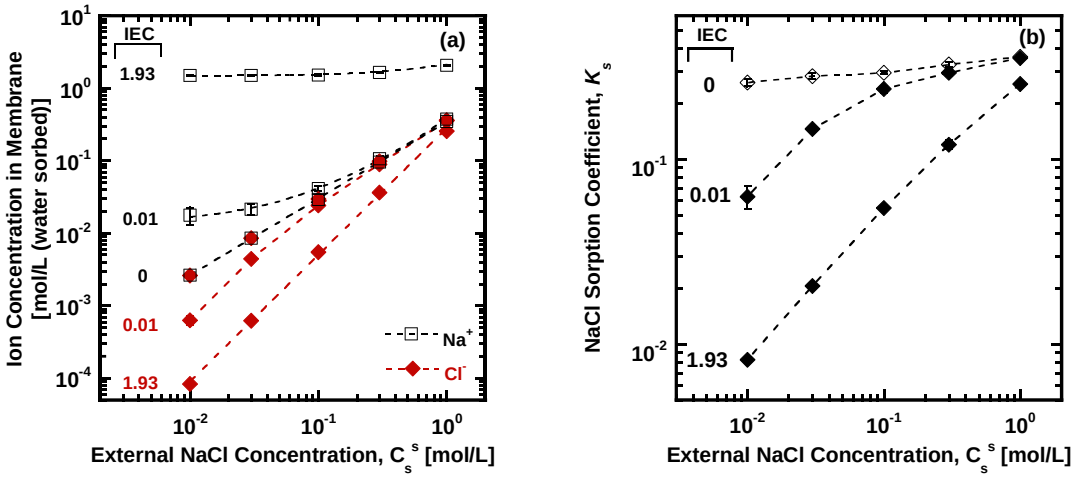

Figure 4.3 The dependence of the (a) sorbed concentrations of Na^+, $C_{Na^+}^{m,w}$, and Cl^-, $C_{Cl^-}^{m,w}$, and (b) salt sorption coefficient on external NaCl concentration in swollen membranes with selected IEC values. The measured K_s of the uncharged membrane at 0.1 M is 0.304 $\pm$ 0.059 (mol/L [water sorbed])/(mol/L [solution]), which is in agreement with previously reported data (e.g., 0.3~0.4 at 0.1M) [38].

Unlike uncharged membranes, Na^+ and Cl^- concentrations in highly charged membranes behave rather differently as C_S^S increases [3, 42]. As shown in Figure 4.3 (a), the Na^+ concentration for the most highly charged membrane considered (IEC value of 1.93 meq/g) is fairly constant, within experimental uncertainty, in dilute NaCl solutions (C_S^S < 0.1 M). This independence of Na^+ sorption on C_S^S is ascribed to two phenomena [3, 42]. First, the sorbed Cl^- concentration at low C_S^S values is orders of magnitude less than the fixed charge concentration, due to strong Donnan exclusion at low C_S^S. The sorbed Na^+ concentration is practically equal to the fixed charge concentration (i.e.,

$C_{Na^+}^{m,w} = C_{\mathrm{A}}^{m,w} + C_{Cl^-}^{m,w} \approx C_{\mathrm{A}}^{m,w}$). Second, the osmotic de-swelling effect is not significant in this dilute region (C_s^s < 0.1 M), so the amount of water sorbed in the membrane is almost constant. Therefore, $C_A^{m,w}$, based on the volume of sorbed water, is essentially independent of C_s^s in the dilute NaCl range (i.e., 0.01-0.1 M), as is the sorbed Na^+ concentration [3, 42]. However, the sorbed Na^+ concentration in the membrane with IEC = 1.93 meq/g increases by about 40% as C_s^s increases from 0.1 to 1 M. This increase is partly due to the increase in $C_A^{m,w}$ stemming from more significant osmotic de-swelling. In addition, the sorbed Cl^- concentration becomes closer to $C_{\mathrm{A}}^{m,w}$ (about one order of magnitude difference at 1 M). Therefore, the total concentration of sorbed Na^+ ends up increasing at higher NaCl concentrations (i.e., 0.1-1 M). About 55% of this increase is caused by osmotic de-swelling, and 45% is caused by the increase in sorbed Cl^- concentration.

In stark contrast, the sorbed Cl^- concentration in the membrane with IEC = 1.93 meq/g increases by more than three orders of magnitude over the entire C_s^s range [cf. Figure 4.3 (a)]. The increase in co-ion (Cl^-) concentration with C_s^s is qualitatively consistent with the Donnan prediction in Eqn. (2.5) [3, 42]. When C_s^s is high (e.g., 1 M), the electrolyte concentration difference between the membrane and solution phases decreases, resulting in a smaller Donnan potential and greater co-ion sorption in the membrane [1].

When C_s^s becomes higher than $C_{\mathrm{A}}^{m,w}$ [e.g., $C_s^s >$ 0.1 M for membrane with IEC = 0.01 meq/g and $C_{\mathrm{A}}^{m,w}$ = 0.02 mol/L in Figure 4.3 (a)], the Donnan potential is significantly reduced, and the ionogenic groups on the polymer backbone exclude co-ions to a much weaker extent than when C_s^s is lower than $C_{\mathrm{A}}^{m,w}$ [42]. Consequently, the

concentration of sorbed Cl^- becomes closer to and even much higher than $C_A^{m,w}$ (i.e., $C_{Cl^-}^{m,w} \gg C_{\mathrm{A}}^{m,w}$). In the later case, the majority of sorbed Na^+ ions are balancing Cl^- ions instead of fixed charges on the polymer backbone (i.e., $C_{Na^+}^{m,w} = C_{\mathrm{A}}^{m,w} + C_{Cl^-}^{m,w} \approx C_{Cl^-}^{m,w}$). For example, as shown in Figure 4.3 (a), C_{A}^{m} of the membrane with IEC = 0.01 meq/L is about 0.02 mol/L (water sorbed). When C_s^s is 0.3 M or higher, the sorbed Cl^- concentration is more than one order of magnitude higher than $C_{\mathrm{A}}^{m,w}$. In this regime ($C_s^s \gg C_{\mathrm{A}}^{m,w}$), charged membranes sorb ions in a similar fashion as that of an uncharged membrane (e.g., for IEC value of 0.01 meq/g, $C_s^s \geq$ 0.3 M).

Figure 4.4 (a) and (b) present the influence of fixed charge concentration on ion sorption at two fixed external NaCl concentrations (0.01 M and 1.0 M). As shown in Figure 4.4 (a), when a relatively small number of charged groups are introduced to the uncharged membrane [i.e., $C_A^{m,w}$ values of 0.02-0.1 mol/L (water sorbed)], the sorbed Cl^- concentration decreases by more than one order of magnitude, so even low levels of fixed charges can exclude co-ions significantly. Ideal Donnan theory predicts a continuous decrease in co-ion sorption as $C_A^{m,w}$ increases, if all other parameters (e.g., C_s^s and Γ) are held constant [cf. Eqn. (2.5)]. However, as $C_A^{m,w}$ increased to about 1-1.5 mol/L (water sorbed), Cl^- sorption decreased to a plateau (within experimental uncertainties), which is not consistent with ideal Donnan theory [i.e., $\Gamma = 1$ in Eqn. (2.5)]. Based on our previous studies, this qualitative deviation from ideal Donnan theory is likely due to the ion activity coefficient ratio, Γ, [defined by Eqn. (2.6)] not being equal to one [1, 3, 29]. Salt mean activity coefficients in aqueous solution deviate from 1 (i.e., $\sqrt{\gamma_+^s \gamma_-^s} = 1$ in infinite dilution) as solution concentration increases (i.e., $\sqrt{\gamma_+^s \gamma_-^s} =$ 0.66 at 1 M for NaCl)

[43]. A quantitative comparison between the experimental and theoretical ion sorption results will be discussed below.

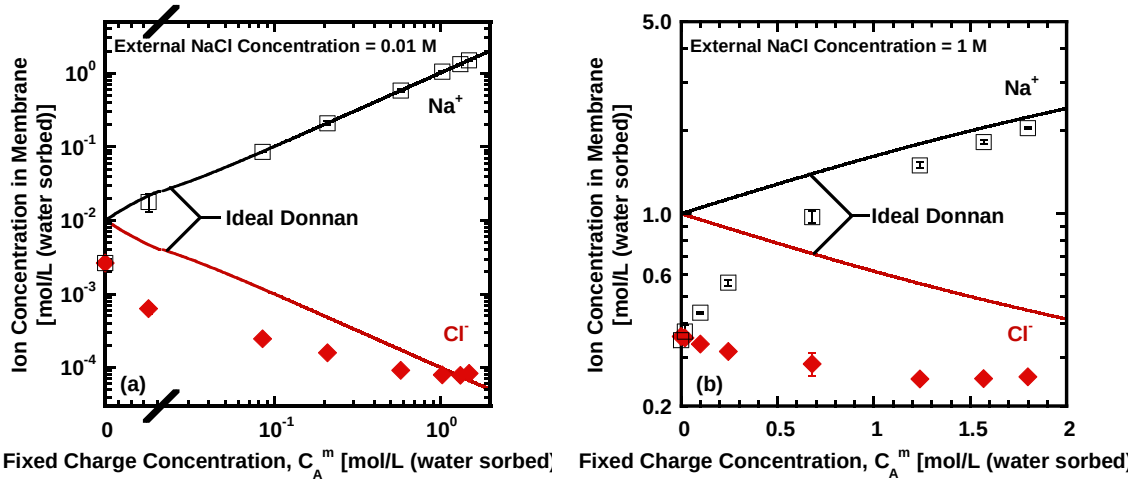

Figure 4.4 The influence of fixed charge concentration on sorbed Na^+ concentration $C_{Na^+}^{m,w}$, and Cl^- concentration, $C_{Cl^-}^{m,w}$, in XL(AMPS-PEGDA) copolymers at a fixed external NaCl concentration of (a) 0.01 M and (b) 1.0 M. An axis break mark was shown in (a) to separate the linear and logarithm scales.

4.2.4 Ion Activity Coefficients in the Membranes

Ion activity coefficients in the membrane, $\gamma_+^m\gamma_-^m$, can be calculated from the experimentally measured ion sorption results, and the mean salt activity coefficients in aqueous solution based on Pitzer model, using Eqn. (2.3). Figure 4.5 (a) shows that $\gamma_+^m\gamma_-^m$ changes by a factor of 20 with changes in $C_A^{m,w}$ at a C_s^s value of 0.01 M. For example, $\gamma_+^m\gamma_-^m$ values in the most highly charged membranes are less than 1 (i.e., $\sqrt{\gamma_+^s\gamma_-^s} =$ 1 in infinite dilution), which is ascribed to strong electrostatic attraction between fixed charges on the polymer backbone and counter-ions (i.e., polyion-ion interaction) [3].

In these membranes, the amount of counter-ions is several orders of magnitude higher than the same ions outside the membrane. To maintain thermodynamic equilibrium between the membrane and solution phases, $\gamma_{\pm}^{m}\gamma_{-}^{m}$ in more highly charged membranes must be low to account for the high concentration of counter-ions [3]. In contrast, $\gamma_{\pm}^{m}\gamma_{-}^{m}$ in the uncharged membrane is as high as 12, which is about 15 times than that in solution (i.e., $\gamma_{\pm}^{s}\gamma_{-}^{s} = 0.8$ at 0.01 M for NaCl). In this case, ion concentrations in the uncharged membrane are much lower than in the external solution, because ions prefer staying in aqueous solution than in the uncharged membrane due to certain polymer-ion and/or water-ion interactions. As a result, $\gamma_{\pm}^{m}\gamma_{-}^{m}$ values must be > 1 in the uncharged membrane.

Figure 4.5 (b) presents Γ calculated from solution mean ion activity coefficients, $\gamma_{\pm}^{s}$, taken from the literature [43] and experimental ion activity coefficients in the membrane, $\gamma_{\pm}^{m}\gamma_{-}^{m}$ [cf. Eqn. (2.3)] [41]. The ideal Donnan theory value of $\Gamma = 1$ is also shown. Γ increases by about 20 times over the entire range of $C_A^{m,w}$ [0-1.5 mol/L (water sorbed)] considered. The large change in Γ further confirms that the original assumptions regarding ion activity coefficients in the ideal Donnan theory are not accurate except by serendipity [i.e., the membrane with an IEC value of 1.46 meq/g in Figure 4.5 (b)] [3, 44].

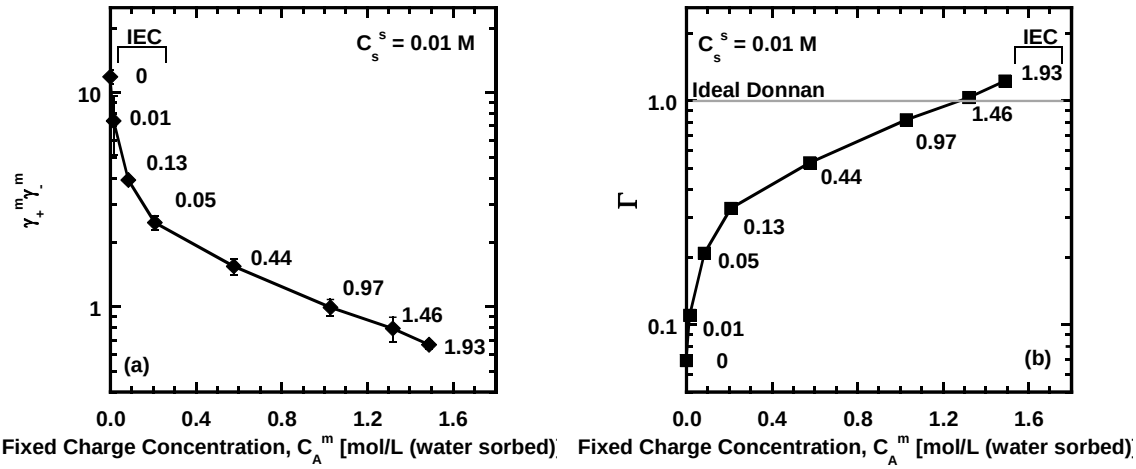

Figure 4.5 The influence of fixed charge concentration on: (a) ion activity coefficients in the membrane, $\gamma_+^m\gamma_-^m$, obtained via Eqn. (3) and (b) ion activity coefficient ratio, Γ .

Figure 4.6 (a) presents the dependence of $\gamma_+^m\gamma_-^m$ on C_s^s at various IEC values. Due to the affinity between fixed charges on the polymer backbone and counter-ions discussed above, $\gamma_+^m\gamma_-^m$ in more highly charged membranes (e.g., IEC values of 0.97-1.93 meq/g) is near or less than 1. $\gamma_+^m\gamma_-^m$ in these membranes increase slightly as C_s^s increases, which is similar to the trend observed in previous studies [3-5, 8, 11, 12, 17, 18, 25, 34, 45, 46]. Some authors ascribed this deviation from ideal Donnan theory to impurities in the polymer matrix [45, 47], polymer heterogeneity [15, 48], and/or the inaccuracy in measuring ion concentrations at low salt concentrations caused by the incomplete separation of the membrane and solution phases [15, 49]. However, this same qualitative behavior has been found in polyelectrolyte solutions where ion activity coefficients were able to be experimentally determined [3, 50, 51]. A new approach,

based on Manning's counter-ion condensation theory from the field of polyelectrolytes [52], can describe the behavior of ion activity coefficients in highly charged membranes [i.e., $C_A^{m,w}$ values of > 2 mol/L (water sorbed)] reasonably well [3, 29]. In contrast, as shown in Figure 4.6 (a), $\gamma_+^m\gamma_-^m$ values in the uncharged membrane decrease as C_s^s increases. A similar behavior is also observed in aqueous solution (i.e., $\gamma_+^s\gamma_-^s$ decreases from 0.8 to 0.4 over the same range of NaCl) due to mobile ion-ion interactions [41, 53]. For weakly charged membranes (e.g., IEC values of 0.01-0.13 meq/g), $\gamma_+^m\gamma_-^m$ behaves in a qualitatively consistent manner between the two limits (i.e., $\gamma_+^m\gamma_-^m$ in uncharged and highly charged membranes).

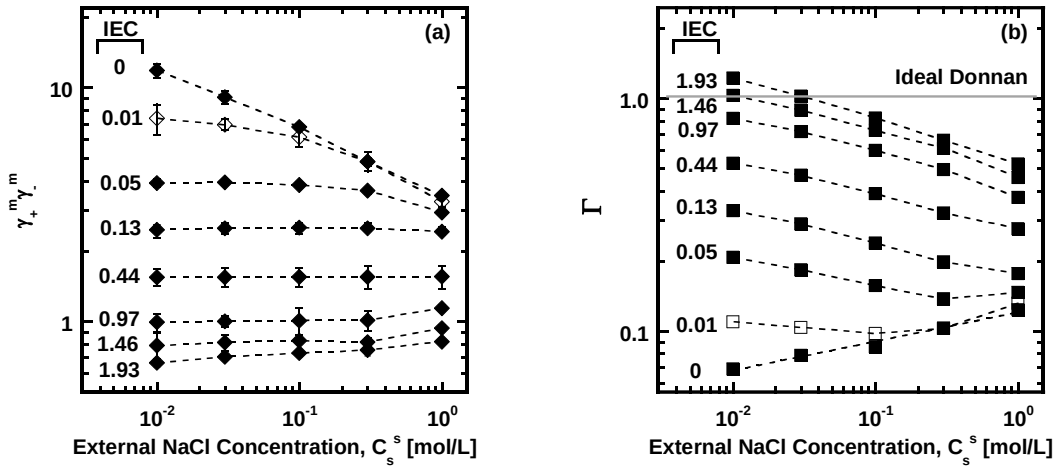

Figure 4.6 The dependence of (a) ion activity coefficients in the membrane, $\gamma_+^m\gamma_-^m$, and (b) Γ, on external NaCl concentration varies with IEC values.

The wide-spread in Γ values shown in Figure 4.6 (b) suggest that the non-idealities in the membrane and solution phases, which are subject to a variety of factors

(e.g., fixed charge concentration, external electrolyte solution concentration), dictate the deviation of Γ from 1 (ideal Donnan theory), resulting in the discrepancy between the experimental and theoretical ion sorption results. However, Manning's couner-ion condensation theory can only predict ion activity coefficients for highly charged membranes, wherein the electrostatic interactions between fixed charges and counter-ions (i.e., polyion-ion) are dominant and ion activity coefficients are less than 1 [3]. There is no comparable, verified model available to describe ion activity coefficients in uncharged and weakly charged membranes, such as those considered in this study. Therefore, there is a strong need for a fundamental, theoretical model to account for electrostatic and other interactions (e.g., polymer-ion, water-ion, ion-ion etc.) in the membrane to describe ion activity coefficients in a wide range of membranes (i.e., ranging from uncharged to highly charged).

4.3 CONCLUSIONS

Water and individual ion (Na^+ and Cl^-) sorption have been studied in a series of uncharged and sulfonated cross-linked hydrogel membranes to investigate the influence of membrane properties (e.g., ion exchange capacity, degree of cross-linking) and external electrolyte solution concentration on water and ion sorption. Water sorption increases as the concentration of charged monomers in the polymers increases. Fixed charge concentration based on the volume of sorbed water increases non-linearly with increasing water uptake and IEC due to charge dilution effects. Fixed charge concentration generally increases as external NaCl concentration increases due to lower water content caused by osmotic de-swelling. There are always equal numbers of sorbed Na^+ and Cl^- ions present in the uncharged membrane. The sorbed Na^+ concentration in a CEM is

significantly larger than the sorbed Cl^- concentration when the external NaCl concentration is low relative to the fixed charge concentration. However, when the external NaCl concentration is higher than the fixed charge concentration, Donnan exclusion can be overwhelmed, and the charged membrane sorbs similar amounts of Na^+ and Cl^- ions, akin to the behavior in an uncharged membrane. Cl^- sorption decreases significantly even in the membrane with the lowest charge density considered in this study, suggesting that a low level of fixed charges can exclude co-ions measurably. Ideal Donnan theory typically cannot qualitatively or quantitatively describe experimental ion sorption isotherms due to the non-idealities of ion activity coefficients in the membrane and solution phases. Ion activity coefficients in the uncharged membrane were much larger than 1, while those in the most highly charged membranes considered were less than 1.

4.4 REFERENCES

[1] F. Helfferich, Ion Exchange, McGraw-Hill Book Co., Inc., New York, 1962.

[2] A.A. Zagorodni, Ion exchange materials: properties and applications, Elsevier, 2006.

[3] J. Kamcev, D.R. Paul, B.D. Freeman, Ion activity coefficients in ion exchange polymers: Applicability of Manning's counterion condensation theory, Macromolecules, 48 (2015) 8011-8024.

[4] W. Bauman, J. Eichhorn, Fundamental properties of a synthetic cation exchange resin, Journal of the American Chemical Society, 69 (1947) 2830-2836.

[5] C. Davies, G. Yeoman, Swelling equilibria with some cation exchange resins, Transactions of the Faraday Society, 49 (1953) 968-974.

[6] G. Boyd, J. Schubert, A. Adamson, The exchange adsorption of ions from aqueous solutions by organic zeolites. I. Ion-exchange equilibria, Journal of the American Chemical Society, 69 (1947) 2818-2829.

[7] H.P. Gregor, A general thermodynamic theory of ion exchange processes, Journal of the American Chemical Society, 70 (1948) 1293-1293.

[8] H.P. Gregor, Gibbs-Donnan equilibria in ion exchange resin systems, Journal of the American Chemical Society, 73 (1951) 642-650.

[9] E. Glueckauf, A theoretical treatment of cation exchangers. I. The prediction of equilibrium constants from osmotic data, Proceedings of the Royal Society of London. Series A. Mathematical and Physical Sciences, 214 (1952) 207-225.

[10] J. Duncan, A theoretical treatment of cation exchangers. II. Equilibria between an ion exchanger and an aqueous solution with a common cation, 214 (1952) 344-355.

[11] J.S. Mackie, P. Meares, The sorption of electrolytes by a cation-exchange resin membrane, Proceedings of the Royal Society of London. Series A. Mathematical and Physical Sciences, 232 (1955) 485-498.

[12] F. Nelson, K.A. Kraus, Anion-exchange studies. XXIII. Activity coefficients of some electrolytes in the resin phase, Journal of the American Chemical Society, 80 (1958) 4154-4161.

[13] G. Hills, P. Jacobs, N. Lakshminarayanaiah, Membrane potentials I. The theory of the emf of cells containing ion-exchange membranes, in: Proceedings of the Royal Society of London A: Mathematical, Physical and Engineering Sciences, The Royal Society, 1961, pp. 246-256.

[14] F. Tye, Absorption of electrolytes by ion-exchange materials, Journal of the Chemical Society (Resumed), (1961) 4784-4789.

[15] E. Glueckauf, R.E. Watts, The Donnan law and its application to ion exchanger polymers, Proceedings of the Royal Society of London. Series A. Mathematical and Physical Sciences, 268 (1962) 339-349.

[16] G. Boyd, K. Bunzl, The Donnan equilibrium in cross-linked polystyrene cation and anion exchangers, Journal of the American Chemical Society, 89 (1967) 1776-1780.

[17] H.P. Gregor, M.H. Gottlieb, Studies on ion exchange resins. VIII. Activity coefficients of diffusible ions in various cation-exchange resins, Journal of the American Chemical Society, 75 (1953) 3539-3543.

[18] M.H. Gottlieb, H.P. Gregor, Studies on ion exchange resins. XI. Activity coefficients of diffusible ions in a strong base anion-exchange resin, Journal of the American Chemical Society, 76 (1954) 4639-4641.

[19] F.G. Donnan, The theory of membrane equilibria, Chemical Reviews, 1 (1924) 73-90.

[20] J.S. Mackie, P. Meares, The diffusion of electrolytes in a cation-exchange resin membrane. I. Theoretical, Proceedings of the Royal Society of London A: Mathematical, Physical and Engineering Sciences, 232 (1955) 498-509.

[21] J.G. Wijmans, R.W. Baker, The solution-diffusion model: a review, Journal of Membrane Science, 107 (1995) 1-21.

[22] H. Yasuda, C.E. Lamaze, L.D. Ikenberry, Permeability of solutes through hydrated polymer membranes. Part I. Diffusion of sodium chloride, Die Makromolekulare Chemie, 118 (1968) 19-35.

[23] G.M. Geise, H.B.Park, A.C. Sagle, B.D. Freeman, J.E. McGrath, Water peameability and water/salt selectivity tradeoff in polymers for desalination, Journal of Membrane Science, 369 (2011) 130-138.

[24] T. Xu, Ion exchange membranes: state of their development and perspective, Journal of Membrane Science, 263 (2005) 1-29.

[25] R.L. Gustafson, Donnan equilibria in polystyrenesulfonate gels, The Journal of Physical Chemistry, 70 (1966) 957-961.

[26] N. Lakshminarayanaisah, Transport phenomena in membranes, Academic Press, New York and London, 1969.

[27] K.S. Pitzer, A thermodynamic model for aqueous solutions of liquid-like density, Reviews in Mineralogy and Geochemistry, 17 (1987) 46.

[28] K. Dorfner, Ion exchangers: properties and applications, Ann Arbor Science Publishers Inc., 1972.

[29] M. Galizia, F.M. Benedetti, D.R. Paul, B.D. Freeman, Monovalent and divalent ion sorption in a cation exchange membrane based on cross-linked poly (p-styrene sulfonate-co-divinylbenzene), Journal of Membrane Science, 535 (2017) 132-142.

[30] P.J. Flory, Principles of polymer chemistry, Cornell University Press, 1953.

[31] J.R. Fried, Polymer science and technology, Pearson Education, 2014.

[32] H.P. Gregor, F. Gutoff, J. Bregman, Studies on ion-exchange resins. II. Volumes of various cation-exchange resin particles, Journal of Colloid Science, 6 (1951) 245-270.

[33] B.R. Sundheim, M.H. Waxman, H.P. Gregor, Studies on ion exchange resins. VII. Water vapor sorption by cross-linked polystyrenesulfonic acid resins, The Journal of Physical Chemistry, 57 (1953) 974-978.

[34] K. Pepper, D. Reichenberg, D. Hale, Properties of ion-exchange resins in relation to their structure. Part IV. Swelling and shrinkage of sulphonated polystyrenes of different cross-linking, Journal of the Chemical Society (Resumed), (1952) 3129-3136.

[35] O. Bonner, A selectivity scale for some monovalent cations on Dowex 50, The Journal of Physical Chemistry, 58 (1954) 318-320.

[36] S. Lindenbaum, C. Jumper, G. Boyd, Selectivity coefficient measurements with variable capacity cation and anion exchangers, The Journal of Physical Chemistry, 63 (1959) 1924-1929.

[37] C. Calmon, Application of volume characteristics of sulfonated polystyrene resins as a tool in analytical chemistry, Analytical Chemistry, 25 (1953) 490-492.

[38] H. Ju, A.C. Sagle, B.D. Freeman, J.I. Mardel, A.J. Hill, Characterization of sodium chloride and water transport in crosslinked poly (ethylene oxide) hydrogels, Journal of Membrane Science, 358 (2010) 131-141.

[39] C. Calmon, Application of volume change characteristics of sulfonated low cross-linked styrene resin, Analytical Chemistry, 24 (1952) 1456-1458.

[40] L. Brannon-Peppas, R.S. Harland, Absorbent polymer technology, Elsevier, 2012.

[41] K.S. Pitzer, G. Mayorga, Thermodynamics of electrolytes. II. Activity and osmotic coefficients for strong electrolytes with one or both ions univalent, The Journal of Physical Chemistry, 77 (1973) 2300-2308.

[42] G.M. Geise, L.P. Falcon, B.D. Freeman, D.R. Paul, Sodium chloride sorption in sulfonated polymers for membrane applications, Journal of Membrane Science, 423-424 (2012) 195-208.

[43] K.S. Pitzer, Thermodynamics of electrolytes. I. Theoretical basis and general equations, The Journal of Physical Chemistry, 77 (1973) 268-277.

[44] J. Kamcev, M. Galizia, F.M. Benedetti, E.-S. Jang, D.R. Paul, B.D. Freeman, G.S. Manning, Partitioning of mobile ions between ion exchange polymers and aqueous salt solutions: importance of counter-ion condensation, Physical Chemistry Chemical Physics, 18 (2016) 6021-6031.

[45] K.A. Kraus, G.E. Moore, Anion exchange studies. V. Adsorption of hydrochloric acid by a strong base anion exchanger, Journal of the American Chemical Society, 75 (1953) 1457-1460.

[46] N. Lakshminarayanaiah, Activity coefficients of small ions in ion-exchange resins, Journal of Polymer Science Part A: General Papers, 1 (1963) 139-149.

[47] D.H. Freeman, V.C. Patel, T.M. Buchanan, Electrolyte uptake equilibria with low cross-linked ion-exchange resins, The Journal of Physical Chemistry, 69 (1965) 1477-1481.

[48] E. Glueckauf, R. Watts, Non-uniformity of cross-linking in ion-exchange polymers, Nature, 191 (1961) 904-905.

[49] D.H. Freeman, Electrolyte uptake by ion-exchange resin, The Journal of Physical Chemistry, 64 (1960) 1048-1051.

[50] M. Nagasawa, I. Kagawa, Colligative properties of polyelectrolyte solutions. IV. Activity coefficient of sodium ion, Journal of Polymer Science, 25 (1957) 61-76.

[51] M. Nagasawa, M. Izumi, I. Kagawa, Colligative properties of polyelectrolyte solutions. V. Activity coefficients of counter-and by-ions, Journal of Polymer Science, 37 (1959) 375-383.

[52] G.S. Manning, Limiting laws and counterion condensation in polyelectrolyte solutions I. Colligative properties, The Journal of Chemical Physics, 51 (1969) 924-933.

[53] R.A. Robinson, R.H. Stokes, Electrolyte solutions, Courier Corporation, 2002.

Chapter 5: Influence of Fixed Charge Concentration and Water Uptake on Ion Sorption in AMPS/PEGDA Membranes[2]

5.1 INTRODUCTION

Ion exchange membranes (IEMs) are used in applications such as electrodialysis (ED), reverse electrodialysis (RED), and fuel cells [1-7]. They are often cross-linked polymers with fixed charge groups (e.g., $-SO_3^-$, $-R_3N^+$) attached to the polymer network [8]. These ionogenic groups selectively permit passage of counterions (i.e., ions bearing the opposite charge as that of the fixed charge groups) over co-ions (i.e., ions bearing the same charge as that of the fixed charge groups) [9-11]. This property is critical to the efficacy of many technologies relying on IEMs [12-14].

Ion sorption and transport through IEMs in contact with electrolyte solutions (e.g., NaCl) can be profoundly influenced by electrostatic interactions between ions and fixed charges [15, 16]. The presence of fixed charges causes an unequal distribution of cations and anions in the membrane via the "Donnan potential" at the membrane/solution interface [8, 17]. This potential acts to keep counterions in the membrane and co-ions in solution (i.e., "Donnan exclusion") [8]. To maintain electroneutrality in the polymer membrane, sorbed counterions must electrically balance the fixed charges on the polymer backbone and any sorbed co-ions in the membrane. Highly selective membranes should sorb many counterions and few co-ions. This effect can be influenced by changing membrane fixed charge concentration [18, 19]. The concentration of fixed charges, $C_A^{m,w}$ (mols of fixed charges per liter of sorbed water), is quantified as follows [8]:

---

[2] This chapter has been adapted from: Yan, N., Kamcev, J., Galizia, M., Jang E.S., Paul, D.R., Freeman, B.D., Influence of fixed charge concentration and wataer uptake on ion sorption in AMPS/PEGDA membranes (in preparation). Yan, N. made the major contributions to this chapter.

$$C_A^{m,w} = 1000 \times \frac{IEC \cdot \rho_w}{w_u} \tag{5.1}$$

where IEC represents ion exchange capacity, expressed as milliequivalents (i.e., mmol) of fixed charges per gram of dry polymer (meq/g), w_u is polymer water uptake (gram of sorbed water per gram of dry polymer), and ρ_w is the density of water [8]. To enhance membrane selectivity for counterions over co-ions, many studies focus on increasing polymer IEC [20, 21]. However, addition of fixed charges in the polymer often increases polymer hydrophilicity [20, 21]. Consequently, increases in IEC are often accompanied by increases in polymer water uptake, and both factors influence C_A^m (and, in turn, ion sorption), but in opposite directions [4, 14]. Establishing structure/property relations in IEMs to guide the preparation of new materials with desired ion sorption and transport properties is typically frustrated by this inability to vary a single variable (e.g., water uptake or $C_A^{m,w}$) at a time to generate better fundamental understanding of ion behavior in IEMs.

To overcome this lack of knowledge in the literature, this study is focused on isolating the effects of fixed charge concentration and water uptake on ion sorption in a series of negatively charged membranes [i.e., cation exchange membranes (CEMs)]. Membrane fixed charge concentration and water uptake were controlled independently by varying the concentration of charged monomer in the pre-polymerization solution and the cross-linker length. As controls, uncharged polymers with different levels of water uptake were prepared with various cross-linker lengths. Finally, experimental ion sorption and ion activity coefficients in membranes equilibrated with NaCl solutions were interpreted using the recently developed Donnan/Manning model [16, 22, 23].

5.2 RESULTS AND DISCUSSIONS

5.2.1 Membrane Water Content and Fixed Charged Concentration

As shown in Table 3.2, at a given n value, an increase in AMPS content (i.e., an increase in IEC) is accompanied by higher water uptake in the polymer (cf. Figure B.1) [33]. At constant IEC, water uptake also increases with increasing PEGDA length (i.e., increasing n value) (cf. Figure B.1). Thus, polymer water uptake can be tuned by adjusting both the AMPS content and PEGDA length [24, 25].

In swollen ion exchange membranes, fixed charge concentration can have a strong influence on ion sorption [16, 18, 22]. In this study, membrane fixed charge concentration increases with increasing AMPS content (i.e., IEC increases) and decreasing PEGDA length (i.e., water uptake decreases. Thus, AMPS content and PEGDA length can be used to control fixed charge concentration. Appropriate values of these two parameters can yield polymers that have either the same water uptake value, but different fixed charge concentrations, or the same fixed charge concentration, but different water uptake values.

5.2.2 Uncharged Membranes

Equilibrium water uptake values measured in aqueous NaCl solutions are shown in Figure 5.1 (a). As cross-linker length decreases, w_u decreases, presumably due to higher cross-link density and the more hydrophobic nature of cross-linkers with fewer ethylene oxide units [24]. All measured values are recorded in the Appendix. For all membranes, w_u decreases slightly (~10%) as external NaCl concentration increases from 0.01 to 1.0 M due to a decrease in water activity as C_s^s increases [15].

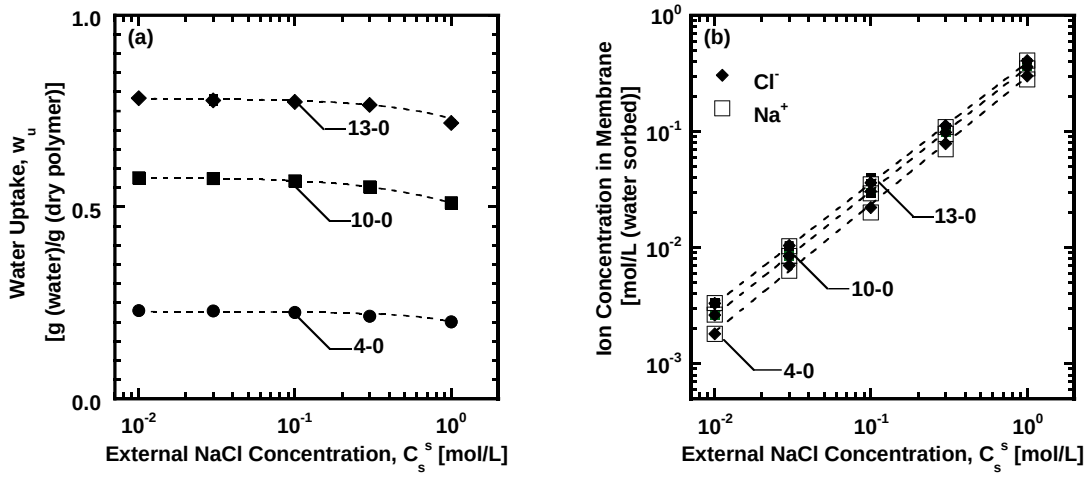

Figure 5.1 The influence of external NaCl concentration on: (a) water uptake and (b) sorbed ion concentrations in uncharged membranes with different cross-linker lengths (n = 13, 10, and 4).

Sodium and chloride concentrations in uncharged membranes are presented in Figure 5.1 (b). To maintain electroneutrality, equal numbers of Na^+ and Cl^- ions sorb into the membrane over the entire range of C_s^s values considered [15]. At fixed C_s^s, less hydrated membranes sorb fewer ions than more hydrated membranes, which is consistent with previous results [24]. Such behavior was ascribed to a polymer ion-excluding effect, which is more pronounced when less water is present in the membrane [24].

To facilitate a quantitative comparison between experimental and theoretical results, experimental salt sorption coefficients were computed from the measured ion concentrations. In uncharged membranes, K_s is related to ion activity coefficients as follows [when $C_A^{m,w}$ = 0 in Eqn. (2.7)] [15]:

$$K_s^w = \left[\frac{\left(\gamma_\pm^s\right)^2}{\gamma_+^m \gamma_-^m}\right]^{\frac{1}{2}} \tag{5.2}$$

In Manning's counterion condensation theory, membrane ion activity coefficients, $\gamma_+^m \gamma_-^m$, would be equal to one for an uncharged membrane, so K_s^w would be equal to $\gamma_\pm^s$ according to Eqn. (5.2). However, the experimental K_s values as shown in Figure 5.2 (a) are well below the $\gamma_\pm^s$ values, which were calculated using the Pitzer model [26]. The discrepancy between the experimental and theoretical results is ascribed to non-ideal ion behavior in the membrane phase (i.e., $\gamma_+^m \gamma_-^m \neq 1$). Additionally, the trends in K_s and $\gamma_\pm^s$ with C_s^s are opposite to each other, $\gamma_\pm^s$ decreases with increasing C_s^s while K_s increases with increasing C_s^s. These trends in K_s^w cannot be captured by Manning's model, which was designed for use with highly charged polyelectrolytes.

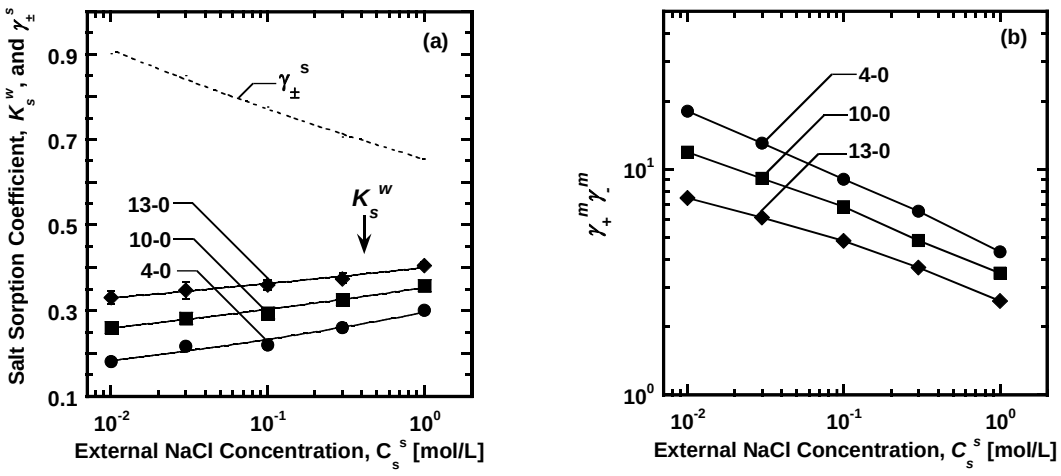

Figure 5.2 Salt sorption coefficient (a) and membrane ion activity coefficients (b) in uncharged membranes with varied water uptake values as a function of external NaCl concentration. For reference, the solution ion activity coefficients, $\gamma_\pm^s$, is shown as a dashed line in Figure 5.2 (a).

Figure 5.2 (b) presents membrane ion activity coefficients using experimentally determined K_s^w and estimated $\gamma_\pm^s$ (i.e., Pitzer model) values via Eqn. (5.2) [27]. $\gamma_+^m\gamma_-^m$ values in uncharged membranes decrease with increasing C_s^s, qualitatively similar to the trend of $\gamma_\pm^s$ observed in Figure 5.2 (a). However, the very high values of $\gamma_+^m\gamma_-^m$, exceeding 10 in some cases, indicating that ions have a strong affinity to remain in the solution than in the membrane phase [24, 28, 29]. Presumably, ions in solution are rejected by membranes due to dielectric exclusion [30], and the electrostatic charges of ions are less stabilized in the membrane than in solution [4], since the dielectric constant of the membrane phase is much smaller than that of the solution phase [4]. Additionally, a competition between sorbed ions and ethylene oxide (EO) groups on the polymer

backbone for water in the polymers may also contribute to the large $\gamma_{\pm}^{m}\gamma_{-}^{m}$ values. More specifically, EO groups and water molecules interact strongly, and approximately 2~3 water molecules are tightly bound to each EO group in XLPEGDA [31], potentially resulting in less "free" water in the polymer for ion solvation. For example, 1000 g of dry sample 13-0 contains 18 mols of EO groups, which can tightly bond with 30~50 mols of water molecules. As shown in Table 3.2, the same amount of dry polymer only sorbs 44 mols of water molecules, according to its water uptake value. Thus, almost all water present in sample 13-0 is "associated" with the EO groups, and similar results are obtained for the other uncharged samples studied, suggesting these uncharged polymers are not thermodynamically favorable environments for ions to dissolve in relative to solution [28, 29]. Consequently, $\gamma_{\pm}^{m}\gamma_{-}^{m}$ values are higher and salt sorption coefficients are lower in materials with lower water uptake, reflecting the more thermodynamically unfavorable environment for ions dissolved in less hydrated samples, where the interactions between polymer segments, water, and ions are more pronounced [28, 29].

5.2.3 Charged Membranes at Constant Fixed Charge Concentration

To prepare samples with constant fixed charge concentration (C_A^m), high IEC membranes must be cross-linked with longer PEGDA chains to increase water sorption. Thus, three membranes (13-1.40, 10-0.97, and 4-0.44) with similar C_A^m values (i.e., measured in DI water) but different pure water uptake values were synthesized (cf. Table 2). As shown in Figure 5.3 (a), membrane water uptake increases as IEC and n increase, due to simultaneously enhanced polymer hydrophilicity and reduced cross-link density (cf. Table 3.2). w_u decreases with increasing external NaCl concentration due to osmotic de-swelling [4, 32]. However, the extent of de-swelling varies in each sample. The most

hydrated membrane de-swells twice as much as the least hydrated one, consistent with previous results [8, 32, 33].

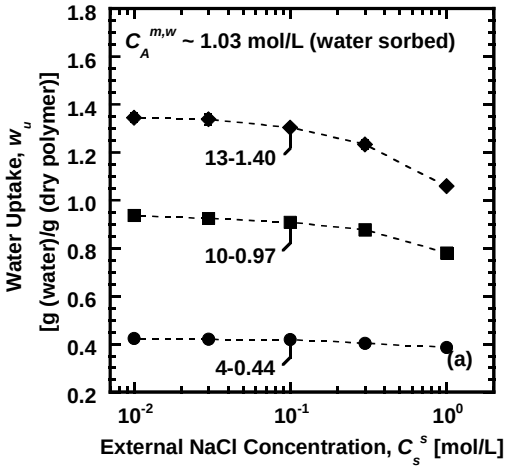

Figure 5.3 The dependence of water uptake on external NaCl concentration in swollen XL(AMPS-PEGDA) membranes having similar fixed charge concentration. The $C_A^{m,w}$ value represents the fixed charge concentration of the sample equilibrated in DI water.

Membrane Na^+ (counterion) and Cl^- (co-ion) concentrations are presented in Figure 5.4 as a function of external NaCl concentration. In Figure 5.4 (a), at low NaCl concentrations (C_S^S < 0.1 M), the sorbed Na^+ concentration is relatively constant and equal in all three samples, within the experimental uncertainty. These observations have two bases. First, the sorbed Cl^- concentration is negligible compared to that of fixed charges in this range of C_S^S due to Donnan exclusion [cf. Figure 5.4 (b)]. Thus, the sorbed Na^+ concentration is approximately equal to the fixed charge concentration ($C_+^{m,\mathrm{w}} = C_\mathrm{A}^{m,w} + C_-^{m,w} \approx C_\mathrm{A}^{m,w}$), and this series of materials was designed to have fixed $C_\mathrm{A}^{m,w}$. Second,

the volume of sorbed water changes little with C_s^s at low C_s^s due to weak osmotic de-swelling [cf. Figure 5.3 (a)], so $C_{\mathrm{A}}^{m,w}$ is essentially constant in this dilute range [16]. As a result, $C_+^{m,w}$ is practically constant and equal in all samples when C_s^s < 0.1 M, which was the desired outcome for these samples. At high NaCl concentrations (C_s^s > 0.1 M), $C_-^{m,w}$ increases due to weaker Donnan exclusion [cf. Figure 5.4 (b)]. $C_{\mathrm{A}}^{m,w}$ also increases due to the reduction in sorbed water caused by stronger osmotic de-swelling at high C_s^s [cf. Figure 5.3 (a)] [16]. Consequently, $C_+^{m,w}$ increases as C_s^s increases above 0.1 M. About 60% of this increase is due to osmotic de-swelling, and 40% is caused by the increase in $C_-^{m,w}$, consistent with results reported elsewhere [32]. The $C_+^{m,w}$ values in the three membranes tend to deviate from each other when C_s^s > 0.1 M. This departure is primarily due to the different levels of osmotic de-swelling in these three membranes, resulting in small differences in $C_{\mathrm{A}}^{m,w}$ values at high C_s^s values. For example, For example, the membrane that de-swells the most (i.e., 13-1.40) has the largest increase in $C_{\mathrm{A}}^{m,w}$ with increasing C_s^s and exhibits the highest $C_+^{m,w}$ value at C_s^s = 1 M (cf. Appendix B).

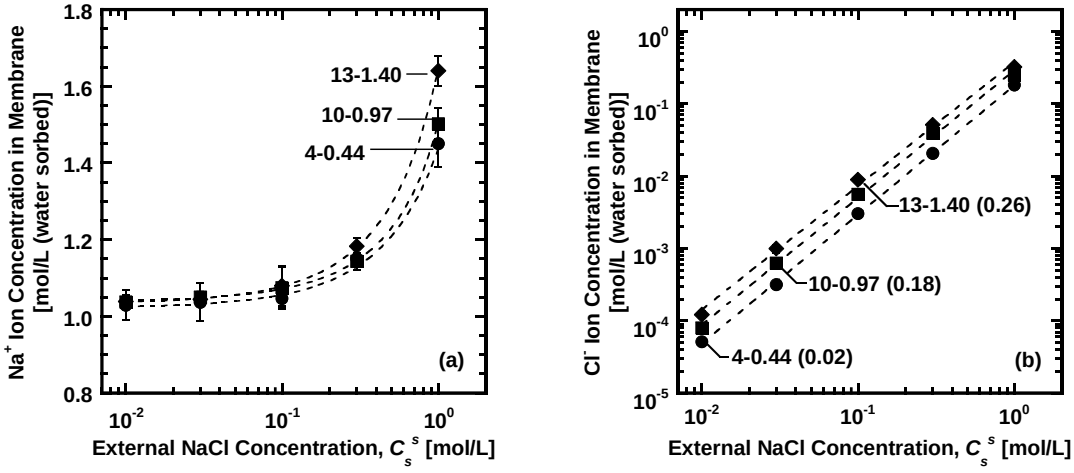

Figure 5.4 Sorbed concentrations of: (a) Na^+, $C_+^{m,w}$, and (b) Cl^-, $C_-^{m,w}$, in swollen XL(AMPS-PEGDA) membranes with a constant fixed charge concentration value of 1.03 mol/L (sorbed water) measured in DI water. Values of the Manning parameters, ξ, are shown in parentheses in Figure 5.4 (b).

Figure 5.4 (b) shows the sorbed Cl^- concentration as a function of external NaCl concentration in membranes having similar fixed charge concentrations. Numerical results of C_+^m and $C_-^{m,\mathrm{w}}$ are recorded in the Appendix. Based on ideal Donnan theory [i.e., $\frac{(\gamma_\pm^s)^2}{\gamma_+^m\gamma_-^m}=1$ in Eqn. (2.5)], membranes having the same $C_{\mathrm{A}}^{m,w}$ value should sorb the same amount of co-ions at fixed C_s^s [34]. In contrast, experimental $C_-^{m,w}$ values in the three membranes are somewhat different, due to differences in the level of non-idealities in the various membranes [22].

Like the uncharged membranes, charged membranes (13-1.40, 10-0.97, and 4-0.44) with constant fixed charge concentration have varied water uptake values (cf. Table 5.1). The dependence of experimental K_s and $\gamma_+^m\gamma_-^m$ values on polymer water uptake is

shown in Figure 5.5 (a) and (b). Experimental K_s values were determined from Eqn. (2.7), and experimental $\gamma_+^m \gamma_-^m$ values were computed from Eqn. (2.2). The Manning parameter, ξ, was calculated based on Eqn. (2.12). As w_u decreases, experimental K_s values decrease and $\gamma_+^m \gamma_-^m$ values increase, similar to the effect of water uptake on salt sorption coefficients and ion activity coefficients observed in uncharged membranes (cf. Figure 5.2). Experimental $\gamma_+^m \gamma_-^m$ values in membranes with lower w_u values are larger than one, suggesting ions are thermodynamically less favored to sorb into the membrane than to remain in the external solution. The high ion activity coefficient values are qualitatively similar to those observed in uncharged membranes. Thus, thermodynamic non-idealities in less hydrated, charged membranes are probably strongly influenced by interactions such as polymer segment-water-ion interactions, as demonstrated in the uncharged membranes.

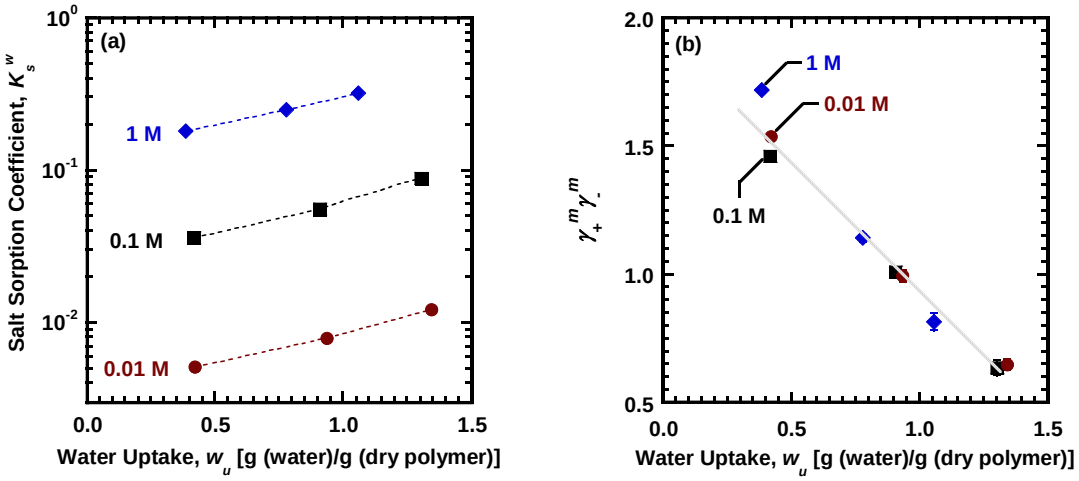

Figure 5.5 The dependence of: (a) salt sorption coefficient and (b) membrane ion activity coefficients on water uptake in swollen XL(AMPS-PEGDA) membranes with similar fixed charge concentration at selected external NaCl concentrations of 0.01, 0.1, and 1 M. The dashed lines were drawn to guide the eye. The membrane fixed charge concentration measured in DI water was about 1.03 mol/L (water sorbed).

For membranes (13-1.40, 10-0.97, and 4-0.44) with similar $C_A^{m,w}$ values, the decrease in water uptake value is accompanied by a decrease in the value of Manning parameter, ξ, which was calculated using Eqn. (2.12). Estimated values for the average distance between fixed charges, b, dielectric constant in the swollen membranes, ε, and the Bjerrum length, λ_B, are recorded in Table 5.1. Among these membranes, the variation in ε (and, therefore, λ_B) is relatively small compared to that of b, so the variation in b among the samples contributes most to the change in ξ [18, 35].

Table 5.1 Computed values for b, ε, λ_B and ξ in the membranes.

Sample	b [Å] [a]	ε [a]	λ_B [Å] [b]	ξ [b]
13-0.33	206.8	48	11.8	0.06
13-1.40	39.4	54	10.3	0.26
10-0.97	60.0	51	10.9	0.18
4-0.44	657	35	15.8	0.02
4-2.18	21.3	49	11.4	0.53

[a] b and ε were estimated based on polymer chemistry and water sorption results, as shown in the Appendix. [b] λ_B and ξ were determined from Eqn. (2.12).

To facilitate understanding effect of ξ on ion activity coefficients and salt sorption coefficients, charged membranes are set to be equilibrated with relatively dilute NaCl solutions, $\gamma_+^m\gamma_-^m$ in (2.13) can be written as follows (as $\frac{C_s^s}{C_A^{m,w}} \to 0$):

$$\gamma_+^m\gamma_-^m = e^{-\xi} \tag{5.3}$$

where $\gamma_+^m\gamma_-^m$ depends only on ξ and should decrease with increasing ξ, presumably due to more favorable interactions between fixed charges and ions because the fixed charges are closer to each other along the polymer chain. Then, K_s in Eqn. (2.14) can be written as follows (as $\frac{C_s^s}{C_A^{m,w}} \to 0$):

$$K_s^w = \frac{C_s^s\left(\gamma_\pm^s\right)^2}{C_A^{m,w}}e^{\xi} \tag{5.4}$$

Thus, K_s^w should increase with increasing ξ at fixed $C_A^{m,w}$ and low C_s^s values, since ions are thermodynamically more favored to stay in membranes having high ξ values [cf. Eqn. (5.3)].

To quantitatively compare experimental and theoretical results estimated by the Donnan/Manning model, Figure 5.6 (a) and (b) present the influence of ξ on experimental salt sorption coefficients and ion activity coefficients in membranes with constant $C_A^{m,w}$ value equilibrated with NaCl solutions of fixed concentrations. Theoretical predictions for K_s^w and $\gamma_+^m \gamma_-^m$ were calculated via Eqn. (5.4) and (5.3), respectively. As ξ increases, experimental K_s^w values increase and $\gamma_+^m \gamma_-^m$ values decrease, qualitatively consistent with the model predictions. Within the experimental uncertainty, the experimental K_s^w and $\gamma_+^m \gamma_-^m$ values can be reasonably described by the theoretical predictions for membranes with higher ξ values (or membranes with higher w_u values), suggesting thermodynamic non-idealities in these membranes are governed by favorable electrostatic interactions between fixed charges and ions, as captured by Manning's model.

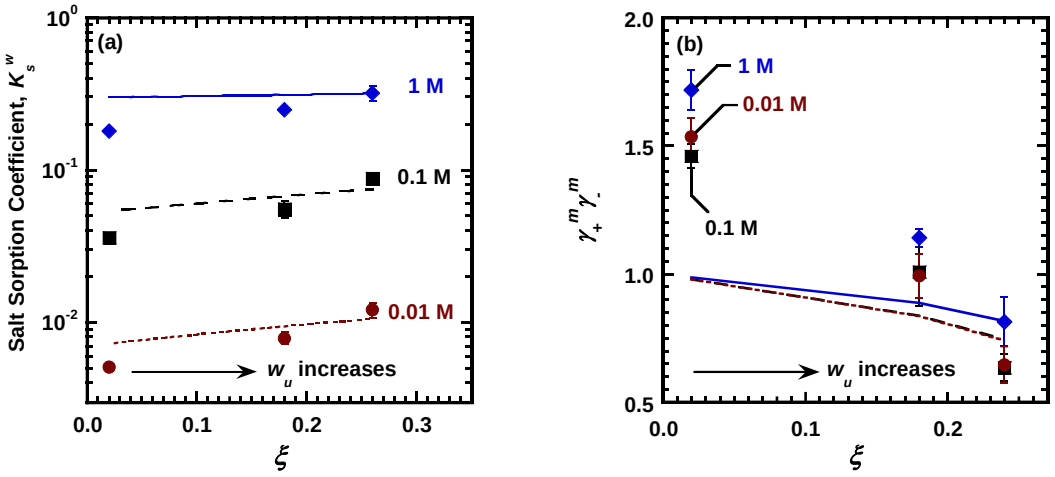

Figure 5.6 The dependence of: (a) salt sorption coefficient and (b) membrane ion activity coefficients on ξ in swollen XL(AMPS-PEGDA) membranes with constant fixed charge concentration at selected external NaCl concentrations of 0.01, 0.1, and 1 M. All symbols represent experimentally determined results. The lines denote the Donnan/Manning model predictions: ⎯ is 1 M, - - is 0.1 M, and ····· is 0.01 M. The membrane fixed charge concentration measured in DI water was about 1.03 mol/L (water sorbed).

However, as ξ decreases (w_u also decreases), the experimental K_s^w values become lower and $\gamma_+^m \gamma_-^m$ values become higher than the theoretical values. As shown in Figure 5.6 (a), the model underestimates co-ion exclusion in the sample with the lowest ξ value (i.e., the least hydrated sample), since the model lines are higher than the symbols. In Figure 5.6 (b), the experimental $\gamma_+^m \gamma_-^m$ values are higher than the theoretically expected values by 50-70% for this ample. Such differences between the experimental and theoretical results suggest that additional interactions such as polymer segment-water-ion interactions, beyond the electrostatic interactions included in Manning's model, contribute to thermodynamic non-idealities in this sample.

As shown in Figure 5.7, the experimental and theoretical K_s^w and $\gamma_+^m\gamma_-^m$ data are plotted as a function of external NaCl concentration. In Figure 5.7 (a) and (b), within experimental uncertainty, the experimental K_s^w and $\gamma_+^m\gamma_-^m$ values can be reasonably described by the theoretical predictions (i.e., no adjustable parameters) for the most hydrated sample (i.e., the sample with the highest ξ value, 13-1.40), similar to results reported elsewhere [16, 18, 22, 36]. In Figure 5.7 (c) and (d), the quantitative agreement between the model predictions and experimental K_s^w and $\gamma_+^m\gamma_-^m$ values for the least hydrated sample (i.e., the sample with the lowest ξ value, 4-0.44) is poor, likely due to thermodynamic non-idealities contributed by unfavorable interactions between polymer segments, water, and ions in such material and not simply governed by electrostatics.

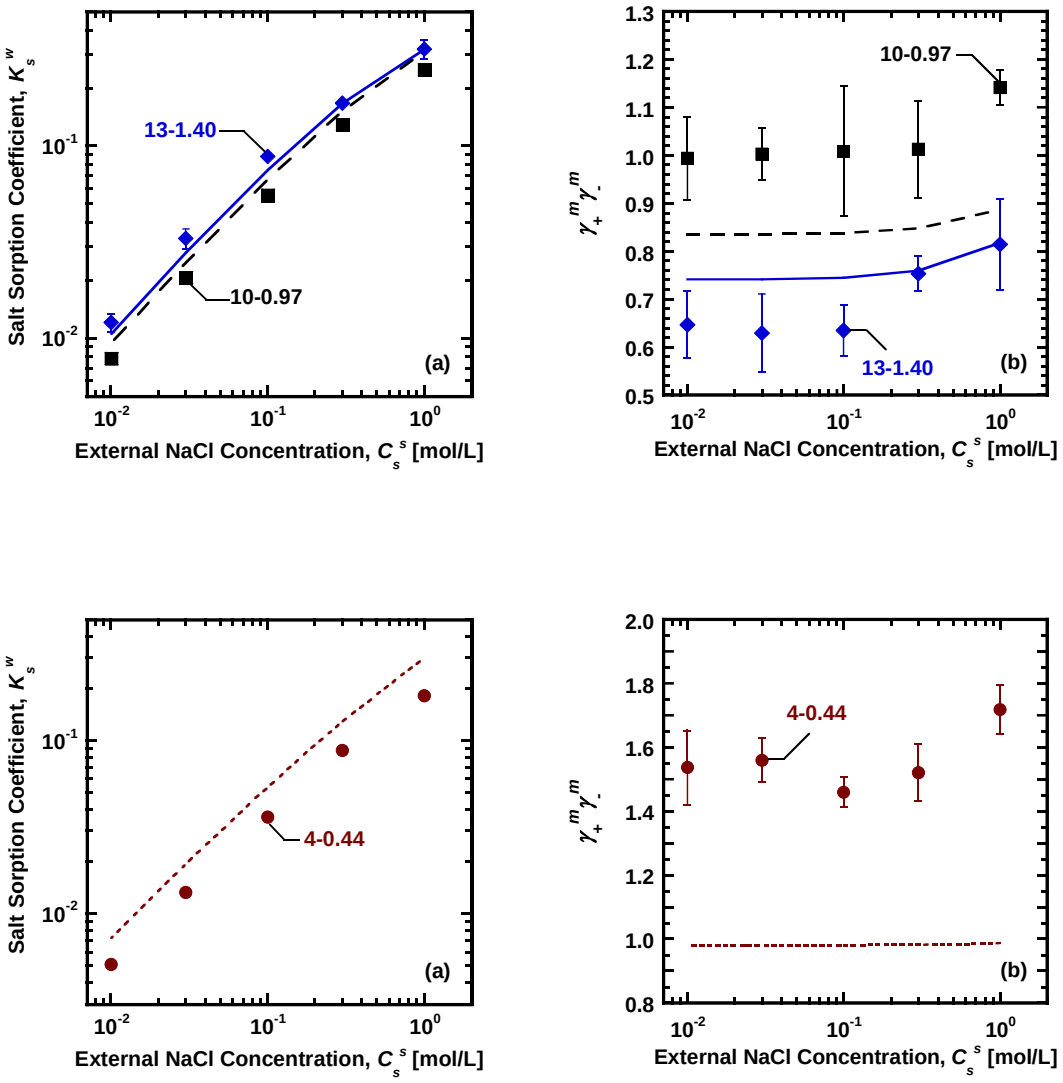

Figure 5.7 Salt sorption coefficient (a) and ion activity coefficients (b) in swollen XL(AMPS-PEGDA) membranes with similar fixed charge concentration. All symbols represent experimentally determined results. The lines indicate the theoretical predictions by the Donnan-Manning model [Eqs. (2.13) and (2.14)]: ⎯ is sample 13-1.40, - - is sample 10-0.97, and ····· is sample 4-0.44. The membrane fixed charge concentration measured in DI water was about 1.03 mol/L (water sorbed).

5.2.4 Charged Membranes at Constant Water Uptake

As described earlier, water uptake in charged membranes increases with increasing IEC and PEGDA chain length (i.e., n). To maintain constant polymer water uptake, membranes with high IEC must be cross-linked with shorter, more hydrophobic PEGDA segments. In this way, samples 4-2.18, 10-0.97, and 13-0.33 were prepared having similar water uptake values but different fixed charge concentrations [cf. Table 3.2].

Figure 5.8 presents membrane water uptake as a function of external NaCl concentration. All membranes exhibit very similar water uptake values over the entire range of C_s^s, within the experimental uncertainty. As shown in Figure 5.8, w_u decreases by ~15% as C_s^s increases due to osmotic de-swelling, the extent of which is similar in all three membranes.

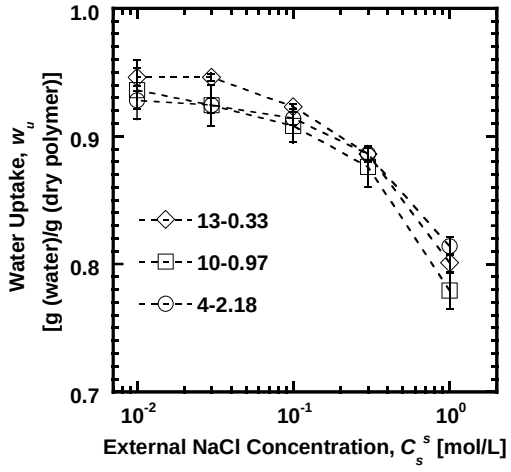

Figure 5.8 The dependence of water uptake on external NaCl concentration in swollen XL(AMPS-PEGDA) membranes having varied fixed charge concentrations but similar pure water uptake value of about 0.94 g (water)/g (dry polymer).

Figure 5.9 presents the sorbed Na^+ and Cl^- concentrations in these membranes. In Figure 5.9 (a), as $C_A^{m,w}$ increases, the sorbed Na^+ concentration increases because, except at high C_s^s, most of the Na^+ ions in each sample are balancing fixed charges on the polymer backbone, as described earlier [16]. In Figure 5.9 (b), the sorbed Cl^- concentration decreases as $C_A^{m,w}$ increases, which qualitatively follows ideal Donnan theory [i.e., Eqn. (2.5)] [18]. Numerical values of $C_+^{m,w}$ and C_-^m are shown in the Appendix.

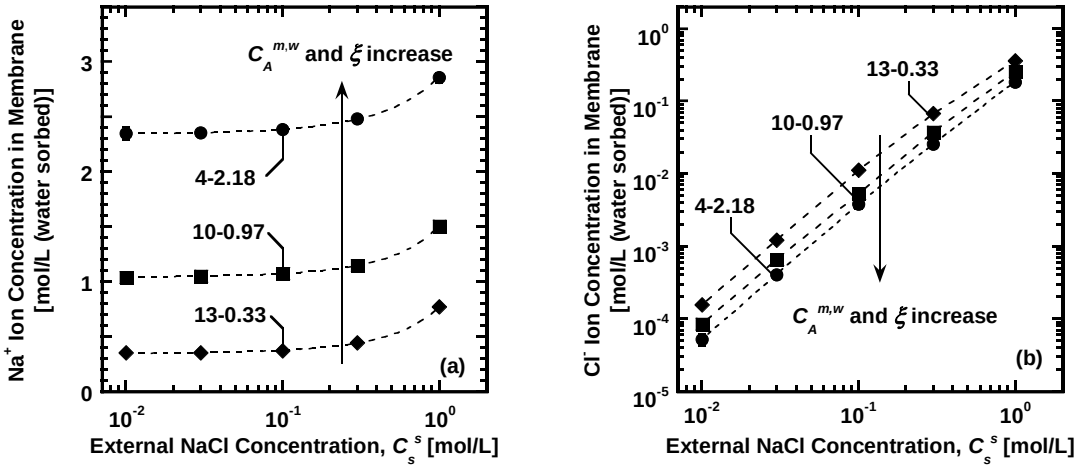

Figure 5.9 The dependence of: (a) sorbed Na^+ ion concentration and (b) sorbed Cl^- ion concentration on external NaCl concentration in swollen XL(AMPS-PEGDA) membranes with similar pure water uptake value of about 0.94 g (water)/g (dry polymer).

Samples with similar water uptake (4-2.18, 10-0.97, and 13-0.33) have concomitantly increased fixed charge concentration and ξ values (cf. Table 5.1), similar to prior studies [18]. To compare experimental results and theoretical predictions, experimental $\gamma_+^m\gamma_-^m$ and K_s values were calculated using Eqn. (2.3) and (2.7), and

theoretical predictions for $\gamma_+^m\gamma_-^m$ and K_s^w were computed via Eqn. (2.13) and (2.14), respectively. K_s^w and $\gamma_+^m\gamma_-^m$ values are presented in Figure 5.10 as a function of ξ. As ξ increases ($C_{\mathrm{A}}^{m,w}$ also increases), experimental $\gamma_+^m\gamma_-^m$ values decrease, qualitatively consistent with predictions from Eqn. (2.20). Based on Eqn. (2.21), K_s should decrease with increasing $C_{\mathrm{A}}^{m,w}$ due to stronger Donnan exclusion and increase with increasing ξ due to more favorable interactions between fixed charges and ions, if C_s^s is kept constant. As shown in Figure 5.10 (a), K_s^w decreases as $C_{\mathrm{A}}^{m,w}$ and ξ increase simultaneously, suggesting the decrease in K_s^w is predominantly due to stronger co-ion suppression at higher $C_{\mathrm{A}}^{m,w}$ values. That is, the level of increase in K_s^w caused by increasing ξ is not sufficient to offset the reduction in K_s^w caused by increasing $C_{\mathrm{A}}^{m,w}$, at least for the samples considered in this study. Deviations between the experimental and theoretical K_s^w and $\gamma_+^m\gamma_-^m$ values are more evident in membranes with the smaller ξ value (i.e., the less highly charged membranes), and $\gamma_+^m\gamma_-^m$ values are larger than one in these materials, similar to the cases observed in less hydrated films. This discrepancy could also be ascribed to thermodynamic non-idealities resulting from unfavorable non-electrostatic interactions between polymer segments, water, and ions that are not captured by Manning's counterion condensation theory.

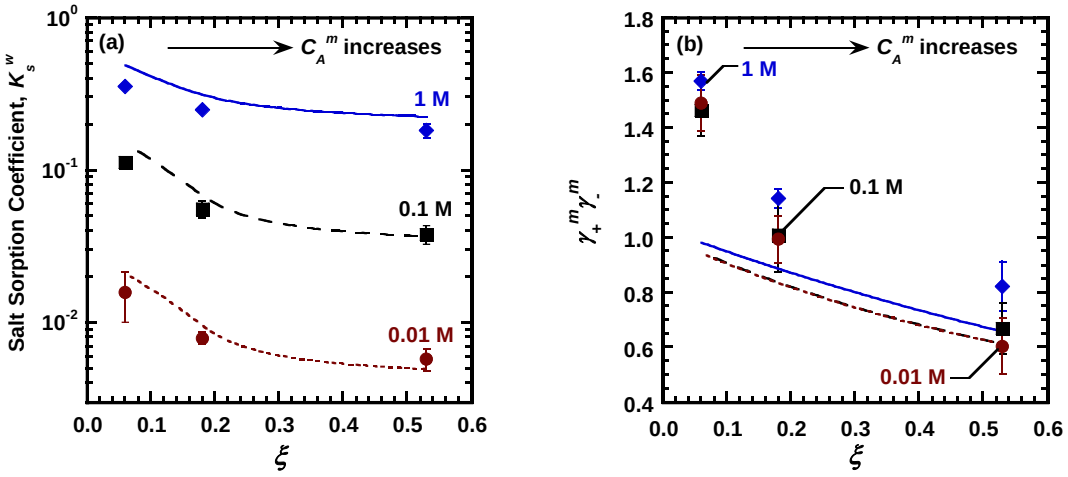

Figure 5.10 The dependence of: (a) salt sorption coefficient and (b) membrane ion activity coefficients on ξ in swollen XL(AMPS-PEGDA) membranes with similar water uptake at selected external NaCl concentrations of 0.01, 0.1, and 1 M. The dashed lines were drawn to guide the eye, and solid lines denote the approximate model predictions based on Eqn. (5.3) and Eqn. (5.4). The water uptake value measured in DI water was about 0.94 g (water)/g (dry polymer).

Experimental K_s^w and $\gamma_+^m\gamma_-^m$ data and theoretical predictions based on the complete Donnan-Manning model are presented in Figure 5.11 (a) and (b), respectively. Results of sample 10-0.97 are not shown here for simplicity. As shown in Figure 5.11 (a) and (b), the experimental K_s^w and $\gamma_+^m\gamma_-^m$ values in the most highly charged membrane considered (i.e., the membrane with the highest ξ value, 4-2.18) are in good agreement with the model predictions (i.e., no adjustable parameters), within experimental error. However, for the least highly charged membrane (e.g., i.e., the membrane with the smallest ξ value, 13-0.33), the model values of K_s^w and $\gamma_+^m\gamma_-^m$ are far from the experimental predictions, likely due to more pronounced thermodynamic non-idealities arising from

unfavorable non-electrostatic interactions between polymer segments, water, and ions in such materials that are not included in Manning's model. Further studies to elucidate the effects of polymer segments on ion behavior in such materials are in progress.

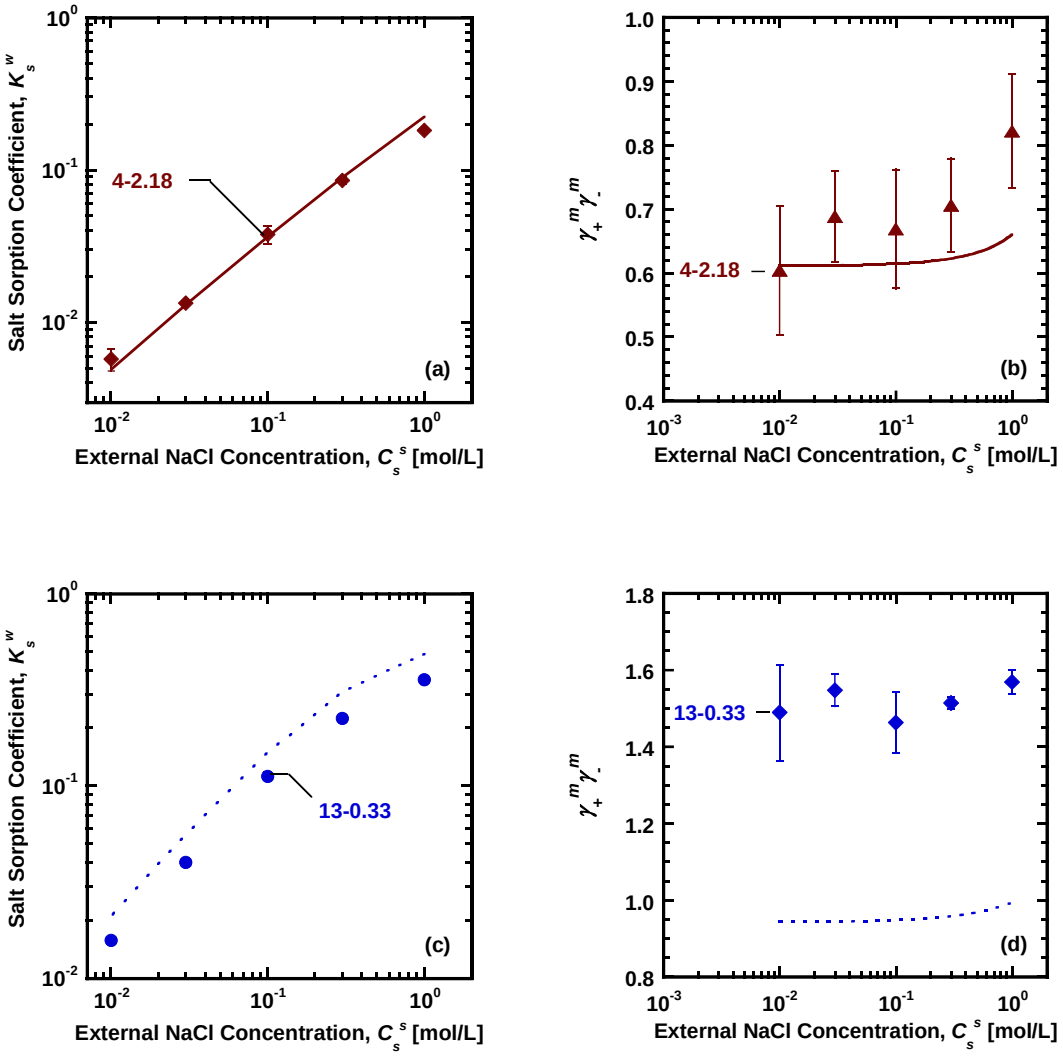

Figure 5.11 Salt sorption coefficient (a) and ion activity coefficients (b) in swollen XL(AMPS-PEGDA) membranes with different fixed charge concentration and ξ values but a constant water uptake. All symbols represent experimentally determined results. The lines indicate the theoretical predictions by the Donnan/Manning model [Eqs. (2.13) and (2.14)]: ▬ is sample 13-1.40, ▬ ▬ is sample 10-0.97, and ····· is sample 4-0.44. The water uptake value measured in Di water was about 0.94 g (water)/g (dry polymer).

5.3 CONCLUSIONS

Ion concentrations and activity coefficients in a series of uncharged and charged membranes equilibrated with NaCl solutions were determined. Ion activity coefficients in uncharged membranes are well above those in aqueous electrolyte solutions, suggesting ions have a much greater affinity for aqueous solution than swollen membranes. Such ion-excluding effects might be due to unfavorable interactions introduced by uncharged polymer segments. However, these interactions cannot be accounted for by Manning's counterion condensation theory to predict or even correlate membrane ion activity coefficients. As a result, experimental ion sorption results in uncharged membranes typically deviate from the theoretical predictions from the Donnan/Manning approach.

Negatively charged membranes with constant fixed charge concentration or constant water uptake were synthesized and characterized. In membranes having the same fixed charge concentration, mobile salt sorption increases and ion activity coefficients decrease with increasing ξ, qualitatively consistent with the model predictions. For membranes with the same water uptake, mobile salt sorption decreases with increasing fixed charge concentration due to stronger Donnan exclusion. The increase in fixed charge concentration is also accompanied by an increase in ξ, which should increase salt sorption (i.e., opposite to the Donnan exclusion effect). However, the increase in ξ is not sufficient to overcome the suppression of co-ion sorption caused by the fixed charges.

Mobile salt sorption and ion activity coefficients in the most hydrated and most highly charged membranes can be reasonably described by the Donnan/Manning model with no adjustable parameters. For less hydrated, weakly charged, or uncharged

membranes, theoretical predictions exhibit poor agreement with experimental results, likely due to non-idealities introduced by polymer segment-water-ion interactions that are not captured by Manning's model. A more comprehensive model accounting for non-idealities in charged polymers, solutions, and uncharged polymers in a unified manner is greatly needed.

5.4 REFERENCES

[1] E. Güler, R. Elizen, D.A. Vermaas, M. Saakes, K. Nijmeijer, Performance-determining membrane properties in reverse electrodialysis, Journal of Membrane Science, 446 (2013) 266-276.

[2] P. Długołęcki, K. Nymeijer, S.J. Metz, M. Wessling, Current status of ion exchange membranes for power generation from salinity gradients, Journal of Membrane Science, 319 (2008) 214-222.

[3] A. Galama, M. Saakes, H. Bruning, H. Rijnaarts, J. Post, Seawater predesalination with electrodialysis, Desalination, 342 (2014) 61-69.

[4] G.M. Geise, D.R. Paul, B.D. Freeman, Fundamental water and salt transport properties of polymeric materials, Progress in Polymer Science, 39 (2013) 1-42.

[5] G.M. Geise, H.S. Lee, D.J. Miller, B.D. Freeman, J.E. McGrath, D.R. Paul, Water purification by membranes: The role of polymer science, Journal of Polymer Science Part B: Polymer Physics, 48 (2010) 1685-1718.

[6] J. Veerman, R.M. De Jong, M. Saakes, S.J. Metz, G.J. Harmsen, Reverse electrodialysis: Comparison of six commercial membrane pairs on the thermodynamic efficiency and power density, Journal of Membrane Science, 343 (2009) 7-15.

[7] S. Maurya, S.-H. Shin, Y. Kim, S.-H. Moon, A review on recent developments of anion exchange membranes for fuel cells and redox flow batteries, RSC Advances, 5 (2015) 37206-37230.

[8] F. Helfferich, Ion Exchange, McGraw-Hill Book Co., Inc., New York, 1962.

[9] P. Meares, Ion exchange membranes: Principles, production and processes, in: Ion Exchange: Science and Technology, Springer, 1986, pp. 529-558.

[10] P. Meares, Ion-exchange membranes, in: Mass Transfer and Kinetics of Ion Exchange, Springer, 1983, pp. 329-366.

[11] H. Strathmann, A. Grabowski, G. Eigenberger, Ion-Exchange Membranes in the Chemical Process Industry, Industrial & Engineering Chemistry Research, 52 (2013) 10364-10379.

[12] Y. Tanaka, S.H. Moon, V.V. Nikonenko, T. Xu, Ion-Exchange Membranes, International Journal of Chemical Engineering, 2012 (2012) 1-3.

[13] T.Sata, Ion exchange membranes: Preparation, characterization, modification and application, Tokuyama Research, Tokuyama City, Japan, 2002.

[14] J. Kamcev, B.D. Freeman, Charged polymer membranes for environmental/energy applications, Annual Review of Chemical and Biomolecular Engineering, 7 (2016) 111-133.

[15] G.M. Geise, L.P. Falcon, B.D. Freeman, D.R. Paul, Sodium chloride sorption in sulfonated polymers for membrane applications, Journal of Membrane Science, 423-424 (2012) 195-208.

[16] J. Kamcev, M. Galizia, F.M. Benedetti, E.-S. Jang, D.R. Paul, B.D. Freeman, G.S. Manning, Partitioning of mobile ions between ion exchange polymers and aqueous salt solutions: importance of counter-ion condensation, Physical Chemistry Chemical Physics, 18 (2016) 6021-6031.

[17] N. Lakshminarayanaisah, Transport phenomena in membranes, Academic Press, New York and London, 1969.

[18] J. Kamcev, D.R. Paul, B.D. Freeman, Effect of fixed charge group concentration on equilibrium ion sorption in ion exchange membranes, Journal of Materials Chemistry A, 5 (2017) 4638-4650.

[19] K. Othmer, Ion Exchange, Kirk-Othmer encyclopedia of chemical technology.

[20] W. Xie, J. Cook, B.D. Freeman, C.H. Lee, J.E. McGrath, Fundamental salt and water transport properties in directly copolymerized disulfonated poly(arylene ether sulfone) random copolymers, Polymer, 52 (2011) 12.

[21] G.M. Geise, B.D. Freeman, D.R. Paul, Characterization of a novel sulfonated pentablock copolymer for desalination applications, Journal of Membrane Science, 24 (2010) 5815-5822.

[22] J. Kamcev, D.R. Paul, B.D. Freeman, Ion activity coefficients in ion exchange polymers: Applicability of Manning's counterion condensation theory, Macromolecules, 48 (2015) 8011-8024.

[23] N. Yan, J. Kamcev, M. Galizia, E.-S. Jang, D.R. Paul, B.D. Freeman, Influence of fixed charge concentration and water uptake on ion sorption in AMPS/PEGDA membranes, In preparation, (2017).

[24] H. Ju, A.C. Sagle, B.D. Freeman, J.I. Mardel, A.J. Hill, Characterization of sodium chloride and water transport in crosslinked poly (ethylene oxide) hydrogels, Journal of Membrane Science, 358 (2010) 131-141.

[25] H. Ju, B.D. McCloskey, A.C. Sagle, V.A. Kusuma, B.D. Freeman, Preparation and characterization of crosslinked poly (ethylene glycol) diacrylate hydrogels as fouling-resistant membrane coating materials, Journal of Membrane Science, 330 (2009) 180-188.

[26] K.S. Pitzer, Thermodynamics of electrolytes. I. Theoretical basis and general equations, The Journal of Physical Chemistry, 77 (1973) 268-277.

[27] K.S. Pitzer, G. Mayorga, Thermodynamics of electrolytes. II. Activity and osmotic coefficients for strong electrolytes with one or both ions univalent, The Journal of Physical Chemistry, 77 (1973) 2300-2308.

[28] R.A. Robinson, R.H. Stokes, Electrolyte solutions, Courier Corporation, 2002.

[29] J.O.M. Bockris, A.K.N. Reddy, M.E. Gamboa-Aldeco, I. NetLibrary, Modern electrochemistry: Volume 1, Ionics, 2nd ed., Kluwer Academic, New York, 2002.

[30] S. Bandini, D. Vezzani, Nanofiltration modeling: the role of dielectric exclusion in membrane characterization, Chemical engineering science, 58 (2003) 3303-3326.

[31] E.-S. Jang, J. Kamcev, K. Kobayashi, N. Yan, M. Galizia, R. Sunjai, H.B. Park, D.R. Paul, B.D. Freeman, Effect of water content on alkali metal chloride sorption in cross-linked poly(ethylene glycol diacrylate), In Preparation, (2017).

[32] N. Yan, D.R. Paul, B.D. Freeman, Water and ion sorption in a series of cross-linked AMPS/PEGDA hydrogel membranes, In preparation, (2017).

[33] P.J. Flory, Principles of polymer chemistry, Cornell University Press, 1953.

[34] F.G. Donnan, Theory of membrane equilibria and membrane potentials in the presence of non-dialysing electrolytes. A contribution to physical-chemical physiology, Journal of Membrane Science, 100 (1995) 11.

[35] G.S. Manning, Limiting laws and counterion condensation in polyelectrolyte solutions I. Colligative properties, The Journal of Chemical Physics, 51 (1969) 924-933.

[36] M. Galizia, F.M. Benedetti, D.R. Paul, B.D. Freeman, Monovalent and divalent ion sorption in a cation exchange membrane based on cross-linked poly (p-styrene sulfonate-co-divinylbenzene), Journal of Membrane Science, 535 (2017) 132-142.

Chapter 6: Ion Transport in a Series of Crosslinked AMPS/PEGDA Hydrogel Membranes[3]

6.1 INTRODUCTION

Ion exchange membranes (IEMs) are actively used and explored for applications such as reverse osmosis, forward osmosis, electrodialysis (ED), reverse electrodialysis (RED), and fuel cells [1-9]. To enhance water/salt separation efficiency and reduce energy cost, these technologies often have specific requirements for membrane ion transport properties [10]. Meeting these specifications requires an understanding and ability to control ion transport through the membranes via tailoring polymer chemical and physical parameters [10, 11]. IEMs have charged functional groups, called fixed charge groups, covalently bound to the polymer backbone. These ionogenic groups can ionize and retain water in the polymer upon exposure to aqueous solution [12]. The fixed charge groups and membrane water content can significantly influence ion transport [13, 14].

Ion transport in nonporous membranes is described by the solution-diffusion model [15, 16]. Ions from the external solution first partition into the upstream face of the membrane, diffuse down the chemical and/or electrical potential gradient, and desorb into the contiguous solution at the membrane's downstream side [12, 16, 17]. Equilibrium ion concentrations in the membrane can be profoundly influenced by fixed charge groups via electrostatic interactions between the fixed charges and ions [18-20]. Typically, counter-ions (i.e., ions bearing a charge opposite to that of the fixed charge groups) are attracted to the membrane from the external aqueous electrolyte solution, and co-ions (i.e., ions bearing

[3] This chapter has been adapted from: Yan, N., Kamcev, J., Jang E.S., Kobayashi, K., Paul, D.R., Freeman, B.D., Ion and Salt Transport in a Series of Crosslinked AMPS/PEGDA Hydrogel Membranes (in preparation). Yan, N. made the major contributions to this chapter.

the same charge as that of the fixed charge groups) are largely excluded from the membrane (i.e., Donnan exclusion) [12]. This exclusion effect is stronger when the fixed charge concentration in the membrane is higher than the electrolyte concentration in solution [12]. At equilibrium, sorbed counter-ions must electrically balance both the fixed charge groups on the polymer backbone and any co-ions sorbed in the membrane.

Ion diffusion is strongly influenced by the water content in a membrane [13, 21]. Water can plasticize polymer chains, thereby facilitating ion diffusion and transport [22]. In addition, fixed charges may affect ion diffusion via electrostatic interactions with sorbed ions [23, 24]. However, methods used to determine membrane transport properties have varied greatly in the literature, and inconsistent results across these studies make fundamental relations between polymer structure and ion transport properties difficult to discern [25-29].

This study focuses on exploring the transport properties of ions in a series of uncharged and negatively charged membranes (i.e., cation exchange membranes, CEMs). The concentration of fixed charge groups in the membrane was systematically controlled by varying the charged monomer content in the pre-polymerization mixture. Ion sorption and ionic conductivity of the membranes were measured as a function of NaCl solution concentrations (i.e., 0.01-1 M). Salt permeability coefficients were also determined. Individual ion diffusion coefficients were calculated using the Nernst-Plank framework [30]. To the best of our knowledge, such information for the same set of uncharged and charged membranes is rarely presented in the literature. Sorption results were interpreted using the Donnan/Manning model [31]. Diffusion and permeation results were

interpreted within the framework of the Mackie and Meares model and the solution-diffusion model [23].

6.2 Results and Discussion

6.2.1 Water Sorption

Water volume fraction values for the samples considered in this study were measured and reported elsewhere [31, 32]. As shown in Table 6.1 for a given value of n (i.e., number of EO units in PEGDA), water volume fraction measured in DI water increases as IEC increases, presumably due to enhanced polymer-water affinity as more hydrophilic fixed charge groups are present in the membrane [12, 32, 33]. Figure 6.1 presents water volume fraction as a function of external NaCl concentration in samples prepared with PEGDA of n = 10. At a given IEC value, as external salt concentration increases, water volume fraction decreases by about 7-12 % due to osmotic de-swelling, since water activity decreases in the external solution [23, 31-33].

Table 6.1 Polymer water uptake, water volume fraction, and fixed charge concentration.

Sample (n-IEC)	w_u [a] [g (water)/g (dry polymer)]	ϕ_w [b] [L (water)/L (swollen membrane)]	$C_A^{m,w}$ [c] [mol/L (water sorbed)]
13-0.44	0.989 ± 0.012	0.547 ± 0.003	0.444 ± 0.005
13-1.40	1.346 ± 0.006	0.634 ± 0.002	1.036 ± 0.005
10-0	0.581 ± 0.006	0.411 ± 0.004	0
10-0.01	0.593 ± 0.014	0.418 ± 0.006	$(1.69 \pm 0.04)\times10^{-2}$
10-0.05	0.619 ± 0.003	0.429 ± 0.003	$(8.40 \pm 0.05)\times10^{-2}$
10-0.13	0.645 ± 0.004	0.440 ± 0.002	0.208 ± 0.005
10-0.44	0.764 ± 0.009	0.487 ± 0.003	0.575 ± 0.007
10-0.97	0.936 ± 0.014	0.546 ± 0.004	1.031 ± 0.015
10-1.46	1.110 ± 0.024	0.593 ± 0.005	1.318 ± 0.029
10-1.93	1.300 ± 0.018	0.633 ± 0.003	1.485 ± 0.021
4-0.44	0.423 ± 0.007	0.353 ± 0.004	1.037 ± 0.017
4-1.93	0.882 ± 0.010	0.544 ± 0.003	2.189 ± 0.025

[a] w_u is the pure water uptake (grams of water per g of dry polymer).

[b] ϕ_w is pure water volume fraction in the swollen membrane (liter of water per L of swollen membrane), and it was calculated via $\phi_w = w_u/(w_u + \rho_w/\rho_p)$, where ρ_p is the density of dry polymer [31, 32].

[c] $C_A^{m,w}$ is the fixed charge concentration, which was determined based on the theoretical IEC values and pure water uptake results via $C_A^{m,w} = IEC \cdot \rho_w/w_u$, , where ρ_w is the density of water [32].

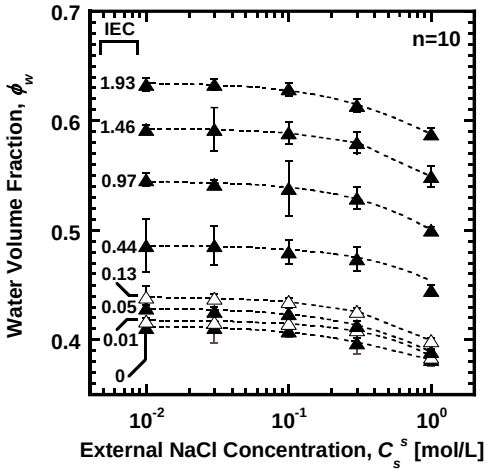

Figure 6.1 Water volume fraction as a function of external NaCl concentration in membranes prepared with PEGDA of n = 10. The uncertainty, determined as the standard deviation from measurements made on at least six samples, was less than 5% of the average of these measurements.

6.2.2 Ion Sorption

6.2.2.1 Cl^- Sorption

Equilibrium Cl^- (i.e., co-ion) concentrations in uncharged and charged membranes prepared with PEGDA of n = 13, 10, and 4 were reported elsewhere [31, 37]. As an example, Figure 6.2 (a) presents Cl^- concentrations in selected membranes (i.e., n =10) as a function of external NaCl concentration, C_s^s. . As C_s^s increases from 0.01 to 1 M, the sorbed Cl^- concentration increases for all samples considered. However, the rate of increase of $C_-^{m,p}$ vs. C_s^s in uncharged and highly charged membranes are different. For example, the Cl^- concentration in the most highly charged membrane (IEC = 1.93 meq/g) increases by over four orders of magnitude as external NaCl concentration increases.

This large increase in co-ion sorption is typical for charged membranes, due to strong Donnan exclusion at low C_s^s values and weakened Donnan exclusion at high C_s^s [18, 19]. In contrast, the Cl^- concentration in the uncharged membrane (labeled "0") only increases by approximately two orders of magnitude, which is proportional to the increase in C_s^s [18].

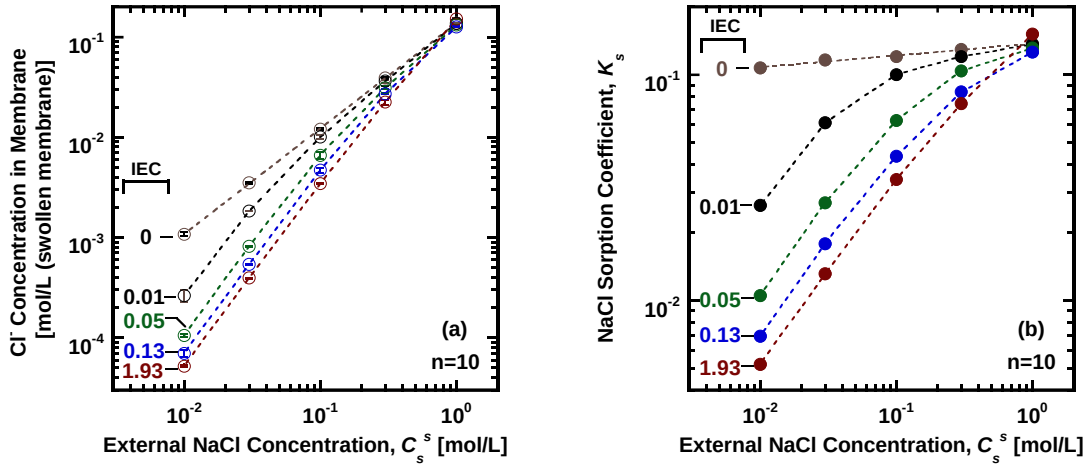

Figure 6.2 The dependence of: (a) sorbed Cl^- concentration, $C_-^{m,p}$, and (b) NaCl sorption coefficient on external NaCl concentration in membranes prepared with PEGDA of n = 10. The uncertainty, determined as the standard deviation from measurements made on at least six samples, was less than 15% of the average of these measurements. The K_s^p value of the uncharged membrane at C_s^s = 0.1 M agrees with previous results reported for XLPEGDA membranes [34].

Salt sorption coefficients were computed from the measured Cl^- concentrations in the membranes via Eqn. (2.7). Figure 6.2 (b) presents NaCl sorption coefficients, K_s^p, as a function of external NaCl concentration. The C_s^s dependence of K_s^p in uncharged

and highly charged membranes is qualitatively different. K_s^p values in the most highly charged membrane (IEC = 1.93 meq/g) exhibit significant variation with C_S^s, while those of the uncharged membrane (IEC = 0) change relatively little with C_S^s, in qualitative agreement with the ideal Donnan model [i.e., $C_A^m = 0$ in Eqn. (2.8)] [18].

Figure 6.3 presents the dependence of experimental NaCl sorption coefficients on IEC values at fixed external NaCl concentrations of 0.01 and 1 M. For comparison, theoretical NaCl sorption coefficients calculated using the Donnan/Manning model [Eqn. (2.14)] are also shown in Figure 6.3. At the lowest salt concentration considered (i.e., C_S^s = 0.01 M), NaCl sorption coefficients initially decrease by about one order of magnitude as IEC increases from 0 to 0.44 meq/g, presumably due to Donnan exclusion induced by increased fixed charge concentration in the membrane (cf. $C_A^{m,w}$ in Table 6.1). Then, K_s^p values are relatively constant at high IEC values (i.e., IEC > 0.44 meq/g). These behaviors are qualitatively consistent with the model predictions [48]. That is, the Donnan exclusion effect is very sensitive to the change in fixed charge concentration when only low levels of fixed charges are introduced to the polymer network [37]. Further addition of fixed charges to an already highly charged polymer would promote co-ion exclusion to a lesser extent [37]. At the highest salt concentration considered (i.e., C_S^s = 1 M), both experimental and theoretical K_s^p values depend relatively weakly on IEC and asymptotically approach that of the uncharged membrane (IEC = 0). This phenomenon indicates the Donnan exclusion effect in charged membranes is greatly reduced at high C_S^s, so the charged membranes sorb co-ions in the same fashion as the uncharged membrane [18].

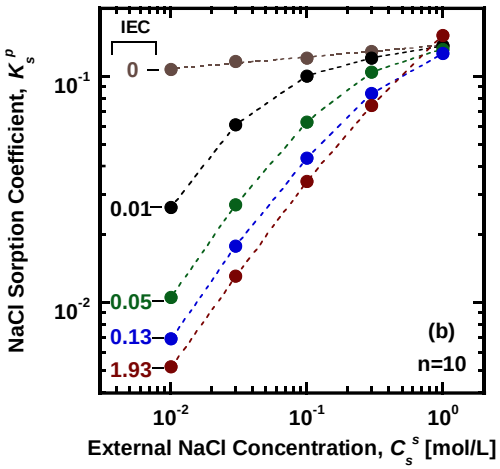

Figure 6.3 NaCl sorption coefficients as a function of IEC value (meq/g) at external NaCl concentrations of 0.01 and 1 M in membranes prepared with PEGDA of n = 10. The filled symbols represent experimental sorption coefficients, and the dashed lines denote predicted salt sorption coefficients according to the Donnan/Manning theory [i.e., Eqn. (2.14)].

The quantitative agreement between the experimental and theoretical values are good in membranes with higher IEC values (i.e., IEC > 0.44 meq/g), suggesting thermodynamic non-idealities in these membranes are governed by strong electrostatic interactions between fixed charges and ions that are captured by Manning's counter-ion condensation theory [33]. For membranes with lower IEC values (i.e., IEC < 0.44 meq/g), For membranes with lower IEC values (i.e., IEC < 0.44 meq/g), the experimental K_s^p values are below the model predictions, likely due to additional thermodynamic non-idealities arising from unfavorable non-electrostatic interactions between polymer segments, water, and ions in such materials [20, 31, 33, 37].

6.2.2.2 Na^+ Sorption

Figure 6.4 presents the sorbed Na^+ concentration (e.g., the counterion concentration in a CEM) as a function of external NaCl concentration, C_s^s. For the uncharged membrane, the C_s^s dependence of $C_+^{m,p}$ resembles that of C_-^m in Figure 6.2 (a), because the membrane contains equal numbers of Na^+ and Cl^- over the entire range of external NaCl concentrations to ensure electroneutrality in the membrane [18]. In contrast, the Na^+ concentration in the membrane of IEC = 1.93 meq/g changes little with external NaCl concentration. This weak C_s^s dependence of $C_+^{m,p}$ is typical for highly charged membranes [19], where the majority of the sorbed sodium ions are electrically balancing fixed charges on the polymer backbone (i.e., $C_+^{m,p} = C_A^{m,p} + C_-^{m,p} \approx C_A^{m,p}$), so the concentration of sodium ions is relatively independent of C_s^s [31, 37]. For samples between these extremes (i.e., IEC of 0.01-1.46 meq/g), $C_+^{m,p}$ exhibits behavior intermediate between the two limiting cases (i.e., the uncharged and most highly charged samples considered).

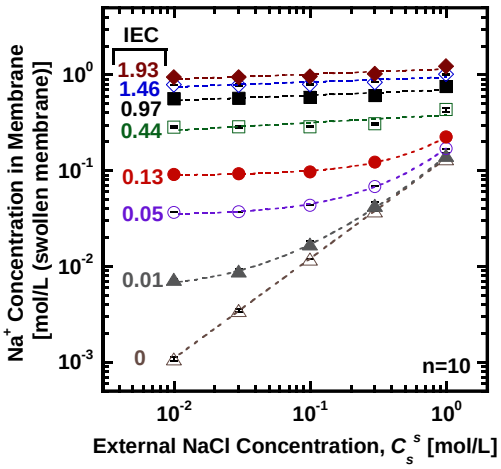

Figure 6.4 The dependence of sorbed Na^+ concentration, $C_+^{m,p}$, on external NaCl concentration in membranes prepared with PEGDA of n = 10. The dashed lines were drawn to guide the eye. The uncertainty, determined as the standard deviation from measurements made on at least six samples, was less than 10% of the average of these measurements.

6.2.3 Ion Diffusion

6.2.3.1 Na^+ Diffusion

The Na^+ diffusion coefficients were computed from the measured ion concentrations, salt permeability coefficient, and membrane ionic conductivity values using the Nernst-Plank approach [cf. Eqn. (2.19)-(2.20)]. Figure 6.5 (a) presents Na^+ diffusion coefficients as a function of upstream NaCl concentration. For each membrane, Na^+ diffusion coefficients are fairly constant at low NaCl concentrations (C_s^s < 0.1 M). Then, D_+^m values decrease by about 25-35% at high NaCl concentrations (C_s^s > 0.1 M). The initial plateau followed by a decrease in Na^+ diffusion coefficients is qualitatively

similar to the trend of polymer water volume fraction (ϕ_w) in Figure 6.1. Additionally, D_+^m values increase as IEC increases, similar to the increase in ϕ_w with increasing IEC (cf. Figure 6.1). The similarities in the dependence of Na^+ diffusion coefficients and water volume fraction on C_S^S and IEC can be qualitatively rationalized by the Mackie and Meares model [cf. Eqn. (2.17))], which predicts that ions diffuse faster in samples with higher water content.

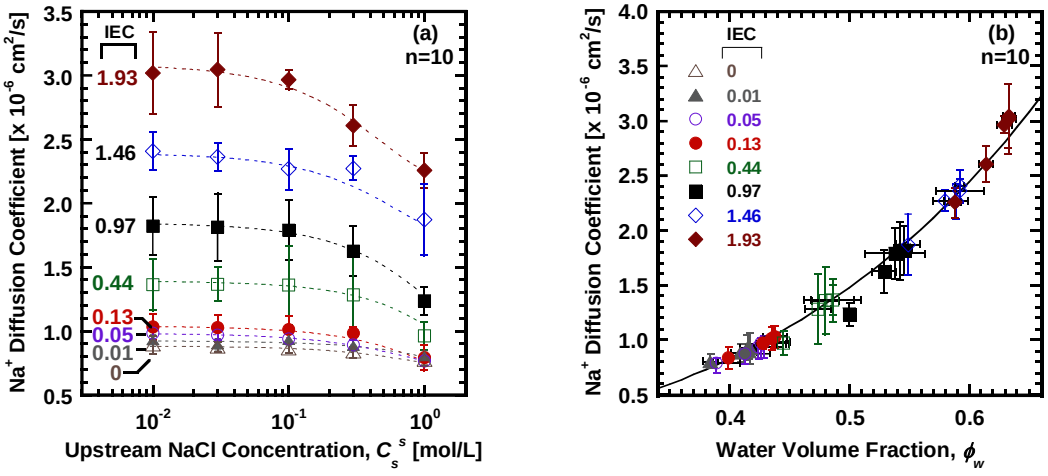

Figure 6.5 Na^+ diffusion coefficients, D_+^m, as a function of: (a) upstream NaCl concentration and (b) polymer water volume fraction in membranes prepared with PEGDA of n = 10. The uncertainty, determined using the propagation error analysis [37], was less than 15% of the average D_+^m value. The dashed lines were drawn to guide the eye, and the solid line represents the Mackie and Meares model predictions [cf. Eqn. (2.17)]. The Na^+ diffusion coefficient in external solution was taken as 13.3×10^{-6} cm^2/s [38].

To quantatitively compare experimental and theoretical results, Figure 6.5 (b) presents the experimental Na^+ diffusion coefficients as a function of water volume fraction

in the membranes. The experimental results are predicted well by the Mackie and Meares model over a wide range of ϕ_w values, regardless of whether ϕ_w was increased by adding fixed charges to the polymer backbone (i.e., varying IEC) or by osmotic de-swelling caused by the increase in external NaCl concentration. Similar agreement was also found in other polymers prepared with PEGDA of n = 13 and n = 4 (cf. Appendix C).

6.2.3.2 Cl^- Diffusion

The Cl^- diffusion coefficients were determined via Eqn. (2.21) and presented in Figure 6.6 (a) as a function of upstream NaCl concentration. For all membranes considered, decreasing IEC values and increasing upstream NaCl concentration lead to decreasing Cl^- diffusion coefficients, primarily due to reduced water content in membranes with lower IEC values and in membranes equilibrated with more concentrated salt solutions. These phenomena agree qualitatively with the Mackie and Meares model [cf. Eqn. (2.17)]. As shown in Figure 6.6 (a), D_-^m values in the uncharged membrane depend somewhat more strongly on C_s^s relative to the weakly charged samples (i.e., IEC = 0.01-0.13 meq/g). The molecular basis for this behavior is not fully understood.

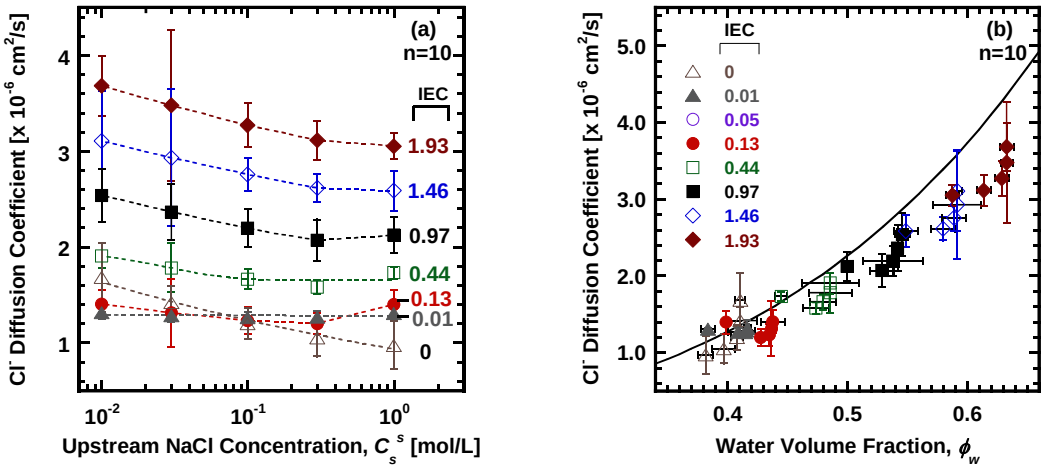

Figure 6.6 Cl^- diffusion coefficients, D_-^m, as a function of: (a) external NaCl concentration and (b) polymer water volume fraction in membranes prepared with PEGDA of n = 10. The uncertainty, determined using the propagation error analysis [37], was less than 25% of the average D_-^m value. The dashed lines were drawn to guide the eye, and solid lines represent the Mackie and Meares model predictions [cf. Eqn. (2.17)]. The Cl^- diffusion coefficient in external solution was taken as 20.3×10^{-6} cm^2/s [38].

Figure 6.6 (b) presents experimental and theoretical D_-^m values as a function of water volume fraction. Given the simple nature of the Mackie and Meares model and that it contains no adjustable parameters, the agreement is reasonable. Some deviation is observed in more highly charged samples for reasons we do not understand at this time. Recently, the effect of electrostatic interactions between fixed charges and ions on ion diffusion coefficient described by Manning's model [24] was found to be small compared to the effect of tortuosity on ion diffusion, as captured by the Mackie and Meares model

[23]. Similar agreement was also obtained in polymers prepared with PEGDA of n = 13 and n = 4 (cf. Appendix C).

6.2.4 Salt Diffusion

Salt diffusion coefficients, determined in concentration gradient driven transport, depend on the concentrations and diffusion coefficients of individual ions in the membrane [cf. Eqn. (2.21)], since every transported ion, driven by a concentration gradient across the membrane, must be electrically balanced by an ion of opposite charge. Apparent salt diffusion coefficients, $\langle \overline{D}_s^{m*} \rangle$, were computed from experimental salt permeability and sorption coefficients via Eqn. (2.18). $\langle \overline{D}_s^{m*} \rangle$ values are presented in Figure 6.7 (a) as a function of upstream NaCl concentration. For all samples, salt diffusion coefficients decrease with increasing C_s^s and decreasing IEC values, primarily due to reduced membrane water content under such conditions, in accordance with the Mackie and Meares model. Interestingly, the C_s^s dependence of $\langle \overline{D}_s^{m*} \rangle$ for highly charged membranes (i.e., IEC > 0.44 meq/g) is nearly identical to that of the Cl^- diffusion coefficients observed in Figure 6.6 (a). This similarity can be rationalized as follows. When a highly charged CEM is equilibrated with a relatively dilute NaCl solution, the sorbed counterion (Na^+) concentration is much higher than that of co-ions (Cl^-) due to Donnan exclusion (i.e., $C_+^{m,p} \gg C_-^{m,p}$). In this limit, Eqn. (2.19) can be simplified as follows:

$$D_s^m \approx \langle \overline{D}_s^{m*} \rangle \approx D_-^m \tag{6.1}$$

Thus, salt diffusion coefficients in highly charged membranes in contact with dilute electrolyte solutions are governd by the diffusion coefficients of co-ions (i.e., the minority species).

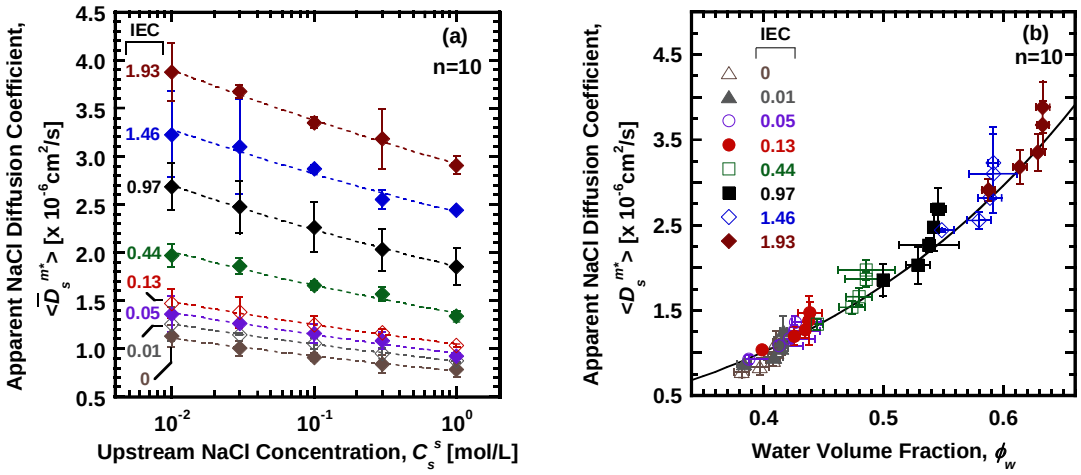

Figure 6.7 Apparent NaCl diffusion coefficients as a function of: (a) upstream NaCl concentration and (b) polymer water volume fraction in membranes prepared with PEGDA of n = 10. The dashed lines were drawn to guide the eye, and the solid line represents the Mackie and Meares model predictions [cf. Eqn. (2.17)]. The uncertainty of $\left\langle \overline{D}_s^{m*} \right\rangle$, determined using the propagation error analysis [37], was less than 15% of the average $\left\langle \overline{D}_s^{m*} \right\rangle$ value.

In Figure 6.7 (b), the experimental $\langle \overline{D}_s^{m*} \rangle$ data are presented as function of polymer water volume fraction together with those predicted by the Mackie and Meares model [41]. Within the experimental uncertainty, the experimental salt diffusion coefficients are well described by the model with no adjustable parameters, suggesting salt diffusion coefficients are mainly affected by water content, similar to results reported elsewhere [23]. Similar agreement was also observed in polymers prepared with PEGDA

of n = 13 and n = 4. This approach provides a tool to predict salt diffusion coefficients, and therefore, salt permeability coefficients in such materials [23].

Figure 6.8 presents the dependence of experimental and theoretical salt diffusion coefficients on IEC at fixed external NaCl concentrations (0.01 and 1 M). Increasing IEC value from 0 to 0.13 meq/g leads to a 50% increase in salt diffusion coefficients. In contrast, as IEC increases from 0.44 to 1.93 meq/g, $\langle \bar{D}_s^{m*} \rangle$ values increase by roughly a factor of two, since polymer water content increases more significantly at high IEC values (i.e., IEC > 0.13 meq/g) than that at low IEC values (i.e., IEC < 0.13 meq/g), consistent with the Mackie and Meares model prediction.

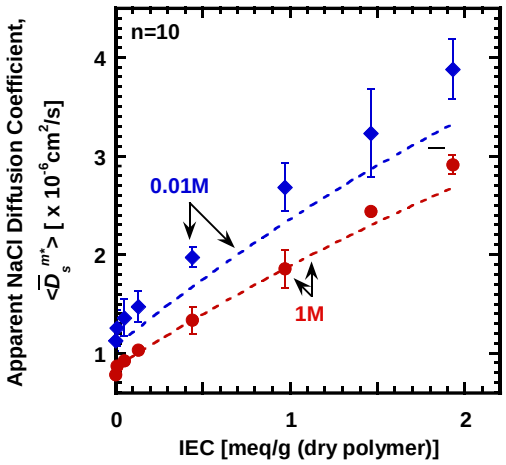

Figure 6.8 Apparent NaCl diffusion coefficient as a function of IEC values (meq/g) at fixed upstream NaCl concentrations of 0.01 and 1 M in membranes prepared with PEGDA of n = 10. The dashed lines denote the Mackie and Meares model prediction [cf. Eqn. (2.17)].

6.2.5 Salt Permeability

Salt permeability coefficients, $\langle P_s \rangle$, are presented as a function of upstream NaCl concentration in Figure 6.9 (a) and (b), respectively. In Figure 6.9 (a), salt permeability coefficients of the uncharged membrane (i.e., IEC = 0) decrease by roughly 12% as C_s^s increases from 0.01-1 M, similar to other XLPEGDA membranes [18]. The decreasing trend of $\langle P_s \rangle$ with increasing C_s^s can be rationalized within the framework of the solution-diffusion model [i.e., $\langle P_s \rangle = K_s \langle \bar{D}_s^{m*} \rangle$], which dictates that salt permeability coefficient is affected by both salt sorption and diffusion coefficients. The salt sorption coefficient (K_s) of the uncharged membrane is relatively constant over the entire range of C_s^s values considered. Thus, the C_s^s dependence of $\langle P_s \rangle$ is predominantly controlled

by that of the salt diffusion coefficient ($\langle \bar{D}_s^{m*} \rangle$), which decreases slightly as C_s^s increases, stemming from the reduced water content due to osmotic de-swelling at high C_s^s [18].

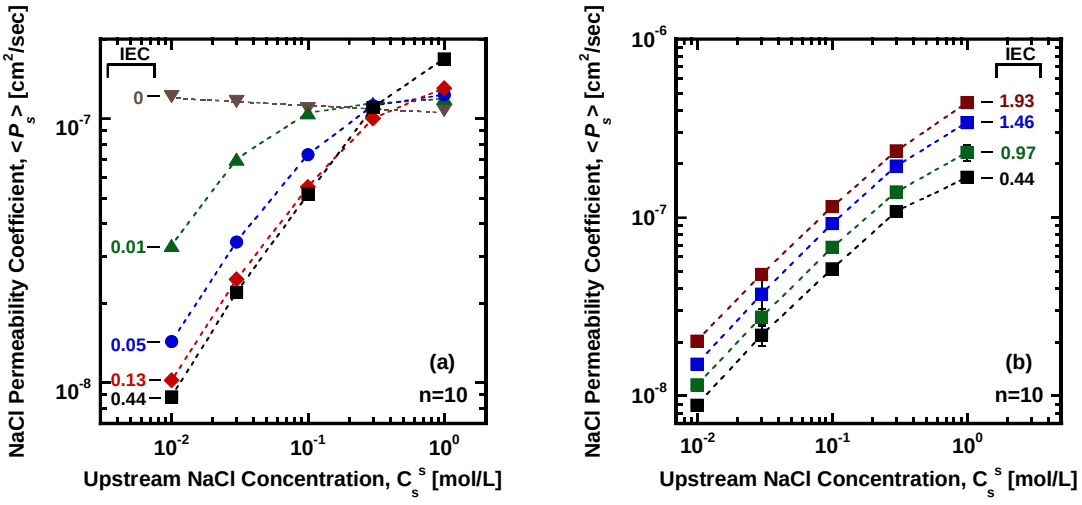

Figure 6.9 The influence of upstream NaCl concentration on salt permeability coefficients of: (a) uncharged and weakly charged membranes (i.e., IEC < 0.44 meq/g) and (b) highly charged membranes (i.e., IEC > 0.44 meq/g). These membranes were prepared with PEGDA of n = 10. The uncertainty, determined as the standard deviation from measurements made on at least six samples, was less than 15% of the average of these measurements. The dashed lines were drawn to guide the eye. The salt permeability coefficient value at C_s^s = 0.1 M agrees results reported for XLPEGDA membranes [7, 12].

In Figure 6.9 (b), $\langle P_s \rangle$ values of the most highly charged membrane (i.e., IEC = 1.93 meq/g) exhibit a strong dependence on C_s^s, which is typical for highly charged membranes due to the influence of fixed charges on salt sorption [cf. Figure 6.2 (b)] [42, 43]. For example, K_s in the samples having an IEC value of 1.93 meq/g increases by about 2 orders of magnitude as C_s^s increases from 0.01 to 1 M, while only a modest

decrease in $\langle \overline{D}_s^{m*} \rangle$ was observed over the same range of C_s^s. Thus, the strong C_s^s dependence of $\langle P_s \rangle$ in this highly charged membrane is governed by that of K_s. For all the other charged membranes (e.g., IEC = 0.01-1.46 meq/g), the dependence of $\langle P_s \rangle$ on C_s^s is in between the trends observed in the uncharged and most highly charged membranes.

The dependence of experimental salt permeability coefficients on IEC values is shown in Figure 6.10. Theoretical salt permeability coefficients were computed from the solution-diffusion model. Salt sorption coefficients were estimated using the Donnan/Manning approach and diffusion coefficients were estimated using the Mackie and Meares model. Interestingly, at the lowest C_s^s value considered (i.e., 0.01 M), the experimental salt permeability coefficients decrease to a minimum followed by a slight increase (~20%) as IEC increases. This phenomenon can be explained by the different dependences of K_s and $\langle \overline{D}_s^{m*} \rangle$ on IEC, as shown in Figure 6.3 and Figure 6.8, respectively. When C_s^s = 0.01 M and IEC values are below about 0.44 meq/g, NaCl sorption coefficients decrease significantly as IEC increases. The decrease in K_s is more dramatic at low IEC values (< 0.44 meq/g) than that observed at high IEC values (> 0.44 meq/g). Increases in IEC are accompanied by increases in water content, so salt diffusion coefficients increase with increasing IEC. The increase in $\langle \overline{D}_s^{m*} \rangle$ is more pronounced at high IEC values (> 0.44 meq/g) than at lower IEC values (< 0.44 meq/g). Consequently, the initial decrease in salt permeability coefficient with increasing IEC is primarily caused by the decrease in salt sorption coefficient, since the diffusion coefficient changes little at low IEC values. Then, salt permeability coefficients reach a minimum and begin to increase with increasing IEC (i.e., > 0.44 meq/g), due to the increase in salt diffusion

coefficient in samples with higher water content. These phenomena can be reasonably well described by the predictions of the Mackie/Meares and Donnan/Manning models at higher IEC values, but there are substantial discrepancies in the weakly charged samples, due to a failure in the Donnan/Manning model to describe sorption coefficients in these materials as discussed above.

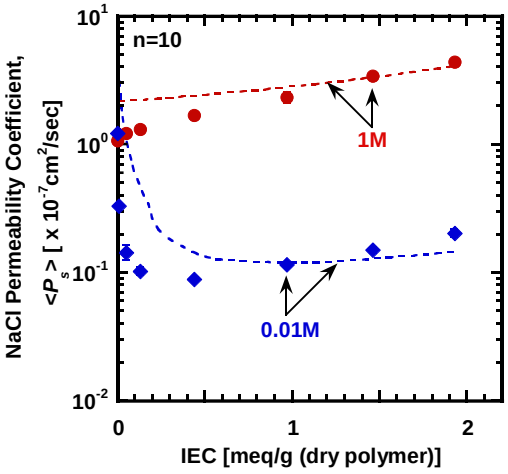

Figure 6.10 The influence of IEC values on salt permeability coefficients at fixed upstream NaCl concentrations of 0.01 and 1 M. Dashed lines denote the product of theoretical salt sorption coefficients estimated by the ideal Donnan theory [cf. Eqn. (2.7)] and salt diffusion coefficients estimated by the Mackie and Meares model [cf. Eqn. (2.17)].

In contrast, when C_s^s = 1 M, salt permeability coefficients increase monotonically with increasing IEC. The IEC dependence of salt permeability coefficient at high C_s^s is mainly governed by the salt diffusion coefficient, since salt solubility in the membrane is relatively independent of IEC at high C_s^s [cf. Figure 6.3]. Thus, $\langle P_s \rangle$ increases essentially in the same fashion as $\langle \bar{D}_s^{m*} \rangle$ with increasing IEC values when C_s^s = 1 M.

6.2.6 Membrane Ionic Conductivity

Membrane ionic conductivity, κ, depends on ion concentrations and diffusion coefficients in the membrane, as set forth in Eqn. (2.19). Figure 6.11 (a) presents membrane ionic conductivity values as a function of NaCl content in the external solution. The C_s^s dependence of κ is qualitatively similar to that of the sorbed Na^+ concentration in the membrane (cf. Figure 6.4). When a CEM is equilibrated with a relatively dilute NaCl solution, $C_+^{m,p} \gg C_-^{m,p}$, so Eqn. (2.19) is simplified as follows:

$$\kappa \approx \frac{F^2}{RT} D_+^m C_+^{m,p} \tag{6.2}$$

where κ depends mainly on the counterion concentrations and diffusion coefficients. The counterions are more numerous in the samples than the co-ions, so they carry most of the current [12]. As C_s^s increases from 0.01 to 1 M, $C_+^{m,p}$ is relatively constant in the most highly charged membrane (i.e., IEC = 1.93 meq/g), as shown in Figure 6.4. D_+^m of this sample also changes little with C_s^s due to relatively constant water content in the membrane [cf. Figure 6.6 (a)]. Consequently, κ is essentially independent of C_s^s in the most highly charged membrane considered, as suggested by Eqn. (6.2).

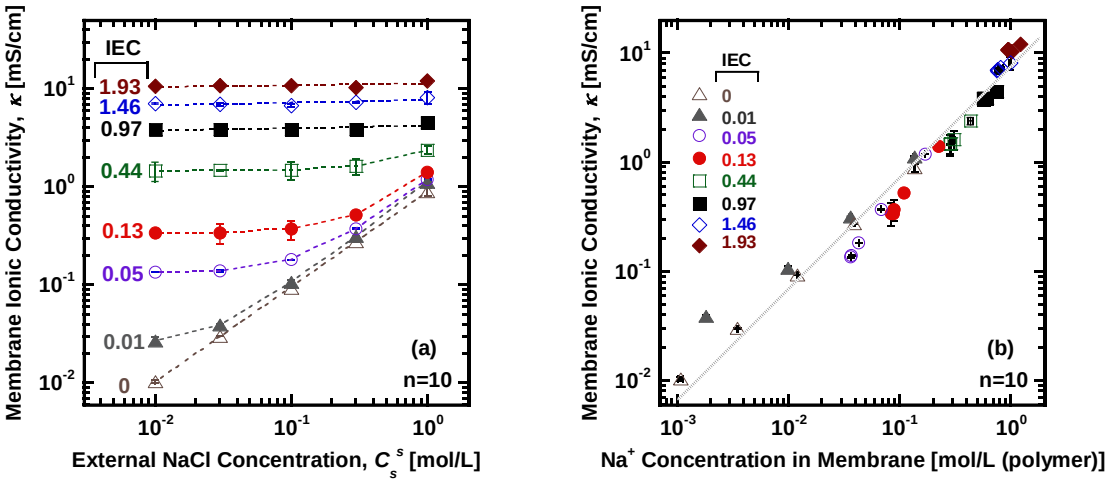

Figure 6.11 The influence of: (a) external NaCl concentration and (b) sorbed Na^+ concentration on membrane ionic conductivity in membranes prepared with PEGDA of n = 10. The uncertainty, determined as the standard deviation from measurements made on at least six samples, was less than 25% of the average of these measurements. The dashed lines were drawn to guide the eye.

Unlike the highly charged membrane, the uncharged membrane's κ value increases by orders of magnitude as C_s^s increases, which is qualitatively similar to the trend of C_+^m with increasing C_s^s in this sample (cf. Figure 6.4). As mentioned earlier, equal numbers of Na^+ and Cl^- sorb in the uncharged membrane to maintain electroneutrality (i.e., $C_+^{m,p} = C_-^{m,p}$). Thus, Eqn. (2.20) can be rewritten as follows:

$$\kappa = \frac{F^2}{RT} C_s^{m,p} (D_+^m + D_-^m) \tag{6.3}$$

where the sorbed salt concentration ($C_s^{m,p} = C_+^{m,p} = C_-^{m,p}$) and both Na^+ and Cl^- diffusion coefficients contribute to the membrane conductivity. Since $C_s^{m,p}$ of the uncharged

membrane has a relatively strong dependence on C_s^s, as shown in Figure 6.4, and ion diffusion coefficients are only weakly dependent on C_s^s [cf. Figure 6.5 (a) and Figure 6.6 (a)], the strong C_s^s dependence of κ of the uncharged membrane is dictated by that of C_s^m.

Motivated by Eqn. (6.2)-(6.3), experimental κ values are presented in Figure 6.11 (b) as a function of the sorbed Na^+ concentration in the membrane. Figure 6.11 (b) shows a good correlation between ionic conductivity and Na^+ concentration in almost all the membranes studied. Ionic conductivity values can be predicted from Eqn. (2.20). where Na^+ and Cl^- diffusion coefficients were estimated using the Mackie and Mears model, Cl^- concentrations were estimated using the Donnan/Manning model, and Na^+ concentrations were computed using Eqn. (2.4). Membrane fixed charge concentration at each external NaCl concentration was estimated using the IEC and water uptake values, as reported elsewhere [32]. Figure 6.12 shows the predicted and measured ionic conductivity results in a parity plot. A reasonably good agreement is found between theoretical and experimental κ values, since no adjustable parameters are used. Some deviations are evident in uncharged and weakly charged samples (i.e., IEC < 0.05), since the Cl^- concentrations in such materials cannot be accurately predicted by the Donnan/Manning model, which was designed for highly charged materials [31]. Minor discrepancy is also found in highly charged samples (i.e., IEC >1.46), which may be due to the effect of polymer-ion interactions on co-ion diffusion that is not captured by the Mackie and Meares model.

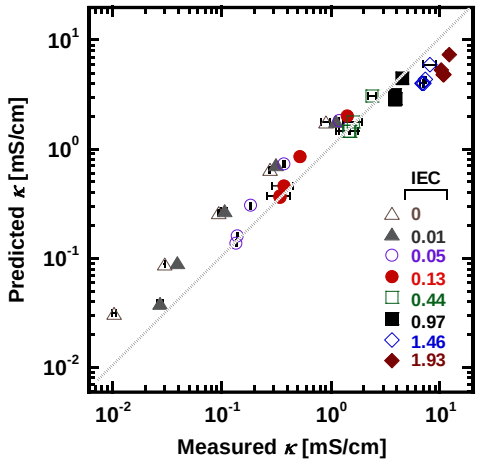

Figure 6.12 The influence of: (a) external NaCl concentration and (b) sorbed Na^+ concentration on membrane ionic conductivity in membranes prepared with PEGDA of n = 10. The uncertainty, determined as the standard deviation from measurements made on at least six samples, was less than 25% of the average of these measurements. The dashed lines were drawn to guide the eye.

6.3 Conclusions

Sorbed ion concentration, salt permeability, and ionic conductivity in a series of uncharged and charged samples were characterized. Ion diffusion coefficients were calculated from these data. Diffusion coefficients were mainly affected by the sample's water volume fraction, which is consistent with the Mackie and Meares model. Model predictions for Na^+ diffusion coefficients agree remarkably well with the experimental results. Reasonable agreement was also found between experimental and theoretical Cl^- diffusion coefficients, considering that no adjustable parameters were used. Minor

deviations were observed in highly charged membranes, likely due to interactions between polymer and ions that are not captured by the Mackie and Meares model.

Salt permeability coefficients depend on salt sorption and diffusion coefficients. The salt concentration dependence of the salt permeability in uncharged membranes was mainly influenced by salt diffusivity and that in charged membranes was dominated by salt solubility. The increase in polymer IEC is often accompanied by simultaneous increases in fixed charge concentration and water content. When a membrane is equilibrated with a dilute electrolyte solution, as IEC increases, salt permeability first decreases due to the depression in salt solubility caused by Donnan exclusion. Then, salt permeability increases slightly owing to the enhancement in salt diffusivity induced by higher water content in the membrane at higher IEC values.

Membrane ionic conductivity depends on sorbed ion concentration and diffusion coefficients in the membrane. The dependence of membrane ionic conductivity on external NaCl concentration correlates well with the sorbed counterion concentration. Reasonably good agreement was found between experimental and predicted ionic conductivity values. Some discrepancy was evident in uncharged and weakly charged samples, since the Donnan/Manning model only describes ion sorption well in highly charged sample but fails in samples that are uncharged or weakly charged.

6.4 REFERENCES

[1] P. Długołęcki, K. Nymeijer, S.J. Metz, M. Wessling, Current status of ion exchange membranes for power generation from salinity gradients, Journal of Membrane Science, 319 (2008) 214-222.

[2] G.M. Geise, D.R. Paul, B.D. Freeman, Fundamental water and salt transport properties of polymeric materials, Progress in Polymer Science, 39 (2013) 1-42.

[3] E. Güler, R. Elizen, D.A. Vermaas, M. Saakes, K. Nijmeijer, Performance-determining membrane properties in reverse electrodialysis, Journal of Membrane Science, 446 (2013) 266-276.

[4] S. Maurya, S.-H. Shin, Y. Kim, S.-H. Moon, A review on recent developments of anion exchange membranes for fuel cells and redox flow batteries, RSC Advances, 5 (2015) 37206-37230.

[5] A. Galama, M. Saakes, H. Bruning, H. Rijnaarts, J. Post, Seawater predesalination with electrodialysis, Desalination, 342 (2014) 61-69.

[6] J. Veerman, R.M. De Jong, M. Saakes, S.J. Metz, G.J. Harmsen, Reverse electrodialysis: Comparison of six commercial membrane pairs on the thermodynamic efficiency and power density, Journal of Membrane Science, 343 (2009) 7-15.

[7] L.F. Greenlee, D.F. Lawler, B.D. Freeman, B. Marrot, P. Moulin, Reverse osmosis desalination: water sources, technology, and today's challenges, Water research, 43 (2009) 2317-2348.

[8] T.Y. Cath, A.E. Childress, M. Elimelech, Forward Osmosis: Principles, Applications, and Recent Development, Journal of Membrane Science, 281 (2006) 70-87.

[9] T.S. Chung, S. Zhang, K.Y. Wang, J. Su, M.M. Ling, Forward osmosis processes: yesterday, today and tomorrow, Desalination, 287 (2012) 78-81.

[10] T.Sata, Ion exchange membranes: Preparation, characterization, modification and application, Tokuyama Research, Tokuyama City, Japan, 2002.

[11] J. Kamcev, B.D. Freeman, Charged polymer membranes for environmental/energy applications, Annual Review of Chemical and Biomolecular Engineering, 7 (2016) 111-133.

[12] F. Helfferich, Ion Exchange, McGraw-Hill Book Co., Inc., New York, 1962.

[13] H. Yasuda, C.E. Lamaze, L.D. Ikenberry, Permeability of solutes through hydrated polymer membranes. Part I. Diffusion of sodium chloride, Die Makromolekulare Chemie, 118 (1968) 19-35.

[14] P. Meares, Ion exchange membranes: Principles, production and processes, in: Ion Exchange: Science and Technology, Springer, 1986, pp. 529-558.

[15] J.G. Wijmans, R.W. Baker, The solution-diffusion model: a review, Journal of Membrane Science, 107 (1995) 1-21.

[16] G.M. Geise, H.S. Lee, D.J. Miller, B.D. Freeman, J.E. McGrath, D.R. Paul, Water purification by membranes: The role of polymer science, Journal of Polymer Science Part B: Polymer Physics, 48 (2010) 1685-1718.

[17] G.S. Park, J. Crank, Diffusion in polymers, Academic Press, New York and London, 1968.

[18] G.M. Geise, L.P. Falcon, B.D. Freeman, D.R. Paul, Sodium chloride sorption in sulfonated polymers for membrane applications, Journal of Membrane Science, 423-424 (2012) 195-208.

[19] J. Kamcev, M. Galizia, F.M. Benedetti, E.-S. Jang, D.R. Paul, B.D. Freeman, G.S. Manning, Partitioning of mobile ions between ion exchange polymers and aqueous salt solutions: importance of counter-ion condensation, Physical Chemistry Chemical Physics, 18 (2016) 6021-6031.

[20] M. Galizia, F.M. Benedetti, D.R. Paul, B.D. Freeman, Monovalent and divalent ion sorption in a cation exchange membrane based on cross-linked poly (p-styrene sulfonate-co-divinylbenzene), Journal of Membrane Science, 535 (2017) 132-142.

[21] J.S. Mackie, P. Meares, The diffusion of electrolytes in a cation-exchange resin membrane. I. Theoretical, Proceedings of the Royal Society of London A: Mathematical, Physical and Engineering Sciences, 232 (1955) 498-509.

[22] P. Meares, Ion-exchange membranes, in: Mass Transfer and Kinetics of Ion Exchange, Springer, 1983, pp. 329-366.

[23] J. Kamcev, D.R. Paul, G.S. Manning, B.D. Freeman, Predicting salt permeability coefficients in highly swollen, highly charged ion exchange membranes, ACS Applied Materials & Interfaces, 9 (2017) 4044-4056.

[24] G.S. Manning, Limiting laws and counterion condensation in polyelectrolyte solutions II. Self‐diffusion of the small ions, The Journal of Chemical Physics, 51 (1969) 934-938.

[25] J. Mackie, P. Meares, The diffusion of electrolytes in a cation-exchange resin membrane. II. Experimental, in: Proceedings of the Royal Society of London A: Mathematical, Physical and Engineering Sciences, The Royal Society, 1955, pp. 510-518.

[26] P. Meares, The conductivity of a cation-exchange resin, Journal of Polymer Science, 20 (1956) 507-514.

[27] P. Meares, Self-diffusion coefficients of anions and cations in a cation-exchange resin, The Journal of Chemical Physics, 55 (1958) 273-279.

[28] P. Meares, D. Dawson, A. Sutton, J. Thain, Diffusion, conduction and convection in synthetic polymer membranes, Berichte der Bunsengesellschaft für physikalische Chemie, 71 (1967) 765-775.

[29] W. McHardy, P. Meares, A. Sutton, J. Thain, Electrical transport phenomena in a cation-exchange membrane II. Conductance and electroosmosis, Journal of Colloid and Interface Science, 29 (1969) 116-128.

[30] N. Lakshminarayanaisah, Transport phenomena in membranes, Academic Press, New York and London, 1969.

[31] N. Yan, J. Kamcev, M. Galizia, E.-S. Jang, D.R. Paul, B.D. Freeman, Influence of fixed charge concentration and water uptake on ion sorption in AMPS/PEGDA membranes, In preparation, (2017).

[32] N. Yan, D.R. Paul, B.D. Freeman, Water and ion sorption in a series of cross-linked AMPS/PEGDA hydrogel membranes, In preparation, (2017).

[33] P.J. Flory, Principles of polymer chemistry, Cornell University Press, 1953.

[34] H. Ju, A.C. Sagle, B.D. Freeman, J.I. Mardel, A.J. Hill, Characterization of sodium chloride and water transport in crosslinked poly (ethylene oxide) hydrogels, Journal of Membrane Science, 358 (2010) 131-141.

[35] F.G. Donnan, Theory of membrane equilibria and membrane potentials in the presence of non-dialysing electrolytes. A contribution to physical-chemical physiology, Journal of Membrane Science, 100 (1995) 11.

[36] J. Kamcev, D.R. Paul, B.D. Freeman, Ion activity coefficients in ion exchange polymers: Applicability of Manning's counterion condensation theory, Macromolecules, 48 (2015) 8011-8024.

[37] P.R. Bevington, D.K. Robinson, J.M. Blair, A.J. Mallinckrodt, S. McKay, Data reduction and error analysis for the physical sciences, Computers in Physics, 7 (1993) 415-416.

[38] L. Yuan-Hui, S. Gregory, Diffusion of ions in sea water and in deep-sea sediments, Geochimica et cosmochimica acta, 38 (1974) 703-714.

[39] M. Jardat, B. Hribar-Lee, V. Vlachy, Self-diffusion coefficients of ions in the presence of charged obstacles, Physical Chemistry Chemical Physics, 10 (2008) 449-457.

[40] M. Jardat, B. Hribar-Lee, V. Dahirel, V. Vlachy, Self-diffusion and activity coefficients of ions in charged disordered media, The Journal of Chemical Physics, 137 (2012) 114507.

[41] R.A. Robinson, R.H. Stokes, Electrolyte solutions, Courier Corporation, 2002.

[42] G.M. Geise, B.D. Freeman, D.R. Paul, Sodium chloride diffusion in sulfonated polymers for membrane applications, Journal of Membrane Science, 427 (2013) 186-196.

[43] J. Kamcev, E.-S. Jang, N. Yan, D.R. Paul, B.D. Freeman, Effect of ambient carbon dioxide on salt permeability and sorption measurements in ion-exchange membranes, Journal of Membrane Science, 479 (2015) 55-56.

Chapter 7: Conclusions and Recommendations

7.1 Conclusions

The goal of this project is to establish a baseline for the relationship between the polymer membrane architecture (e.g., fixed charge concentration, water content, backbone structure) and ion transport (e.g., ion sorption, ion diffusion) properties. Such a relationship will allow for a better understanding of the optimization of next generation membranes.

Chapter 4 reported water and ion sorption properties in charged membranes with charge densities systematically controlled, leading to a better understanding of the fundamental structure/property relations in such materials. As ion exchange capacity (IEC) increased, both water and counter-ion (Na^+) sorption increased. Co-ion (Cl^-) sorption decreased markedly as IEC increased slightly, suggesting that even low levels of fixed charges (IEC value of 0.01 meq/g) exclude co-ions significantly. However, Cl^- sorption became independent of charge density at IEC values of 0.97 meq/g and higher. Experimental values for sorbed Cl^- concentrations deviated from those obtained via ideal Donnan model due to non-idealities of ion activity coefficients in the solution and membrane phases.

Chapter 5 seeked to isolate the effects of water content and charge density on ion sorption properties of charged membranes. At constant charge density, the sorbed mobile salt concentration increases as membrane water content increases. At fixed water content, mobile salt sorption decreases as charge density increases. Salt sorption in the membranes with the highest water content or charge density could be predicted after accounting for the non-idealities in solution and in the membrane. However, this

approach fails for less hydrated or weakly charged membranes due to more pronounced thermodynamic non-idealities introduced by the uncharged polymer segments.

The influence of incorporating fixed charges to the polymer on salt permeability, ionic conductivity, and ion diffusion coefficients is reported in Chapter 6. The polymer's fixed charge group concentration was systematically varied by adjusting the content of charged monomers in the polymer. Salt permeability and ionic conductivity in uncharged and charged membranes were measured in a consistent, unified manner. These properties were determined as a function of NaCl solution concentrations (0.01-1 M). Combining the Solution-Diffusion model and Nernst-Plank equation, individual ion (i.e., Na^+, Cl^-) diffusion coefficients were obtained. Na^+ diffusion coefficients could be described by Meares' tortuosity model remarkably well in all the membranes studied. Model predictions for Cl^- diffusion coefficients agree reasonably with the experimental values. Minor deviations were evident in more highly charged membranes. These discrepancies might be a result of the interactions omitted by Meares' model (e.g., fixed charges-ion, ion-ion, etc.).

7.2 Recommendations for Future Work

7.2.1 Theoretical Model for Ion Activity Coefficients in Uncharged Polymers

Currently, the fundamental underpinning of the uncharged membrane non-idealities (i.e., high ion activity coefficients) is unclear due, in part, to the lack of tools that can experimentally determine ion activity coefficients in the membranes. Thus, some examples of elevated ion activity coefficients observed in aqueous solutions (i.e., ion activity coefficients are experimentally accessible) with added organic chemicals (e.g.,

analogous to a polymer-ion-water system) are presented here. The first example is the formamide-NaCl-water mixture, in which the NaCl activity coefficients systematically increase as the formamide content increases from 0 to 80 wt% in the mixture [1]. The increase in ion activity coefficients was ascribed to the weakened ion-ion interactions in the NaCl solution due to the high dielectric constant of formamide (~110) [1]. As illustrated in Coulomb's law, the electrical force between ionic species decreases as the dielectric constant increases [2]. Thus, depression in ion-ion interactions (favorable for ions to stay in solution) increases the free energy of the system, resulting in higher ion activity coefficients [3]. However, different from formamide, the dielectric constant of XLPEGDA polymers is documented to be approximately10~12 [4], which is less than that of bulk water (~78). Thus the dielectric constant of a polymer-water mixture would be lower than that of bulk water, thereby reducing the ion activity coefficients [5]. However, the opposite phenomenon is observed in uncharged membranes, whose ion activity coefficients are often higher than that of solution. Such behavior cannot be explained solely based on changes in the dielectric constant.

Another example is a sugar-NaCl-water mixture, which exhibits higher NaCl activity coefficients as the sugar concentration increases, because the sugar molecules compete with ions for water via a polar-polar interaction [6]. Similarly, PEGDA chain contains a considerable amount of ethylene oxide (EO) groups (>80 wt%), which are polar and attractive to water molecules as well [7]. Recent DSC results show approximately 2~3 water molecules are tightly bound to one EO group in XLPEGDA [8]. This 'association' between EO groups and water could potentially cause insufficient "free" water for ion solvation. This hypothesis is reasonable since a similar water scarcity

scenario has caused NaCl ion activity coefficients increase in electrolyte solutions [9]. That is, the NaCl activity coefficients increase from 0.4 to 1 as NaCl concentration increases from 1 to 5.3 M (saturation), suggesting a less favored environment for ions to stay at saturation than at 1 M [10]. The higher activity coefficients at saturation has been ascribed to the limited "free" water for ion solvation. For instance, there are approximately 55 mol of water molecules in 1 L of aqueous solution, and it takes almost half of the water molecules to solvate 5 mol of NaCl molecules (i.e., the average reported hydration number for NaCl is about 6) [9]. The reduction in "free" water could disturb the favorable ion-ion interactions and increase the free energy as well as ion activity coefficients of the solution [9]. Similar situations are also found in XLPEGDA membranes as shown in Chapter 5.

Modeling efforts considering ion-water interactions have successfully described the increase of ion activity coefficients in concentrated electrolyte solutions [11]. However, due to the limited studies regarding ion activity coefficients in uncharged membranes together with a lack of theoretical framework guiding the analysis, the explicit interactions (e.g., polymer-ion, water-ion, and/or polymer-water) occurring in uncharged membranes remain unknown. More advanced thermodynamic treatment are needed to elucidate which of these interactions, or combinations of these interactions, are major contributors to the non-idealities in uncharged membranes

7.2.2 Influence of Electro-osmotic Water Flow on Ion Diffusion

As mentioned in Chapter 7, experimental Na^+ (i.e., counter-ions for CEMs) diffusion coefficients were well described by the Mackie and Meares model. However, many previous studies used radioactive tracers to determine membrane counter-ion

diffusion coefficients, whose values were found lower than the theoretical prediction of Mackie and Meares model [12]. This discrepancy was often ascribed to the electrostatic interactions between fixed charges and counter-ions [13]. However, recent studies have verified that the interactions between fixed charges and counter-ions have little impact on ion diffusion rates, even for highly charged membranes [14]. Some authors also claimed the diffusion rates obtained from the tracer method should be lower than those obtained from the ionic conductivity measurements, since electro-osmotic water flow involved in such tests often assists counter-ion diffusion [15], which might fortuitously bring counter-ion diffusion coefficients closer to the model predictions. A quantitative analysis on this aspect needs experimentally determining the electro-osmotic water flux and correct for the its effect on individual ion diffusion coefficient.

7.2.3 Explore Membrane Chemistry on Ion Transport Properties

Studies exploring how different polymer chemistry influences water and ion transport characteristics is of great interest. This work has extensively investigated three series of polymers based on PEGDA and AMPS. However, due to the hydrophilicity of PEGDA, highly charged polymers are often fragile. Thus, replacing PEGDA with more hydrophobic monomers that have similar backbone architecture can effectively generate a more broad range of charged polymers, enabling investigations on the effect of membrane chemistry on ion transport properties. Tables 3 and 4 list possible crosslinkers and monomers that could be used to produce additional series of sulfonated crosslinked hydrogel polymers. A shorter crosslinker will increase the degree of crosslinking and lower the water uptake of the membrane, while the introduction of a more hydrophobic crosslinker or monomer will reduce the water uptake of the membrane.

Table 7.1 Crosslinkers which could be used in this work; n is the degree of polymerization

Poly(ethylene glycol) diacrylate	n > 1	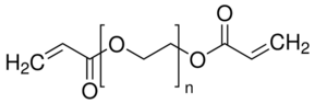
	n = 1	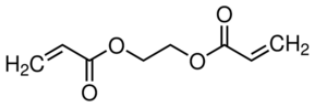
Poly(ethylene glycol) dimethacrylate	n > 1	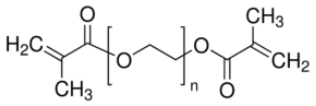
	n = 1	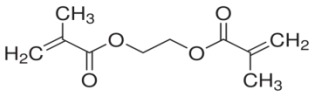
Poly(propylene glycol) diacrylate	n > 1	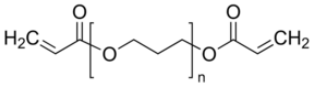
Poly(propylene glycol) dimethacrylate	n > 1	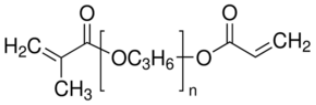
1,3-Butanediol diacrylate		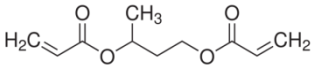
1,4-Butanediol diacrylate		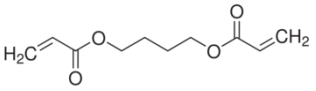
1.4-Butanediol dimethacrylate		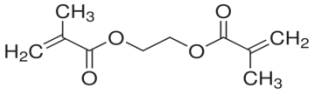

Table 7.2 Alternative monomers that could be used.

2-Sulfoethyl methacrylate		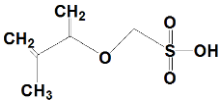
3-Sulfopropyl methacrylate		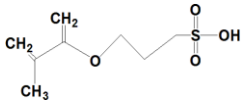
3-Sulfopropyl acrylate		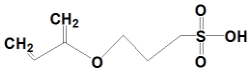
Sodium 4-vinylbenzenesulfonate		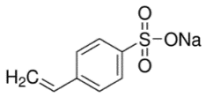
Poly(ethylene glycol) acrylate		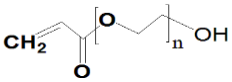
[2-(Methacryloyloxy)ethyl]trimethylammonium chloride		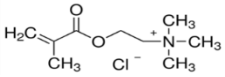
[2-(Acryloyloxy)ethyl]trimethylammonium chloride		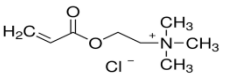
Poly(ethylene glycol) methyl ether acrylate	n > 1	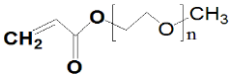
	n = 1	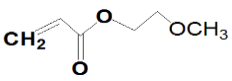
Poly(ethylene glycol) phenyl ether acrylate	n > 1	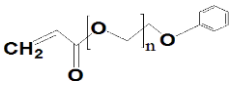
	n = 1	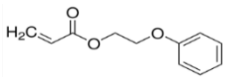

7.3 REFERENCES

[1] F. Hernández-Luis, H.R. Galleguillos, L. Fernández-Mérida, O. González-Díaz, Activity coefficients of NaCl in aqueous mixtures with ε-increasing co-solvent: Formamide–water mixtures at 298.15 K, Fluid Phase Equilibria, 275 (2009) 116-126.

[2] J. Newman, K.E. Thomas-Alyea, Electrochemical systems, John Wiley & Sons, 2012.

[3] K. Oldham, J. Myland, A. Bond, Electrochemical science and technology: Fundamentals and applications, John Wiley & Sons, 2011.

[4] S. Kalakkunnath, D.S. Kalika, H. Lin, R.D. Raharjo, B.D. Freeman, Molecular relaxation in cross-linked poly (ethylene glycol) and poly (propylene glycol) diacrylate networks by dielectric spectroscopy, Polymer, 48 (2007) 579-589.

[5] J. Kamcev, D.R. Paul, B.D. Freeman, Ion activity coefficients in ion exchange polymers: Applicability of Manning's counterion condensation theory, Macromolecules, 48 (2015) 8011-8024.

[6] F. Hernández-Luis, E. Amado-González, M.A. Esteso, Activity coefficients of NaCl in trehalose–water and maltose–water mixtures at 298.15 K, Carbohydrate Research, 338 (2003) 1415-1424.

[7] H. Ju, B.D. McCloskey, A.C. Sagle, V.A. Kusuma, B.D. Freeman, Preparation and characterization of crosslinked poly (ethylene glycol) diacrylate hydrogels as fouling-resistant membrane coating materials, Journal of Membrane Science, 330 (2009) 180-188.

[8] E.-S. Jang, J. Kamcev, K. Kobayashi, N. Yan, M. Galizia, R. Sunjai, H.B. Park, D.R. Paul, B.D. Freeman, Effect of water content on alkali metal chloride sorption in cross-linked poly(ethylene glycol diacrylate), In Preparation, (2017).

[9] J.O.M. Bockris, A.K.N. Reddy, M.E. Gamboa-Aldeco, I. NetLibrary, Modern electrochemistry: Volume 1, Ionics, 2nd ed., Kluwer Academic, New York, 2002.

[10] R.A. Robinson, R.H. Stokes, Electrolyte solutions, Courier Corporation, 2002.

[11] C.C. Chen, H.I. Britt, J. Boston, L. Evans, Local composition model for excess Gibbs energy of electrolyte systems. Part I: Single solvent, single completely dissociated electrolyte systems, AIChE Journal, 28 (1982) 588-596.

[12] J. Kamcev, B.D. Freeman, Charged polymer membranes for environmental/energy applications, Annual Review of Chemical and Biomolecular Engineering, 7 (2016) 111-133.

[13] P. Meares, Self-diffusion coefficients of anions and cations in a cation-exchange resin, The Journal of Chemical Physics, 55 (1958) 273-279.

[14] J. Kamcev, D.R. Paul, G.S. Manning, B.D. Freeman, Predicting salt permeability coefficients in highly swollen, highly charged ion exchange membranes, ACS Applied Materials & Interfaces, 9 (2017) 4044-4056.

[15] P. Meares, Coupling of ion and water fluxes in synthetic membranes*, Journal of Membrane Science, 8 (1981) 295-307.

Appendix A: Supporting Information for Chapter 4[4]

A.1 ATR-FTIR Analysis

Figure A.1 (a) presents the FTIR spectrum of the copolymer XL(AMPS-PEGDA) (40 wt% AMPS) compared to that of the comonomer AMPS and cross-linker PEGDA. In the spectrum of the copolymer, the disappearance of bands at 809 cm^{-1} (CH2=CH twisting/wagging) [1-3], 1189 cm^{-1} (acrylate C=O stretching) [1, 4], 1636 cm^{-1} (CH2=CH stretching) [2, 5, 6], and 1407 cm^{-1} (deformation of CH2=CH) [1, 7] suggests complete acrylate conversion of PEGDA in the polymer. The decrease of absorption peaks in the copolymer at about 920 and 980 cm^{-1} indicates the disappearance of double bonds in AMPS [7, 8].

[4] This chapter has been adapted from: Yan, N., Paul, D.R., Freeman, B.D., Water and ion sorption in a series of cross-linked AMPS/PEGDA hydrogel membranes (in preparation). Yan, N. made the major contributions to this chapter.

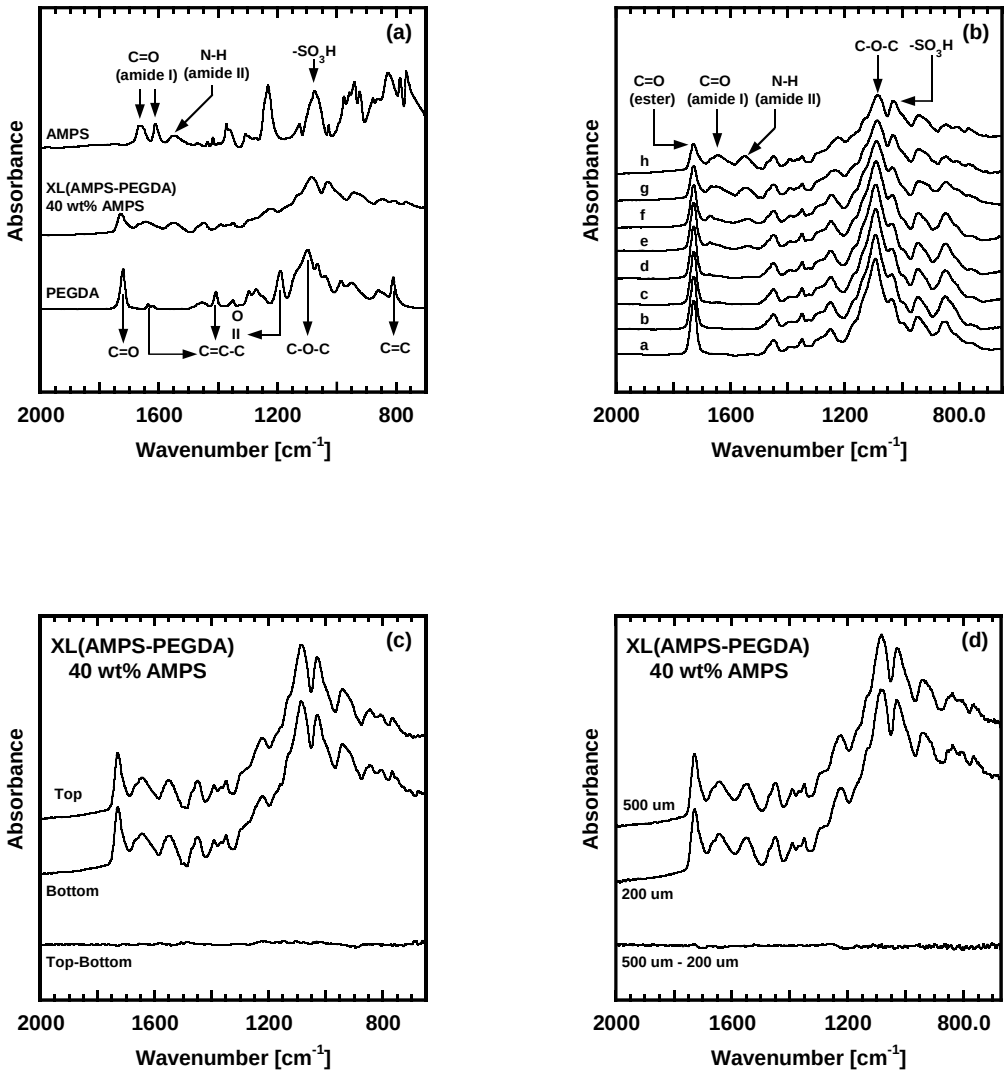

Figure A.1 FTIR spectra of: (a) copolymer XL(AMPS-PEGDA), comonomer AMPS, and cross-linker PEGDA, (b) XL(AMPS-PEGDA) with varied AMPS content (wt%): a-0, b-0.2, c-1, d-3, e-9, f-20, g-30, h-40, (c) two surfaces of a XL(AMPS-PEGDA) film and the subtraction spectrum between them, and (d) two XL(AMPS-PEGDA) films of different thickness and the subtraction spectrum between them.

The structure of the copolymer XL(AMPS-PEGDA) can be verified by the FTIR spectra shown in Figure A.1 (a). The two characteristic absorption peaks for PEGDA at 1720 cm^{-1} (ester C=O stretching) [9-11] and 1097 cm^{-1} (ether C-O-C stretching) [12-14] appear in the spectrum of the copolymer. Moreover, the typical absorption peaks for AMPS at 1656 and 1611 cm^{-1} (amide I, C=O stretching) [15, 16], 1550 cm^{-1} (amide II, N-H bending) [17-19], 1075 cm^{-1} (-SO_3H, S=O stretching) [20-24] are also evident in the spectrum of the copolymer. This evidence confirms the presence of AMPS and PEGDA in the copolymer. Figure S1 (b) depicts the FTIR spectra of films with different AMPS content. The spectrum of XLPEGDA (0 wt% AMPS) is consistent with that reported in previous studies [25]. Superimposing the spectra shows that the intensity of the characteristic peaks is a function of the monomer composition in the copolymer. When AMPS content is low (0.2 wt%, IEC of 0.01 meq/g), the characteristic amide groups peaks are weak. The intensity of the peaks (e.g., amide I and II, and the sulfonic acid group) corresponding to the AMPS moiety increases with increasing AMPS content in the copolymer. Additionally, the decrease of AMPS content in the copolymer is accompanied by an enhancement of the peaks (e.g., ester and ether groups) arising from the PEGDA moiety.

Figure A.1 (c) presents a comparison of the spectra of a typical copolymer's top and bottom surfaces. During copolymerization, UV light reaches the top surface of the membrane first and travels through the depth of the membrane [1]. For a membrane with a thickness of about 500 μm, there is an insignificant difference between the two surfaces, which implies that UV light has been able to reach the bottom surface to initiate the copolymerization. As presented in Figure A.1 (d), from comparing the spectra of the

same polymer cast with thickness of 500 μm and 200 μm, the difference between the two spectra is negligible. Therefore, the copolymerization effectiveness is independent of membrane thickness over the thickness range considered.

A.2 THERMAL ANALYSIS

Thermal stabilities of the polymers were investigated by thermogravimetric analysis (TGA) in a nitrogen stream. Figure A.2 presents the TGA curves of the homopolymers XLPEGDA, PAMPS, and the copolymer XL(AMPS-PEGDA) (40 wt% AMPS). As seen in Figure A.2, the scan of XLPEGDA shows only one degradation step in the temperature range from 230 to 480 ℃, after which the weight loss change is negligible [2]. However, the TGA curves of PAMPS and the copolymer show a multi-stage decomposition procedure. The initial 6% weight loss occurs before 185 ℃, which may be due to the evaporation of moisture (e.g., water bound to the sulfonic acid group) [3]. The second weight loss stage (185-260 ℃) is mainly ascribed to the cleavage of weak cross-links and the decomposition of amide groups [4, 5]. The polymers decompose in a single step above 260 ℃ due to the loss of sulfonic acid groups and the scission of the main chain of PEGDA, then followed by the breaking of primary chemical bonds (e.g., C-C covalent bonds) above 350 ℃ [4].

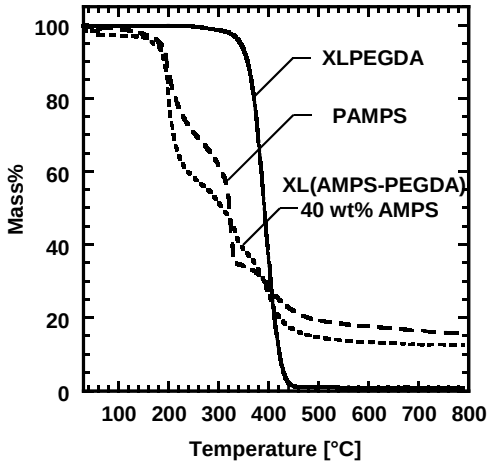

Figure A.2 TGA profiles of homopolymers XLPEGDA, PAMPS, and copolymer XL(AMPS-PEGDA) with 40 wt% AMPS.

The DSC thermograms of the homopolymers XLPEGDA, PAMPS, and the copolymers are collected in Figure A.3. The onset, midpoint, and endpoint temperature of the glass transition of each polymer are recorded in Table S1. The midpoint of the heat capacity change was reported as T_g, which for the homopolymers XLPEGDA and PAMPS were found to be -23 ℃ and 118 ℃, in agreement with literature values [6]. The literature reported T_g values of linear PAMPS ranges from 67 ℃ to 126 ℃ [5, 7-16] due to differences in polymer preparation, molecular weight, and measurement method [6, 17]. The glass transition in PAMPS was found to be rather broad and weak, which could be due to the low heat capacity change associated with its glass transition [15, 18].

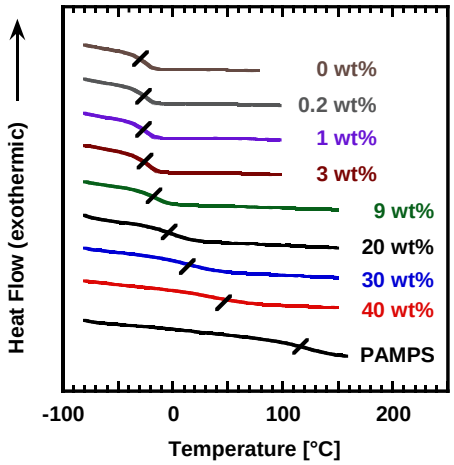

Figure A.3 DSC thermograms (second heating scan) are displaced vertically for clarity. The midpoint of the glass transition in each polymer was identified.

The thermomechanical properties of the homopolymer XLPEGDA and select copolymers are presented in Figure A.4. The thermomechanical characteristic of the linear polymer PAMPS could not be obtained due to its powder state. Table A.1 also presents the onset temperature of storage modulus (E'), peak temperature of loss modulus (E''), and peak temperature of loss tangent (tan δ). The difference in T_gs between DSC and DMA values is in a reasonable range that has been found in other PEG-based and/or sulfonated polymers [19-23].

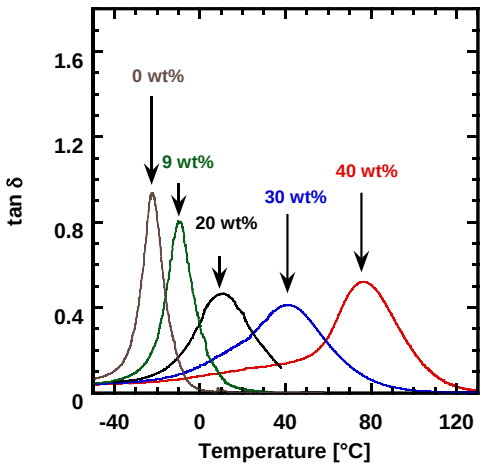

Figure A.4: DMA tan δ-temperature curves (frequency = 1 Hz, heating rate = 2 °C/min) in polymers with varied AMPS content (wt %). Select DMA scans (i.e. AMPS content 0.2-3 wt%) are not shown for clarity. The arrows point at the peak of the tan δ-temperature curve.

The homogeneity of a copolymer can be probed by DSC as well as DMA, the latter being a more sensitive technique to detect segmental chain motions than DSC [20, 24]. Generally, the detection of two glass transitions corresponding to those of the component homopolymers could be caused by partial or complete phase separation [25]. The single T_g of all the copolymers located between the T_gs of the two component homopolymers suggests homogeneity of the copolymers studied here [26-28]. In addition, the T_g of a homogeneous polymer can be greatly influenced by the copolymer composition [8, 22]. As demonstrated in Figure A.3, Figure A.4, and Table A.1, T_gs, assigned as the midpoint (DSC) and tan δ peak (DMA) of the glass transition, progressively shift to higher temperatures as AMPS content increases, indicating the dependence of T_g on polymer composition.

Table A.1 The onset, midpoint, and endpoint temperatures of the glass transition (DSC) and the onset temperature of the storage modulus (E'), the peak temperature of the loss modulus (E'') and loss tangent (tan δ) of the glass transition (DMA). T_g s of the polymers were determined as the midpoint temperature of the glass transition (DSC) and the peak temperature of the tan δ-temperature curve (DMA).

AMPS [wt%]	**DSC**				**DMA**		
	Onset Temp [°C]	Mid Temp [°C]	Endpoint Temp [°C]	ΔT [°C][a]	Temp at E'_{onset} [°C]	Temp at E''_{peak} [°C]	Temp at tan δ_{peak} [°C]
0	-30	-23	-20	10	-31	-30	-22
0.2	-30	-23	-19	11	-31	-30	-22
1	-29	-22	-18	11	-30	-29	-21
3	-28	-20	-16	12	-27	-26	-18
9	-24	-14	-8	16	-21	-19	-10
20	-16	0	15	31	-8	-8	10
30	-7	14	43	50	7	[b]	41
40	6	42	72	66	41	60	75
100	87	118	132	46	-	-	-

[a] $\Delta T = T_{endpoint} - T_{onset}$. [b] Not distinguishable

The mechanical relaxation characterized by tan δ-temperature curve shows an evident "shoulder" between -25 °C to 15 °C. This 'shoulder' only exists in the copolymers as AMPS content increases to 20 wt% and higher. It is not detected in the XLPEGDA homopolymer. This phenomenon has been observed in other hydrophilic PEO-based and/or sulfonated polymers [44, 45], and may suggest occurrence of a secondary relaxation (e.g., localized bond movements, side chain movements) as the material warms and expands. This relaxation could involve the release of small amounts of water bound to the relaxed polymer chains [42, 45, 51]. Therefore, these 'shoulders'

could be attributed to the moisture bound to the hydrophilic sulfonate groups in AMPS and/or the relaxation related to AMPS component in the copolymer.

The T_g of a copolymer can be estimated by an empirical rule of mixtures model assuming no interaction between the components [29]. The dependence of T_g on the copolymer composition and the T_gs of the respective homopolymers is described by the following equation [29]:

$$T_g = w_1 T_{g,1} + w_2 T_{g,2} \quad \text{(A.1)}$$

where w_1 and w_2 are the mass fractions of the two components in the copolymer, $T_{g,1}$, and $T_{g,2}$ are the glass transition temperatures of the pure component homopolymer, respectively. With the experimentally measured T_gs of XLPEGDA and PAMPS, the copolymer's glass transition temperature can be estimated using Eqn. (A.1). The experimental T_gs are in reasonable agreement with the model predictions as shown in Figure A.5.

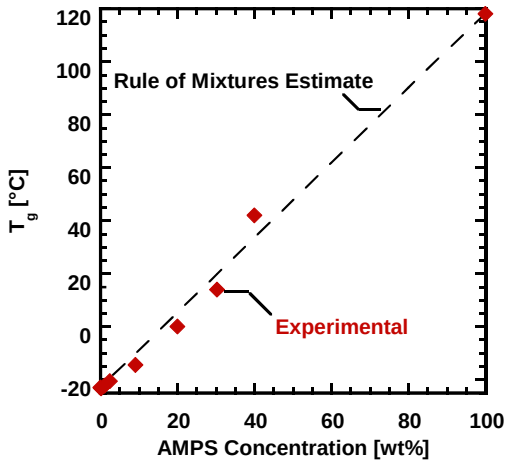

Figure A.5 Dependence of T_gs measured by DSC on polymer composition. The dashed line is the estimate based on the rule of mixtures.

A.3 REFERENCES

[1] A.C. Sagle, H. Ju, B.D. Freeman, M.M. Sharma, PEG-based hydrogel membrane coatings, Polymer, 50 (2009) 756-766.

[2] K. Wang, J. Guan, F. Mi, J. Chen, H. Yin, J. Wang, Q. Yu, A novel method for preparation of cross-linked PEGDA microfibers by low-temperature photopolymerization, Materials Letters, 161 (2015) 317-320.

[3] C. Soykan, R. Coşkun, S. Kirbağ, E. Şahin, Synthesis, characterization and antimicrobial activity of poly (2-acrylamido-2-methyl-1-propanesulfonic acid-co-crotonic acid), Journal of Macromolecular Science Part A: Pure and Applied Chemistry, 44 (2007) 31-39.

[4] Y. Aggour, Thermal degradation of copolymers of 2-acrylamido-2-methylpropanesulphonic acid with acrylamide, Polymer Degradation and Stability, 44 (1994) 71-73.

[5] C. Zhang, A.J. Easteal, Study of poly (acrylamide-co-2-acrylamido-2-methylpropane sulfonic acid) hydrogels made using gamma radiation initiation, Journal of Applied Polymer Science, 89 (2003) 1322-1330.

[6] J. Illescas, Y.S. Ramírez-Fuentes, G. Zaragoza-Galan, P. Porcu, A. Mariani, E. Rivera, PEGDA-based luminescent polymers prepared by frontal polymerization, Journal of Polymer Science Part A: Polymer Chemistry, 53 (2015) 2890-2897.

[7] M.B. Huglin, J.M. Rego, S.R. Gooda, Comments on thermal transitions in some polyelectrolyte complexes, Macromolecules, 23 (1990) 5359-5361.

[8] L. Chikh, S. Girard, D. Teyssie, O. Fichet, Proton conducting PAMPS networks: From flexible to rigid materials, Journal of Applied Polymer Science, 107 (2008) 3672-3680.

[9] Y. Shen, J. Xi, X. Qiu, W. Zhu, A new proton conducting membrane based on copolymer of methyl methacrylate and 2-acrylamido-2-methyl-1-propanesulfonic acid for direct methanol fuel cells, Electrochimica Acta, 52 (2007) 6956-6961.

[10] K. Kabiri, H. Mirzadeh, M.J. Zohuriaan-Mehr, M. Daliri, Chitosan-modified nanoclay-poly (AMPS) nanocomposite hydrogels with improved gel strength, Polymer International, 58 (2009) 1252-1259.

[11] U. Sen, O. Acar, A. Bozkurt, A. Ata, Proton conducting polymer blends from poly (2, 5-benzimidazole) and poly (2-acrylamido-2-methyl-1-propanesulfonic acid), Journal of Applied Polymer Science, 120 (2011) 1193-1198.

[12] H. Erdemi, A. Bozkurt, W.H. Meyer, PAMPSA-IM based proton conducting polymer electrolytes, Synthetic Metals, 143 (2004) 133-138.

[13] Y.H. Lee, J.Y. Lee, D.S. Lee, A novel conducting soluble polypyrrole composite with a polymeric co-dopant, Synthetic Metals, 114 (2000) 347-353.

[14] S. Günday, A. Bozkurt, W.H. Meyer, G. Wegner, Effects of different acid functional groups on proton conductivity of polymer-1, 2, 4-triazole blends, Journal of Polymer Science Part B: Polymer Physics, 44 (2006) 3315-3322.

[15] A. Martinez-Felipe, Z. Lu, P.A. Henderson, S.J. Picken, B. Norder, C.T. Imrie, A. Ribes-Greus, Synthesis and characterisation of side chain liquid crystal copolymers containing sulfonic acid groups, Polymer, 53 (2012) 2604-2612.

[16] R. Coşkun, C. Soykan, A. Delibaş, Study of free-radical copolymerization of itaconic acid/2-acrylamido-2-methyl-1-propanesulfonic acid and their metal chelates, European Polymer Journal, 42 (2006) 625-637.

[17] C. Zhang, A.J. Easteal, Study of free-radical copolymerization of N-isopropylacrylamide with 2-acrylamide-2-methyl-1-propanesulphonic acid, Journal of Applied Polymer Science, 88 (2003) 2563-2569.

[18] H. Every, M. Forsyth, D. MacFarlane, Plasticized single conductung polyelectrolytes based on poly (AMPS), Ionics, 2 (1996) 53-62.

[19] P.E. Inc., DMA - A beginner's guide Roylance, 2001.

[20] K.P. Menard, Dynamic mechanical analysis: a practical introduction, CRC press, 2008.

[21] J.D. Menczel, R.B. Prime, Thermal analysis of polymers: fundamentals and applications, John Wiley & Sons, 2014.

[22] H.J. Oh, B.D. Freeman, J.E. McGrath, C.H. Lee, D.R. Paul, Thermal analysis of disulfonated poly (arylene ether sulfone) plasticized with poly (ethylene glycol) for membrane formation, Polymer, 55 (2014) 235-247.

[23] Z. Bai, M.D. Houtz, P.A. Mirau, T.D. Dang, Structures and properties of highly sulfonated poly (arylenethioethersulfone) s as proton exchange membranes, Polymer, 48 (2007) 6598-6604.

[24] P. Gabbott, Principles and applications of thermal analysis, John Wiley & Sons, 2008.

[25] R.A. Basheer, A.R. Hopkins, P.G. Rasmussen, Dependence of transition temperatures and enthalpies of fusion and crystallization on composition in polyaniline/nylon blends, Macromolecules, 32 (1999) 4706-4712.

[26] J. Qiao, T. Hamaya, T. Okada, Chemically modified poly (vinyl alcohol)-poly (2-acrylamido-2-methyl-1-propanesulfonic acid) as a novel proton-conducting fuel cell membrane, Chemistry of Materials, 17 (2005) 2413-2421.

[27] S. Goh, H. Chan, C. Ong, Miscible blends of conductive polyaniline with tertiary amide polymers, Journal of Applied Polymer Science, 68 (1998) 1839-1844.

[28] Z. Li, E. Ruckenstein, Improved surface properties of polyaniline films by blending with Pluronic polymers without the modification of the other characteristics, Journal of Colloid and Interface Science, 264 (2003) 362-369.

[29] J.R. Fried, Polymer science and technology, Pearson Education, 2014.

Appendix B: Supporting Information for Chapter 5[5]

B.1 Water Uptake and Fixed Charge Concentration

Equilibrium pure water uptake in three series of uncharged and charged membranes is presented as a function of IEC value in in Figure B.1. For each series of membranes (i.e., prepared using the same PEGDA chain length), w_u increases by roughly 20-40% as IEC increases. An IEC increase is often accompanied by an increase in polymer-water affinity and a decrease in polymer cross-link density, v_t [1]. However, the level of decrease in v_t (i.e., 30-40%) for each series of membranes has a negligible effect on water uptake, based on predictions of the Flory-Rehner theory [2, 3]. Thus, the increase in w_u with increasing IEC is mainly caused by increases in polymer hydrophilicity.

[5] This chapter has been adapted from: Yan, N., Kamcev, J., Galizia, M., Jang E.S., Paul, D.R., Freeman, B.D., Influence of fixed charge concentration and wataer uptake on ion sorption in AMPS/PEGDA membranes (in preparation). Yan, N. made the major contributions to this chapter.

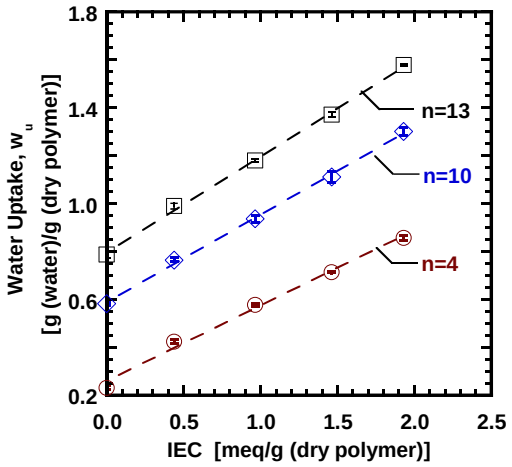

Figure B.1 The dependence of water uptake on IEC. Dashed lines were drawn to guide the eye. The water uptake values were measured by equilibrating the samples in DI water.

Among membranes having constant IEC, w_u increases by a factor of 2~4 as PEGDA chain length, n, increases from 4 to 13. Increases in n reduce polymer cross-link density, providing less elasticity to restrict membrane swelling, and increase the concentration of hydrophilic ethylene oxide groups [4, 5]. Based on the Flory-Rehner model, about 80% of this increase is due to the enhanced polymer hydrophilicity (i.e., the Flory polymer-water interaction parameter decreases), and 20% is caused by the reduction in v_t [2].

Figure B.2 shows the membrane fixed charge concentration, C_A^m, correlated with IEC and water uptake (i.e., $C_A^m = \frac{IEC}{w_u}$). Thus, at a given PEGDA chain length (i.e., n), C_A^m increases non-linearly with increasing IEC due to the concomitant increase in IEC and

w_u [6]. For polymers having the same IEC, their C_A^m decreases as n increases, mainly due to the increase in polymer water uptake [1].

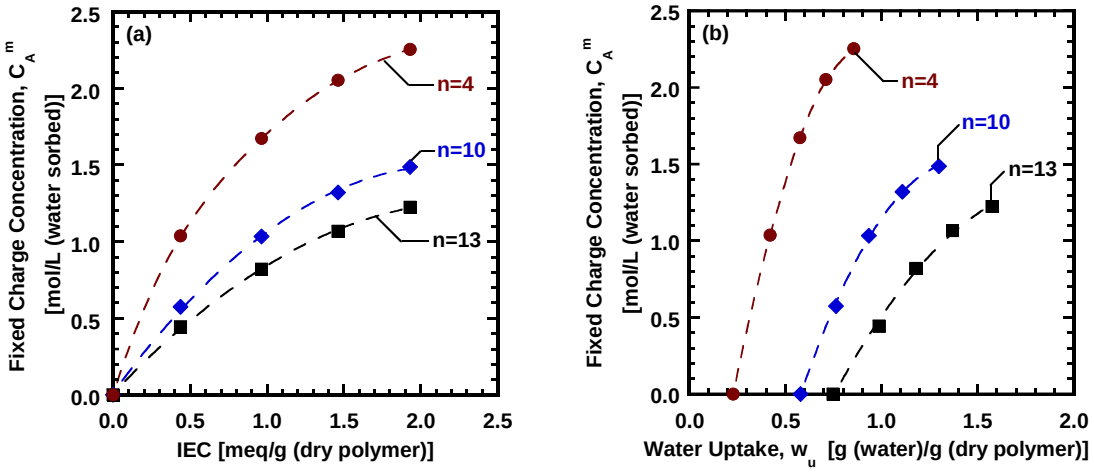

Figure B.2 The influence of: (a) IEC and (b) water uptake on fixed charge concentration.

B.2 Charge Distance

The average distance between successive fixed charges on the polymer chain can be estimated based on the polymer composition. The XL(AMPS-PEGDA) membranes considered in this study are all transparent and likely homogeneous [6]. The polymer chains are assumed to be extended between cross-links, and the charged groups are uniformly distributed along the polymer chain as envisioned in Manning's model [7]. Therefore, the average number of cross-linkers (PEGDA) between two charged monomers

(AMPS) can be determined from the mass ratio of PEGDA/AMPS and their corresponding molecular weights. For example, the dry polymer of sample 4-2.18 (i.e., a polymer having an IEC value of 2.18 meq/g cross-linked with PEGDA of n = 4) contains 9.76 g of AMPS and 8 g of PEGDA. Thus, the molar ratio of PEGDA/AMPS is about 1:1, indicating there is approximately one PEGDA molecule for each AMPS molecule. Figure B.3 provides a schematic of the possible distance between two fixed charge groups (-SO_3H) assuming a representative segment of the polymer network is in a zig-zag conformation [7]. Since the projected distance is about 2.5 Å for the C-C-C bond and 2.1 Å for C-O-C bond [8], the estimated distance between neighboring -SO_3H groups (i.e., the projected distance of the red chain segment in) is about 21 Å for the sample 4-2.18. The dielectric constant, ε, in the swollen polymer is estimated as the sum of the dielectric constants of pure water (~78 at ambient conditions) and XLPEGDA (~12) [9] multiplied by their volume fractions in the swollen polymer, as described elsewhere [7]. Thus, the calculated ξ value using Eqn. (2.12) for sample 4-2.18 is 0.53. The other calculated b, ε, λ_B, and ξ values were calculated similarly and are recorded in Table 5.1.

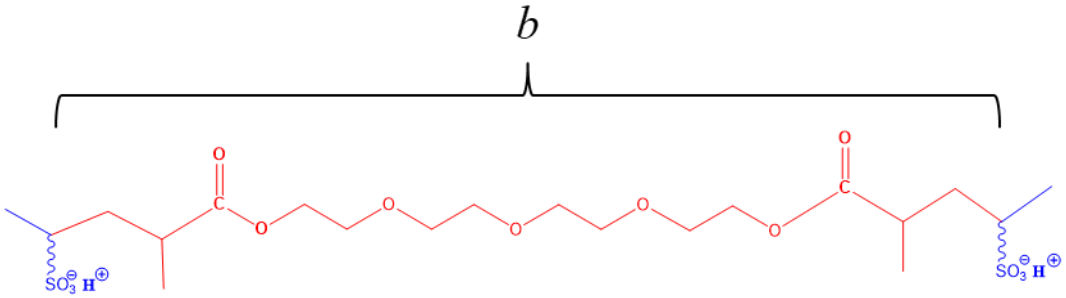

Figure B.3 A segment chain between two charged groups in a zig-zag conformation.

B.3 THEORETICAL PREDICATIONS BY DONNAN AND MANNING THEORIES

From Eqs. (2.13)-(2.14), membrane mobile salt sorption coefficient, K_s, and ion activity coefficients, $\gamma_+^m\gamma_-^m$, depend on external salt concentration, C_s^s, fixed charge concentration, C_A^m, and ξ (i.e., fixed charge distribution) [10]. When C_s^s and ξ are held constant, the effect of C_A^m on ion sorption and activity coefficients can be examined. Thus, Eqs. (2.13)-(2.14) were numerically solved for K_s and $\gamma_+^m\gamma_-^m$ in four variously charged membranes at constant ξ (ξ = 0.1, no counter-ion condensation). The results are presented in Figure B.4 (a) and (b), respectively. C_A^m varies from 0.01 to 10 mol/L (water sorbed), within the range typically reported in literature [11]. For each membrane, C_A^m is assumed to be independent of C_s^s (i.e., membrane volume is constant) [12].

Figure B.4 (a) shows K_s as a function of C_s^s in membranes having the same ξ but different C_A^m. As C_A^m increases from 0.01 to 10 mol/L (water sorbed), K_s decreases by 3 orders of magnitude, presumably due to stronger co-ion exclusion effect [12]. As mentioned earlier, co-ion exclusion effect depends on Donnan potential at the membrane/solution interface [1]. Based on Donnan theory, higher C_A^m can increase Donnan potential (at constant C_s^s), which promotes co-ion exclusion [1, 13]. For all the membranes, K_s appears to increase with increasing C_s^s. However, the dependence of K_s on C_s^s varies with C_A^m value. For example, at high C_A^m [e.g., 10 mol/L (water sorbed)], K_s increases exponentially as C_s^s increases, due to weakened co-ion exclusion effect at high C_s^s [6, 14]. This behavior is typical for charged membranes [10, 14]. At high C_s^s, fixed charges are "screened" by ions, resulting in less effective C_A^m and co-ion exclusion [10, 14]. In contrast, at low C_A^m [e.g., 0.01 mol/L (sorbed water)], K_s is about one over the entire range of C_s^s. In this case ($C_A^m \leq C_s^s$), co-ion exclusion is no longer effective due to the "screening" effect. Consequently, this membrane behaves like an

uncharged membrane, where the salt concentrations are equal in the membrane and solution phases [i.e., $K_s = 1$ as $\frac{C_A^m}{C_s^s} \to 0$ in Eqn. (2.8)] [14].

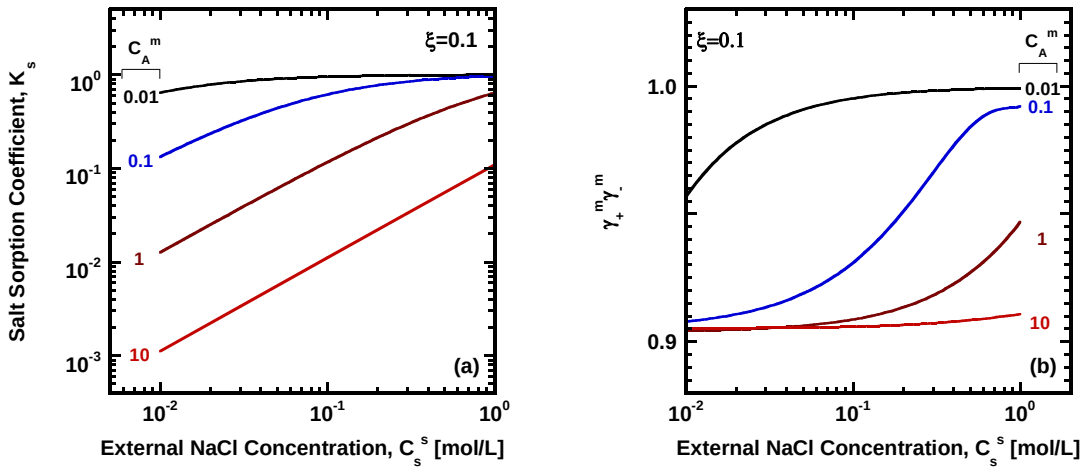

Figure B.4 Calculated (a) mobile salt sorption coefficients and (b) ion activity coefficients as a function of the external NaCl concentration in four imaginary membranes having constant ξ of value 0.1 and different fixed charge concentrations [mol/L (water sorbed)].

Figure B.4 (b) plots $\gamma_+^m \gamma_-^m$ as a function C_s^s in the membranes at constant ξ [cf. Eqn. (2.14)]. $\gamma_+^m \gamma_-^m$ can characterize non-ideal ion behaviors in membranes. Non-idealities typically arise when ions interact with other species (e.g., ion-ion, polyion-ion, etc.). A phase is considered ideal if no interactions are present (i.e., $\gamma_+^m \gamma_-^m = 1$). Normally, $\gamma_+^m \gamma_-^m < 1$ means ions are attracted to the membrane. Oppositely, $\gamma_+^m \gamma_-^m > 1$ means ions are excluded from the membrane. As shown in Figure B.4 (b), all predicted $\gamma_+^m \gamma_-^m$ values are below one. The deviation of membrane ion activity coefficients from ideal case is predominantly due to the electrostatic interactions between counter-ions and

fixed charges on the polymer chain [15]. Studies show, counter-ions (e.g., Na^+) typically have stronger affinity to fixed charges (e.g., $-SO_3^-$) in the membrane than co-ions (e.g., Cl^-) in solution [16]. Thus, the favorable interactions between counter-ions and fixed charges lead to a lower system free energy, and, in turn, $\gamma_+^m\gamma_-^m$ falls below one [7, 13, 17, 18]. In addition, $\gamma_+^m\gamma_-^m$ appears to decrease (5~10%) with increasing C_A^m at fixed C_S^s. According to Manning, $\gamma_+^m\gamma_-^m$ values depend on the extent of polyion-ion interactions [17], which is determined by the concentrations of interacting species (i.e., fixed charges and mobile ions) [7]. In IEMs, sorbed mobile ion concentration is typically negligible relative to that of fixed charges, due to co-ion exclusion. As a result, the contribution of mobile ions to the magnitude of polyion-ion interactions is much smaller than that of fixed charges. Thus, as C_A^m increases, polyion-ion interactions become stronger and, in turn, system free energy and $\gamma_+^m\gamma_-^m$ decrease [7, 17].

Figure B.4 (b) shows that the trends of $\gamma_+^m\gamma_-^m$ with C_S^s exhibit different shapes in membranes having different C_A^m values. For example, at high C_A^m [e.g., 10 mol/L (water sorbed)], $\gamma_+^m\gamma_-^m$ changes little with C_S^s and shows an asymptotic leveling at low C_S^s (i.e., $C_A^m \gg C_S^s$). This scenario occurs because the fixed charge concentration significantly exceeds that of sorbed mobile ions due to strong co-ion exclusion effect at low C_S^s. Thus, only C_A^m contributes to the extent of polyion-ion interactions, which keeps unchanged if C_A^m is constant. According to Manning, as $\frac{C_A^m}{C_S^s} \to \infty$ in Eqn. (2.13), $\gamma_+^m\gamma_-^m$ approaches an asymptotic value equal to $\exp(-\xi)$ [i.e., $\exp(-0.1) \approx 0.9$ in Figure B.4 (b)]. In contrast, when $C_A^m = 0.01$ mol/L (water sorbed), $\gamma_+^m\gamma_-^m$ initially increases by 5% as C_S^s increases, followed by a plateau at unity. This leveling at high C_S^s occurs when all fixed charge groups are effectively taken off the polymer chain (i.e.,

$C_A^m \to 0$), or when they are fully "screened" by concentrated ions ($C_A^m \ll C_s^s$). In each scenario, the interactions between fixed charges and counter-ions are weak due to less effective fixed charges. When the only interactions (i.e., polyion-ion) considered by Manning vanish, the system is analogous to an ideal solution, where the ion activity coefficients equal to one.

To investigate the influence of ξ on K_s and $\gamma_+^m\gamma_-^m$, Figure B.5 (a) and (b) present K_s and $\gamma_+^m\gamma_-^m$ values in the membranes having constant C_A^m [1 mol/L (water sorbed)] but different ξ (1~0.01, no counter-ion condensation). As shown in Figure B.5 (a), K_s in all membranes increase dramatically with increasing C_s^s due to the weakened co-ion exclusion effect at high C_s^s. This behavior is qualitatively similar to that observed in Figure B.4 (a) at high C_A^m. At fixed C_s^s (e.g., 0.01 mol/L), K_s decreases by 50% as ξ ($= \frac{\lambda_B}{b}$) decreases from 1 to 0.1. If λ_B is assumed constant (i.e., same dielectric constant and conditions), the decrease in ξ indicates increasing fixed charge distance, b. That is, the fixed charges are less densely distributed on the polymer, which generates relatively isolated electric fields along the chain. Consequently, the attractions between fixed charges and counter-ions are reduced, resulting in less mobile counter-ion (i.e., mobile salt) sorption as ξ decreases. Interestingly, K_s only decreases by 20% as ξ decreases from 0.1 to 0.01. In this case, b increases to an extent that the interactions between isolated fixed charges and counter-ions are very weak, and, in turn, mobile counter-ions are no longer experiencing the attractions from fixed charges. The weak interactions eventually change little as ξ continues decreasing and, therefore, K_s, subjective to this interaction, becomes insensitive to ξ change.

Figure B.5 (b) shows $\gamma_+^m\gamma_-^m$ as a function of C_S^s in the membranes with constant C_A^m but different ξ. At high ξ (0.5 and above), the trends of $\gamma_+^m\gamma_-^m$ against C_S^s are qualitatively similar to that demonstrated in Figure B.4 (b) when $C_A^m = 1$ mol/L (water sorbed). As described earlier, $\gamma_+^m\gamma_-^m$ approaches an asymptotic value at low C_S^s [i.e., $\gamma_+^m\gamma_-^m = \exp(-\xi)$ as $\frac{C_A^m}{C_S^s} \to \infty$ in Eqn. (2.13)] and curves towards one at high C_S^s [i.e., $\frac{C_A^m}{C_S^s} \to 0$ in Eqn. (2.13)] [12]. However, at low ξ (0.1 and below), $\gamma_+^m\gamma_-^m$ approaches 1. This ideal behavior ($\gamma_+^m\gamma_-^m = 1$) results from the depressed polyion-ion interactions due to the less densely distributed fixed charges on the polymer as ξ decreases. When such interactions diminish, the system is essential ideal, as mentioned earlier [12, 17].

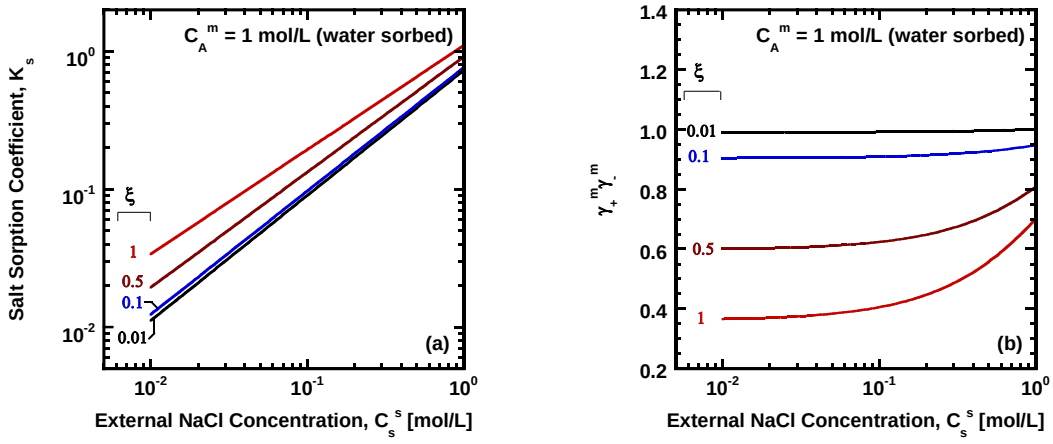

Figure B.5 The influence of ξ on the (a) mobile salt sorption coefficient and (b) ion activity coefficients as a function of the external NaCl concentration in hypothetical membranes having constant fixed charge concentration of value 1 mol/L (water sorbed).

Based on the analysis presented above (i.e., $\xi < 1$), one can expect increasing C_A^m at constant ξ can simultaneously decrease K_S (i.e., stronger co-ion exclusion) and

$\gamma_+^m\gamma_-^m$ (i.e., stronger polyion-ion interactions). On the other hand, increasing ξ (i.e., more densely distributed fixed charges) at constant C_A^m can increase K_s (i.e., more counter-ion sorption) while decreasing $\gamma_+^m\gamma_-^m$. These results will be useful in understanding the subsequent experimental sorption data. However, certain model limits must be considered. That is, Manning's model was originally developed for densely charged polyelectrolytes in aqueous solution. One would assume highly charged membranes equivalent to cross-linked polyelectrolytes, since electrostatic interactions between fixed charges and ions captured by polyelectrolyte theory are dominant in highly charged membranes [7]. However, such assumption might be inappropriate when the membrane is less charged or uncharged. For example, the ion activity coefficients predicted by Manning's model are always below one. Because polyelectrolyte solution is identical to an ideal solution when all fixed charges are effectively "neutralized" [i.e., $\frac{C_A^m}{C_s^s} \to 0$ in Eqn. (2.13)] [17]. Thus, ion activity coefficients in polyelectrolyte solution can not exceed those in ideal solution. However, this upper limit of ion activity coefficients does not apply to membranes. Indeed, the ion activity coefficients in uncharged membranes were reported to be much larger than one, likely due to unfavorable interactions between polymer backbone and ions [6]. However, further studies are needed to extend Manning's model to account for non-idealities introduced by uncharged polymer segments.

B.4 REFERENCES

[1] F. Helfferich, Ion Exchange, McGraw-Hill Book Co., Inc., New York, 1962.

[2] N.A. Peppas, E.W. Merrill, Poly (vinyl alcohol) hydrogels: Reinforcement of radiation-crosslinked networks by crystallization, Journal of Polymer Science: Polymer Chemistry Edition, 14 (1976) 441-457.

[3] P.J. Flory, Principles of polymer chemistry, Cornell University Press, 1953.

[4] H. Ju, A.C. Sagle, B.D. Freeman, J.I. Mardel, A.J. Hill, Characterization of sodium chloride and water transport in crosslinked poly (ethylene oxide) hydrogels, Journal of Membrane Science, 358 (2010) 131-141.

[5] H. Ju, B.D. McCloskey, A.C. Sagle, V.A. Kusuma, B.D. Freeman, Preparation and characterization of crosslinked poly (ethylene glycol) diacrylate hydrogels as fouling-resistant membrane coating materials, Journal of Membrane Science, 330 (2009) 180-188.

[6] N. Yan, D.R. Paul, B.D. Freeman, Water and ion sorption in a series of cross-linked AMPS/PEGDA hydrogel membranes, In preparation, (2017).

[7] J. Kamcev, D.R. Paul, B.D. Freeman, Ion activity coefficients in ion exchange polymers: Applicability of Manning's counterion condensation theory, Macromolecules, 48 (2015) 8011-8024.

[8] P.C. Hiemenz, T.P. Lodge, Polymer chemistry, CRC press, 2007.

[9] S. Kalakkunnath, D.S. Kalika, H. Lin, R.D. Raharjo, B.D. Freeman, Molecular relaxation in cross-linked poly (ethylene glycol) and poly (propylene glycol) diacrylate networks by dielectric spectroscopy, Polymer, 48 (2007) 579-589.

[10] J. Kamcev, M. Galizia, F.M. Benedetti, E.-S. Jang, D.R. Paul, B.D. Freeman, G.S. Manning, Partitioning of mobile ions between ion exchange polymers and aqueous salt solutions: importance of counter-ion condensation, Physical Chemistry Chemical Physics, 18 (2016) 6021-6031.

[11] T. Xu, Ion exchange membranes: state of their development and perspective, Journal of Membrane Science, 263 (2005) 1-29.

[12] J. Kamcev, D.R. Paul, B.D. Freeman, Effect of fixed charge group concentration on equilibrium ion sorption in ion exchange membranes, Journal of Materials Chemistry A, 5 (2017) 4638-4650.

[13] F.G. Donnan, Theory of membrane equilibria and membrane potentials in the presence of non-dialysing electrolytes. A contribution to physical-chemical physiology, Journal of Membrane Science, 100 (1995) 11.

[14] G.M. Geise, L.P. Falcon, B.D. Freeman, D.R. Paul, Sodium chloride sorption in sulfonated polymers for membrane applications, Journal of Membrane Science, 423-424 (2012) 195-208.

[15] R.A. Robinson, R.H. Stokes, Electrolyte solutions, Courier Corporation, 2002.

[16] M. Nagvekar, F. Tihminlioglu, R.P. Danner, Colligative properties of polyelectrolyte solutions, Fluid Phase Equilibria, 145 (1998) 15-41.

[17] G.S. Manning, Limiting laws and counterion condensation in polyelectrolyte solutions I. Colligative properties, The Journal of Chemical Physics, 51 (1969) 924-933.

[18] M. Galizia, F.M. Benedetti, D.R. Paul, B.D. Freeman, Monovalent and divalent ion sorption in a cation exchange membrane based on cross-linked poly (p-styrene sulfonate-co-divinylbenzene), Journal of Membrane Science, 535 (2017) 132-142.

Appendix C: Supporting Information for Chapter 6[6]

C.1 Solution-Diffusion Model

The solution-diffusion mechanism has been one of the most useful models for interpreting mass transport phenomenon in dense, non-porous membranes [1-3]. The model often describes chemical potential gradient across a homogeneous membrane as the overall driving force for the movement of penetrants [1, 4-7]. To derive mathematical equations for describing mass transport in the membrane, assumptions such as continuous concentration gradient and uniform pressure (i.e., at the feed pressure value) across the membrane are made, and the latter one allows the membrane to maintain mechanical equilibrium [1, 2, 8]. Figure C.1 shows a schematic of the chemical potential and concentration profiles in a membrane where salt transport occurs. The symbols shown in this figure have the following meanings: μ = chemical potential, c = concentration, J = molar flux. The phases external to the membrane surfaces at $x = 0$ and $x = L$ indicate the feed and permeate streams, respectively.

[6] This chapter has been adapted from: Yan, N., Kamcev, J., Jang E.S., Kobayashi, K., Paul, D.R., Freeman, B.D., Ion and Salt Transport in a Series of Crosslinked AMPS/PEGDA Hydrogel Membranes (in preparation). Yan, N. made the major contributions to this chapter.

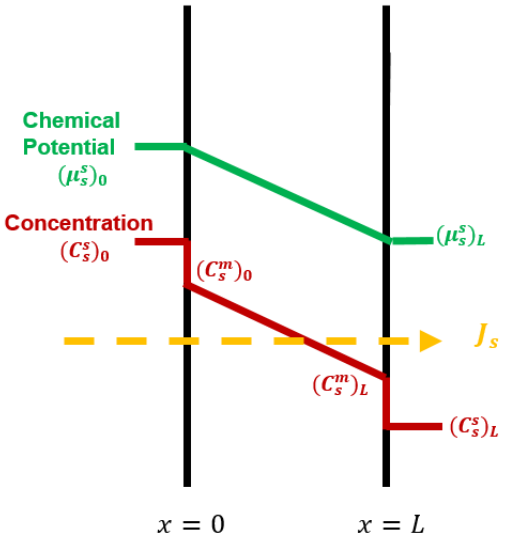

Figure C.1 Schematic of the chemical potential and concentration gradient in a dense, non-porous membrane.

As shown in Figure C.1, there is a continuous chemical potential gradient throughout the membrane based on the assumption that the solutions are in equilibrium with the membrane at both the feed and permeate interfaces [1, 9]. Thus, the molar flux of penetrant i, J_i [mol/(cm^{-2} sec $^{-1}$)], is described as the product of penetrate concentration, C_i, driving force, $d\mu_i/dx$, and a constant as follows (i.e. no applied pressure) [1, 2, 10].

$$J_i = -\frac{D_i}{RT} C_i \frac{d\mu_i}{dx} \tag{C.1}$$

where $d\mu_i/dx$ is the chemical potential gradient across the membrane at x direction. In a typical salt permeation measurement, the driving force arises from the penetrant

concentration difference across the membrane. Therefore, the chemical potential can be expressed as [1].

$$\mu_i = \mu_i^0 + RTlna_i = \mu_i^0 + RTln(\gamma_i C_i) \tag{C.2}$$

where μ_i^0 is the reference chemical potential, R is the gas constant, T is absolute temperature, a_i is the activity of penetrant i (i.e., water, salt, ion), which can be written as the product of activity coefficient, γ_i, and concentration, C_i. Combining Eqn. (C.1)-(C.2) gives:

$$J_i = -D_i C_i \left[\frac{dlnC_i}{dx} + \frac{dln\gamma_i}{dx}\right] = -D_i \left[1 + \frac{dln\gamma_i}{dC_i}\right]\frac{dC_i}{dx} = -D_i \beta_i \frac{dC_i}{dx} \tag{C.3}$$

where $\beta_i (= 1 + \frac{dln\gamma_i}{dC_i})$ is defined as the thermodynamic factor (or activity factor), which describes the thermodynamic non-ideality effect involved in the process [11, 12]. When $\gamma_i = 1$ (ideal solution), $\beta_i = 1$, and the expression of flux reduces to the form of Fick's law [1].

In a typical salt permeation test, the molar salt flux can be expressed as follows:

$$J_s = -D_s^m \beta_s \frac{dC_s^m}{dx} = -D_s^{m*} \frac{dC_s^m}{dx} \tag{C.4}$$

where the subscripts refer to components (s-salt), and the superscripts refer to polymer phases (s-solution, m-membrane) [3, 13, 14]. D_s^m is the local salt diffusion coefficient, and D_s^{m*} is the effective local salt diffusion coefficient inheritably containing the non-ideal thermodynamic effect (i.e., β_s). Determination of D_s^{m*} will be discussed subsequently. β_s can be determined by knowing the ion activity coefficients in the

membrane (i.e., computed from the experimental ion sorption results) [15] as demonstrated later. Therefore, D_s^m can be calculated after accounting for the non-ideal thermodynamic effect as follows:

$$D_s^m = \frac{1}{\beta_s} D_s^{m*} \tag{C.5}$$

Integrating Eqn. (S4) across the membrane thickness gives the momentary steady state salt fluxas follows [2]:

$$J_s = \frac{\langle \bar{D}_s^{m*} \rangle K_s}{L} [(C_s^m)_0 - (C_s^m)_L] \tag{C.6}$$

where $(C_s^m)_0$ and $(C_s^m)_L$ are the salt concentrations at the feed and permeate sides of the membrane, respectively, L is the swollen membrane thickness, $\langle \bar{D}_s^{m*} \rangle$ is the concentration averaged, apparent salt diffusion coefficient, and K_s is the mobile salt (i.e., equal to co-ion concentration in charged membranes) sorption coefficient.

To determine K_s, one has to assume the solutions are in equilibrium with the membrane at both the feed and permeate interfaces. Thus, equating the chemical potentials at the interfaces ($\mu_s^s = \mu_s^m$) leads to the definition of K_s [1, 9]:

$$\frac{(C_s^m)_L}{(C_s^s)_L} = \frac{(C_s^m)_0}{(C_s^s)_0} = K_s \tag{C.7}$$

Substituting $(C_s^m)_0$ and $(C_s^m)_L$ in Eqn. (C.6) using the relations in Eqn. (C.7) gives:

$$J_s = \frac{\langle \bar{D}_s^{m*} \rangle K_s}{L} [(C_s^s)_0 - (C_s^s)_L] \tag{C.8}$$

where $(C_s^s)_0$ and $(C_s^s)_L$ are the solution salt concentrations at the feed and permeate streams, respectively. One typically defines a concentration averaged, integral salt permeability coefficient $\langle P_s \rangle$ as follows:

$$\langle P_s \rangle = \langle \bar{D}_s^{m*} \rangle K_s \tag{C.9}$$

where $\langle P_s \rangle$ and can be experimentally determined using the approach presented subsequently, K_s can be determined via salt sorption experiments and, therefore, $\langle \bar{D}_s^{m*} \rangle$ can be computed via Eqn. (C.9).

C.2 Determination of Integral Salt Permeability

When a membrane separates two compartments of salt solutions with constant volume, the upstream and downstream concentrations are set $(C_s^s)_0$ and $(C_s^s)_L$, respectively. Combining Eqn. (C.8) and (C.9) yields [1]:

$$J_s = \frac{\langle P_s \rangle}{L} [(C_s^s)_0 - (C_s^s)_L] \tag{C.10}$$

In a typical salt permeation test conducted in a pair of diffusion cells, the downstream cell usually contains pure water [i.e., $(C_s^s)_L = 0$], therefore, Eqn. (C.10) can be written as [16]:

$$J_s = \frac{\langle P_s \rangle}{L} (C_s^s)_0 \tag{C.11}$$

In the downstream cell, the time dependence of increased salt quantity arising from salt transport is related to a transient mass balance as follows [17]:

$$\frac{d[(C_s^s)_L[t] \cdot V]}{dt} = AJ_s \tag{C.12}$$

where $(C_s^s)_L[t]$ is the downstream salt concentration at time t, V is the volume of the downstream cell, and A is the membrane area contacting the solutions. Combining Eqn. (C.10) and (C.12) gives:

$$\frac{d[(C_s^s)_L[t] \cdot V]}{dt} = A\frac{\langle P_s \rangle}{L}\left[(C_s^s)_0[t] - (C_s^s)_L[t]\right] \tag{C.13}$$

where $(C_s^s)_0[t]$ is the upstream salt concentration at time t. Assuming a mass balance exists in the upstream cell as well:

$$(C_s^s)_0[t] = (C_s^s)_0[0] - (C_s^s)_L[t] \tag{C.14}$$

where $(C_s^s)_0[0]$ is the initial upstream salt concentration ($t = 0$). Combining Eqn. (C.13) and (C.14) yields:

$$\frac{d[(C_s^s)_L[t]]}{\left[(C_s^s)_0[0] - 2(C_s^s)_L[t]\right]} = \frac{\langle P_s \rangle A}{VL}dt \tag{C.15}$$

Rearranging Eqn. (C.15) gives:

$$\frac{d[(C_s^s)_L[t]/(C_s^s)_0[0]]}{\left[1 - 2(C_s^s)_L[t]/(C_s^s)_0[0]\right]} = \frac{\langle P_s \rangle A}{VL}dt \tag{C.16}$$

Therefore,

$$d\ln\left\{1 - 2\frac{(C_s^s)_L[t]}{(C_s^s)_0[0]}\right\} = -2\frac{\langle P_s \rangle A}{VL}dt \tag{C.17}$$

Integrating Eqn. (C.17) yields:

$$\int_0^{(C_s^s)_L[t]/(C_s^s)_0[0])} d\ln\left\{1-2\frac{(C_s^s)_L[t]}{(C_s^s)_0[0]}\right\} = -2\frac{\langle P_s\rangle A}{VL}\int_0^t dt \tag{C.18}$$

The rearranged integral of Eqn. (C.18) is:

$$\frac{VL}{-2A}\ln\left\{1-2\frac{(C_s^s)_L[t]}{(C_s^s)_0[0]}\right\} = \langle P_s\rangle t \tag{C.19}$$

where $(C_s^s)_L[t]$ can be recorded using a conductivity meter (i.e., conductivity can be converted to salt concentration) with respect to time. Therefore, plotting $\frac{VL}{-2A}\ln\left\{1-2\frac{(C_s^s)_L[t]}{(C_s^s)_0[0]}\right\}$ vs. t gives the slope equal to $\langle P_s\rangle$ [18].

However, $\langle P_s\rangle$ measured using the aforementioned method does not account for the frame of reference effect (i.e., convection) [12]. Thus, the apparent salt diffusion coefficient $\langle \bar{D}_s^{m*}\rangle$ obtained using $\langle P_s\rangle$ via Eqn. (C.9) needs to be corrected for the frame of reference effect to get an effective average diffusion coefficient, $\langle D_s^{m*}\rangle$ [12].

C.3 Correcting the Frame of Reference (Convection) Effect

The Fick's first law of diffusion as described above considers the moles of solute (e.g., salt, ion) transported through molecular motions [19]. In a polymer system, it is more appropriate to use mass flux instead of molar flux due to the infinitely large molecular weight of the cross-linked polymer. Therefore, the molar salt flux in Eqn. (S4) can be converted to a mass salt flux by multiplying the molecular weight of the penetrant salt as follows:

$$n_s = -D_s^{m*}\frac{d\rho_s^m}{dx} \tag{C.20}$$

where n_s is mass flux of salt due to diffusive molecular motions, ρ_s^m is the salt mass concentration in the swollen membrane [g (salt)/L (swollen membrane)]. The integral salt permeability $\langle P_s \rangle$ in Eqn. (C.11) can be also expressed as:

$$\langle P_s \rangle = \frac{n_s L}{(C_s^s)_0 M_s} \tag{C.21}$$

where M_s is the molecular weight of the salt. Similarly, the hydraulic water permeability, P_w, can be expressed as follows:

$$P_w = \frac{n_w L}{\rho_w (\Delta p - \Delta \pi)} \tag{C.22}$$

where ρ_w is the density of water, $\Delta \pi$ is the osmotic pressure difference across the membrane. In a typical salt permeation test, the hydrostatic pressure applied on the membrane is zero ($\Delta p = 0$).

The mass of salt can be also transported by the convective motion of solvent (e.g., water) [19]. For example, in a typical salt permeation experiment, water flux is in the opposite direction of that of salt due to the osmotic pressure difference across the membrane (i.e., $\Delta \pi$). Thus, the true salt mass flux (corrected for convection) is expressed as follows:

$$n_s = j_s + \omega_s (n_s + n_w + n_p) \tag{C.23}$$

where n_s is the combined salt mass flux (diffusive + convective), ω_s is the mass fraction of salt in the membrane [g (salt)/g (polymer + water + salt)], which will be discussed later,

n_w is the mass flux of water, and n_p is the mass flux of the polymer (~0). Combining Eqn. (C.2) and (C.23) gives the effective local salt diffusion coefficient, D_s^{m*}, as follows:

$$D_s^{m*} = \frac{[n_w \omega_s - n_s(1-\omega_s)]dx}{d\rho_s^m} \tag{C.24}$$

Assuming a continuous salt mass concentration gradient across the membrane at x direction [12]:

$$(\omega_s)_x = (\omega_s)_0 - [(\omega_s)_0 - (\omega_s)_L]\frac{x}{L} \tag{C.25}$$

where $(\omega_s)_0$ and $(\omega_s)_L$ are the salt mass concentrations at the upstream and downstream interfaces, respectively. $(\omega_s)_x$ is the salt mass concentration at the position with a distance of x from the upstream interface. In a salt permeation test, the downstream side salt concentration is typically negligible relative to that of the upstream side within the short timescale of the experiment. Thus, integrating Eqn. (C.24) with the boundary conditions $(\omega_s)_L = 0$ and $(\rho_s^m)_L = 0$ yields:

$$\langle D_s^{m*} \rangle (\rho_s^m)_0 = \frac{n_w L(\omega_s)_0}{2} - n_s L\left[1 - \frac{(\omega_s)_0}{2}\right] \tag{C.26}$$

Combining Eqn. (C.7), (C.21), (C.22), and (C.26), the effective average salt diffusion coefficient (corrected for the frame of reference effect), $\langle D_s^{m*} \rangle$, in a salt permeation process is expressed as follows:

$$\langle D_s^{m*} \rangle = \frac{\langle P_s \rangle}{K_s}\left[1 - \frac{(\omega_s)_0}{2}\right] + \frac{P_w \rho_w \Delta\pi (\omega_s)_0}{2M_s (C_s^m)_0} \tag{C.27}$$

Substituting $\langle \bar{D}_s^{m*} \rangle = \frac{\langle P_s \rangle}{K_s}$ in Eqn. (C.27) using Eqn. (C.9), $\langle D_s^{m*} \rangle$, can be determined as follows:

$$\langle D_s^{m*} \rangle = \langle \bar{D}_s^{m*} \rangle \left[1 - \frac{(\omega_s)_0}{2} \right] + \frac{P_w \rho_w \Delta\pi (\omega_s)_0}{2 M_s (C_s^m)_0} \tag{C.28}$$

where the sorbed salt (e.g., co-ion for charged membranes) concentration at the upstream face of the membrane, $(C_s^m)_0$ can be experimentally measured, and the salt mass fraction in the membrane, $(\omega_s)_0$, can be computed based on the sorbed salt and water content, the water permeability, P_w, can be determined from the osmotic water flux measurements. Procedures to determine $(\omega_s)_0$ and P_w will be discussed subsequently.

C.4 NERNST-PLANK EQUATION

Different from the neutral molecules (i.e., water, salt), ionized species are also subjective to the force of an externally applied electric filed. Ionic flux is therefore affected by both the concentration and electric potential gradients across the membrane. The driving force in this case is electrochemical potential defined as follows [20]:

$$\mu_i = \mu_i^0 + RTlna_i + z_i F\psi = \mu_i^0 + RTln(\gamma_i C_i) + z_i F\psi \tag{C.29}$$

where z_i is the valence of the penetrant ion i (e.g., $+$ is cation, $-$ is anion), F is Faraday's constant, ψ is the electric potential. Based on Teorell's theory, ionic flux can be expressed as the product ion concentration, C_i, and ion velocity, v_i, as follows [21]:

$$J_i = C_i v_i = C_i u_i A_i \tag{C.30}$$

where u_i is the ionic mobility, A_i is the driving force for ion movements. Assuming the validity of the Einstein equation (i.e., linear relation between u_i and D_i) [10]:

$$u_i = \frac{F}{RT} D_i \tag{C.31}$$

Substituting u_i in Eqn. (C.30) using the relation in Eqn. (C.31) gives:

$$J_i = \frac{D_i}{RT} C_i A_i = \frac{D_i}{RT} C_i \frac{d\mu_i}{dx} \tag{C.32}$$

where the general driving force was substituted with the one-directional electrochemical potential gradient (i.e., $A_i = \frac{d\mu_i}{dx}$), and the ionic flux expression has the same form of that in the Fick's law. Combining Eqn. (C.29) and Eqn. (C.32) yields the expression for the ionic flux with a convection term [20]:

$$J_i = -D_i C_i \left[\frac{dln(\gamma_i C_i)}{dx} + \frac{z_i F}{RT} \frac{d\psi}{dx}\right] + C_i \nu_x \tag{C.33}$$

where ν_x is the velocity of the convective fluid (e.g., solvent) at x direction. When the convective term is neglected and all ionic solutions are ideal (γ_i= 1), Eqn. (C.33) reduces to the best-known form of the Nernst-Plank equation [20]:

$$J_i = -D_i \left[\frac{dC_i}{dx} + \frac{z_i F C_i}{RT} \frac{d\psi}{dx}\right] \tag{C.34}$$

where the ionic flux is essentially composed of the ion diffusion driven by the concentration gradient (the first term in the bracket) and ion migration driven by the electric field (the second term in the bracket).

However, the ion activity coefficients in the membrane are typically far from ideality (i.e., not equal to unity), therefore, the ionic flux in a membrane is expressed as follows [12]:

$$J_i^m = -D_i^m \left[\beta_i \frac{dC_i^m}{dx} + \frac{z_i F C_i^m}{RT} \frac{d\psi}{dx} \right] \tag{C.35}$$

where J_i^m, D_i^m, β_i, and C_i^m are the ionic flux, diffusion coefficient, thermodynamic factor, and concentration the penetrant i in the swollen membrane.

C.5 Ion Diffusion (No External Electric Field)

Absent of an external electric filed, a net transference of ionic flux in the membrane must be zero, therefore, for a 1:1 electrolyte [12]:

$$J_+ = J_- = J_s \tag{C.36}$$

where J_s is the coupled salt flux. In a charged membrane with the fixed charge concentration of C_A^m, a charge balance exists [17]:

$$C_+^m + \omega C_A^m = C_-^m \tag{C.37}$$

where ω is the sign of the fixed charge groups ($\omega = -1$ for a negatively charged membrane, $\omega = 1$ for a positively charged membrane. Differentiating Eqn. (C.37) at x direction yields:

$$\frac{dC_+^m}{dx} = \frac{dC_-^m}{dx} = \frac{dC_s^m}{dx} \tag{C.38}$$

where C_s^m is the mobile salt concentration in the membrane. Eqn. (C.37) means the concentration gradient across the membrane is constant. Combining Eqn. (C.35), (C.36), and (S50) yields the local electric field gradient experienced by cations and anions [12]:

$$\frac{d\psi}{dx} = -\frac{RT}{F}\left(\frac{D_+^m\beta_+ + D_-^m\beta_-}{D_+^m\beta_+C_+^m + D_-^m\beta_-C_-^m}\right)\frac{dC_s^m}{dx} \tag{C.39}$$

where D_+^m and D_-^m are the cation and anion diffusion coefficients in the membrane. Combining Eqn. (C.35) and (C.39), one can express the molar salt flux in a membrane as follows [12]:

$$J_s^m = -\left(\frac{D_+^m D_-^m(\beta_+C_-^m + \beta_-C_+^m)}{D_+^m C_+^m + D_-^m C_-^m}\right)\frac{dC_s^m}{dx} \tag{C.40}$$

Eqn. (C.40) is another way to express the Fick's law with the individual ionic thermodynamic effect included. Generally, in uncharged and moderately charged membranes, the ion activity coefficient of counter-ion and co-ion are equal to the mean salt activity coefficients (e.g., $\gamma_+ = \gamma_- = \gamma_s$) [22], therefore, $\beta_+ = \beta_- = \beta_s$, and Eqn. (C.40) becomes:

$$J_s^m = -\beta_s\left(\frac{D_+^m D_-^m(C_-^m + C_+^m)}{D_+^m C_+^m + D_-^m C_-^m}\right)\frac{dC_s^m}{dx} \tag{C.41}$$

Comparing Eqn. (C.41) to Eqn. (C.4), the local salt diffusion coefficient can be expressed in terms of individual ion concentrations (C_-^m and C_+^m) and diffusion coefficients (D_-^m and D_+^m) as follows [12]:

$$D_s^m = \frac{D_+^m D_-^m(C_-^m + C_+^m)}{D_+^m C_+^m + D_-^m C_-^m} \tag{C.42}$$

Eqn. (C.42) describes the coupled diffusion coefficient of a salt molecule in terms of the individual ions. In an uncharged membrane, $C_-^m = C_+^m$, therefore, Eqn. (C.42) reduces to:

$$D_s^m = \frac{2D_+^m D_-^m}{D_+^m + D_-^m} \tag{C.43}$$

Eqn. (C.43) also apples to the salt diffusion coefficient in a 1:1 strong electrolyte solution as follows:

$$D_s^s = \frac{2D_+^s D_-^s}{D_+^s + D_-^s} \tag{C.44}$$

where the superscript 's' represents the solution phase.

C.6 Ion Migration (No Concentration Gradient)

In the absence of an ionic concentration gradient, ionic flux driven by the electric potential gradient reduces to the following form [10]:

$$J_i = -\frac{z_i F}{RT} D_i C_i \frac{d\psi}{dx} \tag{C.45}$$

where J_i is equivalent to a current density since the ionized species are current carriers under an electric field. F is Faraday's constant, R is the gas constant, and T is the absolute temperature. The electric current carried by the ith ion, I_i (C/s), is expressed by [10]:

$$I_i = -z_i F A J_i = \frac{z_i^2 F^2 A}{RT} D_i C_i \frac{d\psi}{dx} \tag{C.46}$$

where A is the cross-sectional area in a linear system. Thus, the total electric current, I_i, is the sum of all the individual ionic current [20]:

$$I = \sum_i I_i = \frac{F^2 A}{RT} \frac{d\psi}{dx} \sum_i z_i^2 D_i C_i \tag{C.47}$$

Integrating Eqn. (C.47) gives [20]:

$$I = \frac{F^2 A}{RT} \frac{\Delta E}{l} \sum_i z_i^2 D_i C_i \tag{C.48}$$

where l is the distance over which the electric potential gradient, ΔE (V), is applied. The resistance, R (Ω), is defined by Ohm's law [20]:

$$\frac{1}{R} = \frac{A}{l\rho} = \frac{I}{\Delta E} = \frac{F^2 A}{RTl} \sum_i z_i^2 D_i C_i \tag{C.49}$$

where ρ is the resistivity having units of $\Omega \cdot \mathrm{cm}$, and the conductivity, κ, $(\mathrm{S/cm})$is given by [20]:

$$\kappa = \frac{1}{\rho} = \frac{F^2}{RT} \sum_i z_i^2 D_i C_i \tag{C.50}$$

For a membrane equilibrated in a 1:1 strong electrolyte solution, the membrane ionic conductivity, κ, can be rewritten as [10]:

$$\kappa = \frac{F^2}{RT} (D_+^m C_+^m + D_-^m C_-^m) \tag{C.51}$$

C.7 MASS FRACTION OF SALT

The mass fraction of salt in a membrane, ω_s, equilibrated with an external electrolyte solution is given by [23]:

$$\omega_s = \frac{C_s^m M_s}{C_s^m M_s + \phi_w(1 + 1/w_u)} \tag{C.52}$$

where C_s^m is the salt concentration in the membrane [mol/L (swollen membrane)], ϕ_w is the water volume fraction [L (sorbed water)/L (swollen membrane)], and w_u is the polymer water uptake [g (water)/g (dry polymer)]. Exemplary ω_s values for an uncharged (i.e., 10-0) and charged (i.e., 10-1.93) membranes are presented in Figure C.2 as a function of external NaCl concentration. At low external NaCl concentrations, ω_s in sample 10-1.93 is lower than that in sample 10-0 due to Donnan exclusion. When C_s^s = 1M, their ω_s values are nearly identical, which is due to reduced Donnan exclusion at high C_s^s values. These results are consistent with the salt sorption coefficient results in the main text.

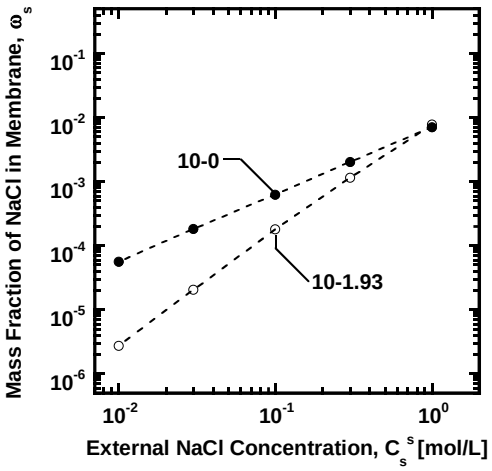

Figure C.2 NaCl mass fraction in the uncharged XLPEGDA membrane (i.e., 10-0) and charged XL (AMPS-PEGDA) membrane (i.e., 10-1.93) as a function of external NaCl concentration.

C.8 Effective Average Salt Diffusion Coefficient

After correcting for the frame of reference effect, the effective average salt diffusion coefficient, $\langle D_s^{m*} \rangle$, is presented in Figure C.3 together with $\langle \bar{D}_s^{m*} \rangle$ as a function of upstream NaCl concentration [12].

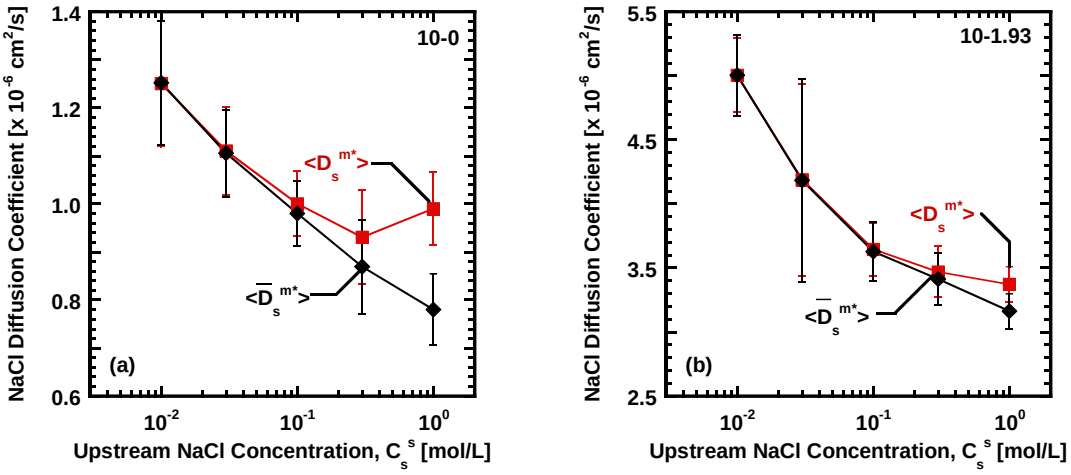

Figure C.3 The apparent and effective average diffusion coefficients, $\left\langle \overline{D}_s^{m*} \right\rangle$, and $\left\langle \overline{D}_s^{m} \right\rangle$, for: (a) sample 10-0 and (b) sample 10-1.93.

As shown in Figure C.3, the effect of frame of reference is negligible for both membranes considered [i.e., $\langle D_s^{m*} \rangle \approx \langle \overline{D}_s^{m*} \rangle$] at low upstream NaCl concentrations ($C_s^s <$ 0.3 M), due to the low mass salt fraction, $(\omega_s)_0$, and water flux, n_w, at these conditions [cf. Eqn. (C.28)]. However, at higher C_s^s values (> 0.3 M), $\langle D_s^{m*} \rangle$ is higher than $\langle \overline{D}_s^{m*} \rangle$, so the frame of reference effect is more pronounced at higher salt concentrations. These observations are consistent with results from prior studies [12].

C.9 Effective Local Diffusion Coefficient

The effective local salt diffusion coefficient, D_s^{m*}, can be calculated as follows [12]:

$$D_s^{m*} = \frac{d\{\langle D_s^{m*}\rangle[(\rho_s^m)_0 - (\rho_s^m)_L]\}}{d\rho_s^m} \tag{C.53}$$

where ρ_s^m is the mass concentration of salt in the membrane. As shown in Figure C.4, $\langle D_s^{m*}\rangle[(\rho_s^m)_0 - (\rho_s^m)_L]$ is plotted against ρ_s^m, so the relation between D_s^{m*} and ρ_s^m can be obtained using an empirical model fitting method [12].

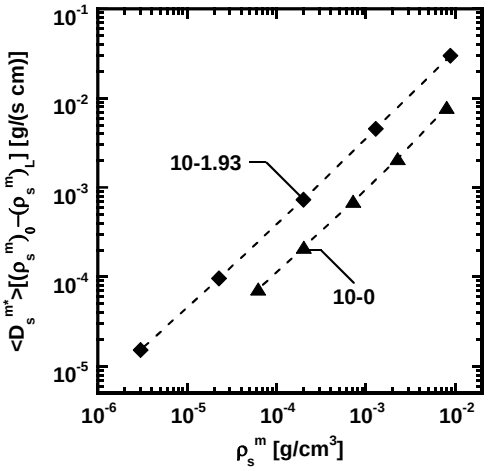

Figure C.4 The influence of ρ_s^m on $\left\langle \overline{D}_s^m \right\rangle \left(\rho_s^m\right)_0$ in samples 10-0 and 10-1.93.

In Figure C.4, data points for sample 10-0 were fit to an empirical power law model (dashed line):

$$\langle D_s^{m*}\rangle \rho_s^m = 0.60 \times 10^{-6} (\rho_s^m)^{0.94} \tag{C.54}$$

The fitting parameters extracted from Eqn. (C.54) were used to determine D_s^{m*} as follows:

$$D_s^{m*} = 0.56 \times 10^{-6}(\rho_s^m)^{-0.06} \tag{C.55}$$

The empirical power law expression for sample 10-1.93 is given by:

$$\langle D_s^{m*}\rangle \rho_s^m = 2.69 \times 10^{-6}(\rho_s^m)^{0.99} \tag{C.56}$$

Then, D_s^{m*} for sample 10-1.93 is expressed as:

$$D_s^{m*} = 2.62 \times 10^{-6}(\rho_s^m)^{-0.01} \tag{C.57}$$

The effective local salt diffusion coefficient and the effective average salt diffusion coefficient are presented in Figure C.5 (a) and (b), respectively.

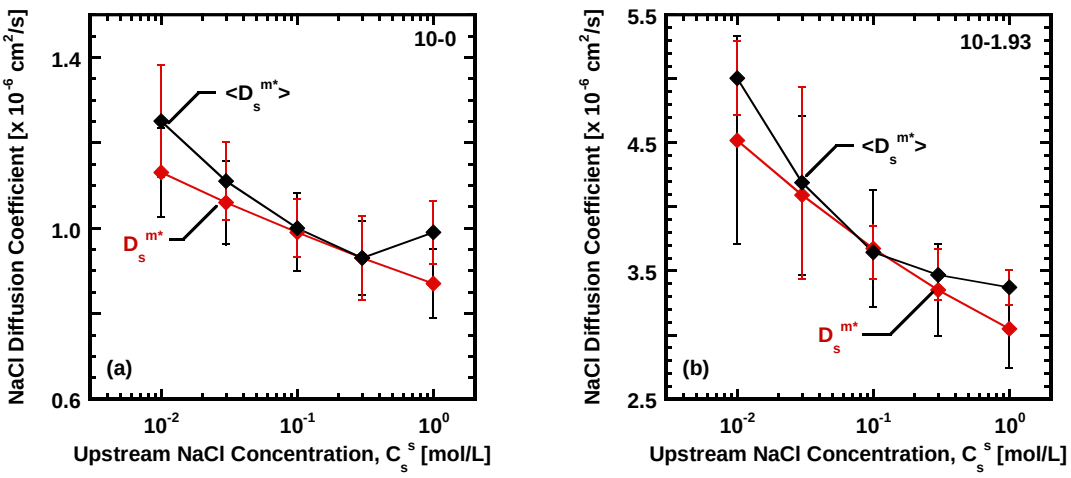

Figure C.5 Effective average, $\left\langle \overline{D_s}^{m*} \right\rangle$, and effective local salt diffusion coefficients, D_s^{m*}, for samples: (a) 10-0 and (b) 10-1.93.

For both samples, the effective local salt diffusion coefficient is almost the same as the effective average diffusion coefficient ($\langle D_s^{m*} \rangle = D_s^{m*}$), within experimental uncertainty, similar to prior reports [12]. The same behavior was also found in the other samples studied.

C.10 Local Salt Diffusion Coefficient

Quantifying non-ideal thermodynamic effects on diffusion coefficients requires ion activity coefficient data in the membrane [12]. According to Manning's model, the individual ion activity coefficient in a charged membrane that does not undergo counter-ion condensation would be the same for cation and anion [22]. Thus, the mean ion activity coefficient in the membrane, $\gamma_{\pm}^{m}$, can be defined in the same manner as in solution [22]:

$$\gamma_{\pm}^{m} = \sqrt{\gamma_{+}^{m}\gamma_{-}^{m}} \tag{C.58}$$

where $\gamma_{+}^{m}\gamma_{-}^{m}$ can be computed from experimental salt sorption results, as discussed elsewhere [24]. Figure C.6 presents mean ion activity coefficient as a function of external NaCl concentration.

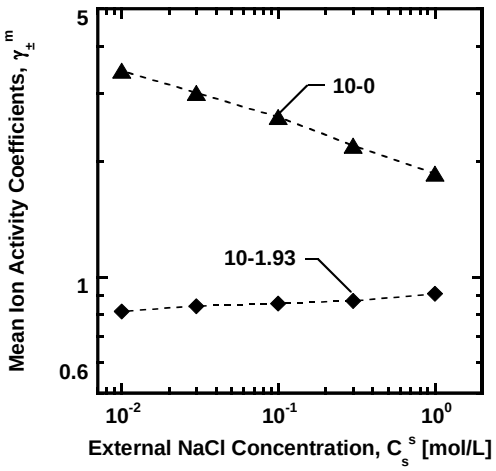

Figure C.6 The dependence of mean ion activity coefficient in the membrane as a function of the external NaCl concentration for samples 10-0 and 10-1.93.

The thermodynamic correction factor for salt diffusion coefficients can be calculated as follows [11]:

$$\beta_s = \left(1 + \frac{dln\gamma_{\pm}^{m}}{dlnC_s^m}\right) \tag{C.59}$$

Plotting $ln\gamma_{\pm}^{m}$ vs. lnC_s^m gives β_s by fitting the data to a power law model, as shown in Figure C.7.

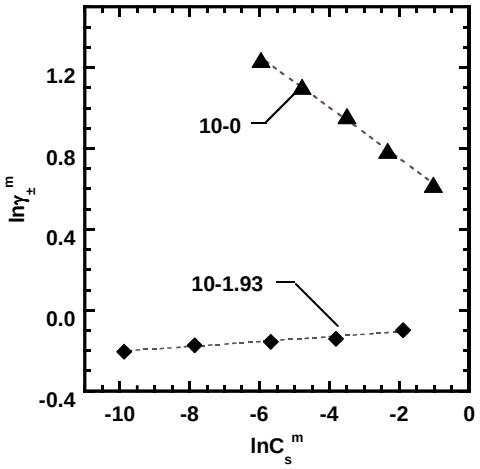

Figure C.7 Determination of β_s in samples 10-0 and 10-1.93.

Fitting the data of sample 10-0 to an empirical power law model (dashed line) gives:

$$\beta_s = \left(1 + \frac{dln\gamma_{\pm}^{m}}{dlnC_s^m}\right) = 1 - 0.13 = 0.87 \tag{C.60}$$

where the slope of $ln\gamma_{\pm}^{m}$ vs. lnC_s^m is negative because ion activity coefficients of uncharged membranes typically decrease as salt concentration in the membrane increases [24]. For sample 10-1.93:

$$\beta_s = \left(1 + \frac{dln\gamma_{\pm}^{m}}{dlnC_s^m}\right) = 1 + 0.02 = 1.02 \tag{C.61}$$

where the slope of $ln\gamma_{\pm}^{m}$ vs. lnC_s^m is a small positive number since the ion activity coefficient of the charged membrane increases slightly as the membrane sorbed salt concentration increases [15]. Such behavior is qualitatively consistent with other charged membranes studied [12].

Combining Eqn. (C.5), (C.59), and (C.61), the local NaCl diffusion coefficient, D_s^m, which accounts for both the frame of reference and non-ideal thermodynamic effects can be calculated [12]. D_s^m values are presented in Figure C.8 together with the effective local diffusion coefficient, D_s^{m*}, as a function of upstream NaCl concentration.

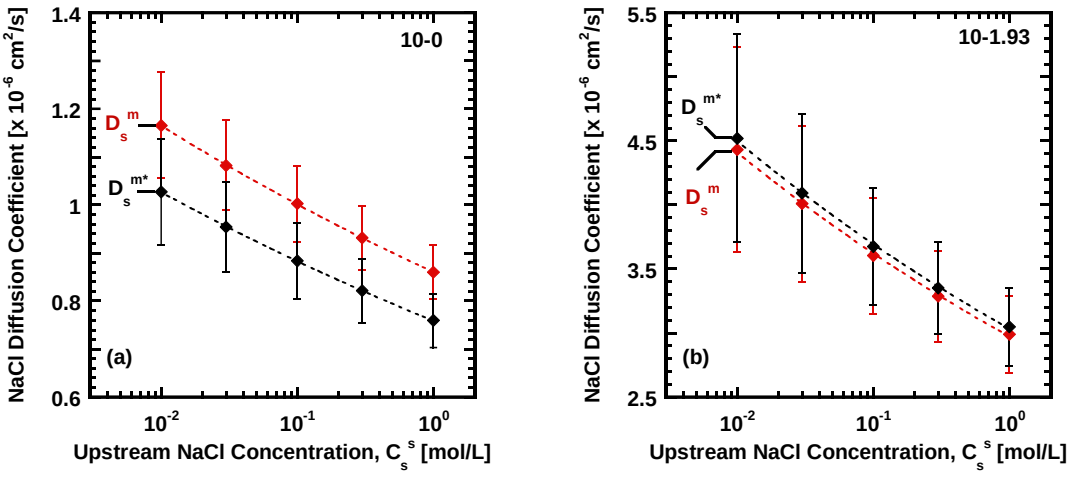

Figure C.8 Local salt diffusion coefficient, D_s^m, compared with the effective local salt diffusion coefficient, D_s^{m*}, for samples: (a) 10-0 and (b) 10-1.93.

As shown in Figure C.8 (a), the local salt diffusion coefficient is systematically higher than the effective local diffusion coefficient by about 18%, because β_s is less than 1 for the uncharged membrane [cf. Eqn. (C.59)]. As shown in Figure C.8 (b), D_s^m is slightly smaller than D_s^{m*} by about 5%, due to the small value of β_s [cf. Eqn. (C.61)]. However, these small differences are within experimental the uncertainties, similar to results reported for other charged membranes [12]. The same result was also obtained in the other samples studied.

C.11 Comparing Local and Apparent Salt Diffusion Coefficients

Figure C.9 presents local and apparent salt diffusion coefficients as a function of upstream NaCl concentration. For the uncharged membrane (i.e., 10-0), the local salt diffusion coefficient is slightly larger than the apparent one, since both frame of reference and thermodynamic non-ideality effects act to increase the apparent salt diffusion coefficien [cf. Figure C.2 (a) and Figure C.6 (a)]. However, the difference between D_s^m and $\langle \overline{D}_s^{m*} \rangle$ is within the experimental uncertainty. For the most highly charged membrane considered (i.e.,10-1.93), D_s^m and $\langle \overline{D}_s^{m*} \rangle$ are nearly identical considering the experimental uncertainty. Correcting for the frame of reference effect increased salt diffusion coefficients [cf. Figure C.2 (b)], and salt diffusion coefficients decreased slightly after accounting for the thermodynamic non-ideality effect [cf. Figure C.6 (b)]. Both effects somewhat offset each other in the charged membrane, which is similar to results elsewhere [12]. The same conclusion applies to all the other samples studied.

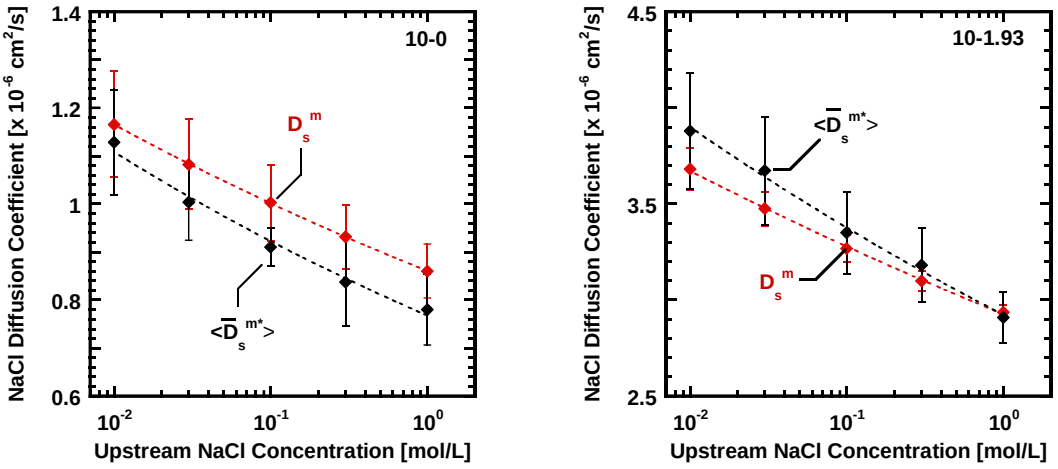

Figure C.9 Effect of upstream NaCl concentration on local salt diffusion coefficient, D_s^m, compared with the apparent salt diffusion coefficient, $\left\langle \overline{D}_s^{m*} \right\rangle$, for samples: (a) 10-0 and (b) 10-1.93.

C.12 MEMBRANE IONIC CONDUCTIVITY MEASUREMENTS

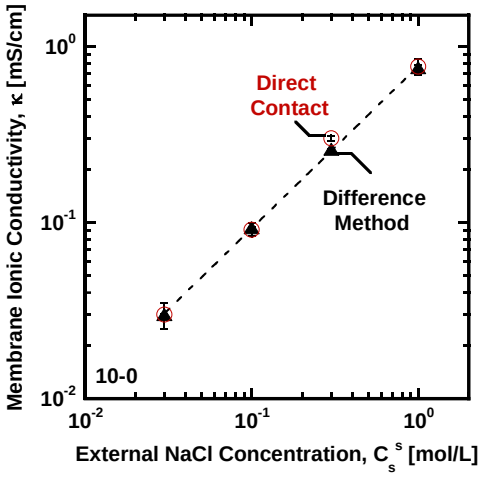

Figure C.10 Membrane ionic conductivity in sample 10-0 measured using difference and direct contact method [25]. κ values obtained using these two methods are identical, within the experimental uncertainty.

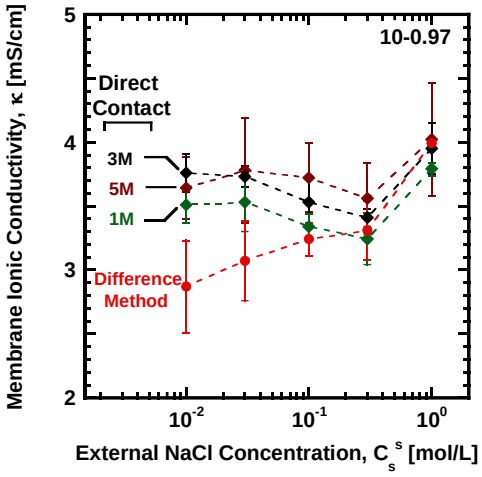

Figure C.11 Membrane ionic conductivity in sample 10-0.97 measured using the direct contact method [25] with dipping solution concentrations of 1, 3 and 5 M and using the difference method [25]. κ values obtained using the direct contact method are indistinguishable when the dipping solution is above 3 M, within experimental uncertainty.

C.13 MEMBRANE TRANSPORT PROPERTIES (I.E., PEGDA N = 13 AND N = 4)

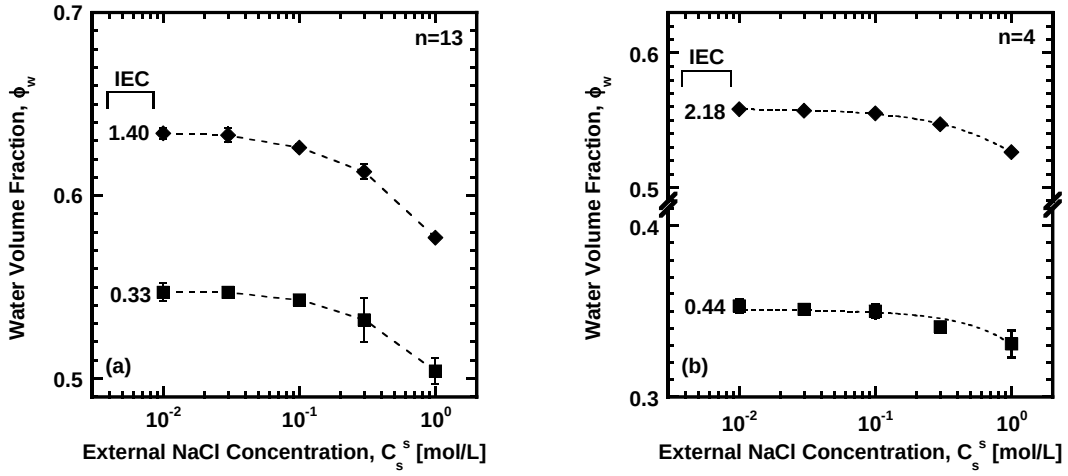

Figure C.12 Membrane water volume fraction in selected charged XL(AMPS-PEGDA) membranes prepared with PEGDA of (a) n =13 and (b) n = 4.

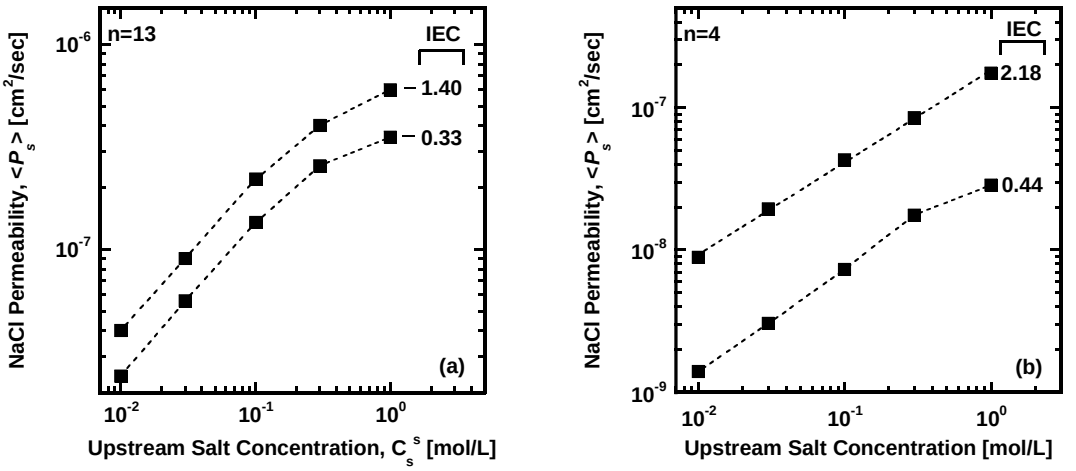

Figure C.13 Membrane salt permeability coefficients in selected charged XL(AMPS-PEGDA) membranes prepared with PEGDA of (a) n =13 and (b) n = 4.

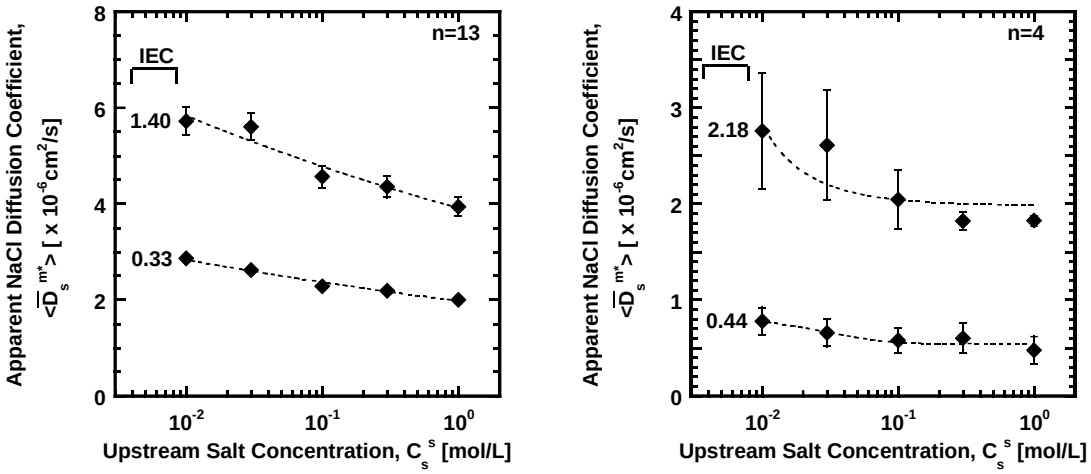

Figure C.14 Membrane apparent salt diffusion coefficients in selected charged XL(AMPS-PEGDA) membranes prepared with PEGDA of (a) n =13 and (b) n = 4.

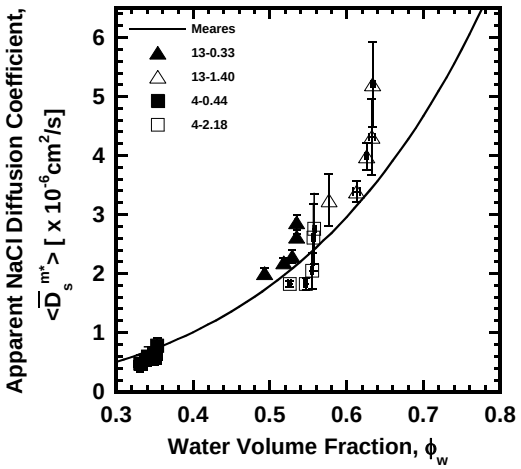

Figure C.15 Membrane apparent salt diffusion coefficients in selected charged XL(AMPS-PEGDA) membranes prepared with PEGDA of n =13 and n = 4 compared with Meares' model predictions, represented by the solid line.

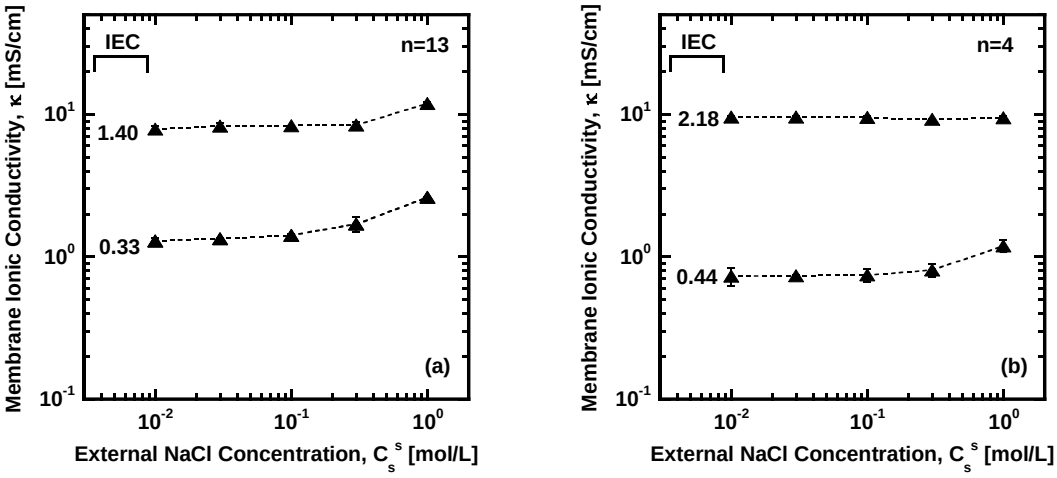

Figure C.16 Membrane ionic conductivity in selected charged XL(AMPS-PEGDA) membranes prepared with PEGDA of n =13 and n = 4.

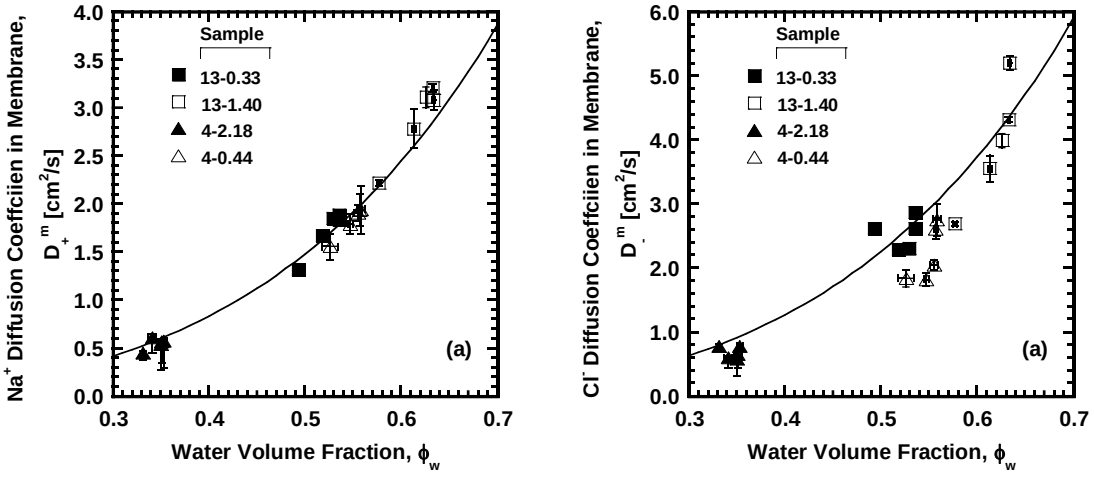

Figure C.17 Na^+ diffusion coefficients, D_+^m, (a) and Cl^- diffusion coefficients, D_-^m, (b) as a function of polymer water volume fraction in membranes prepared with PEGDA of n =13 and n = 4. The solid lines represent the Mackie and Meares model predictions.

C.14 REFERENCES

[1] J.G. Wijmans, R.W. Baker, The solution-diffusion model: a review, Journal of Membrane Science, 107 (1995) 1-21.

[2] D.R. Paul, Reformulation of the solution-diffusion theory of reverse osmosis, Journal of Membrane Science, 241 (2004) 371-386.

[3] G.M. Geise, D.R. Paul, B.D. Freeman, Fundamental water and salt transport properties of polymeric materials, Progress in Polymer Science, 39 (2013) 1-42.

[4] U. Merten, Flow Relationships in Reverse Osmosis, I & EC Fundamentals, 2 (1963) 229-232.

[5] H.K. Lonsdale, U. Merten, R.L. Riley, Transport properties of cellulose acetate osmotic membranes, Journal of Applied Polymer Science, 9 (1965) 1341-1362.

[6] H.K. Lonsdale, U. Merten, M. Tagami, Phenol Transport in Cellulose Acetate Membranes, Journal of Applied Polymer Science, 11 (1967) 1807-1820.

[7] U. Merten, Desalination by Reverse Osmosis, The M.I.T. Press, 1966.

[8] D.R. Paul, The Role of Membrane Pressure in Reverse Osmosis, Journal of Applied Polymer Science, 16 (1972) 771-852.

[9] R.W. Baker, Membrane Technology and Applications, John Wiley & Sons Ltd: West Sussex, England, 2004.

[10] N. Lakshminarayanaisah, Transport phenomena in membranes, Academic Press, New York and London, 1969.

[11] R.A. Robinson, R.H. Stokes, Electrolyte solutions, Courier Corporation, 2002.

[12] J. Kamcev, D.R. Paul, B.D. Freeman, Accounting for Frame of Reference and Thermodynamic Non-Idealities When Calculating Ion Diffusion Coefficients in Ion Exchange Membranes, Journal of Membrane Science, 537 (2017) 396-406.

[13] C.E. Reid, E.J. Breton, Water and Ion Flow Across Cellulosic Membranes, Journal of Applied Polymer Science, 1 (1959) 133-143.

[14] C.E. Reid, J.R. Kuppers, Physical Characteristics of Osmotic Membranes of Organic Polymers, Journal of Applied Polymer Science, 2 (1959) 264-272.

[15] J. Kamcev, D.R. Paul, B.D. Freeman, Ion activity coefficients in ion exchange polymers: Applicability of Manning's counterion condensation theory, Macromolecules, 48 (2015) 8011-8024.

[16] G.M. Geise, H.S. Lee, D.J. Miller, B.D. Freeman, J.E. McGrath, D.R. Paul, Water purification by membranes: The role of polymer science, Journal of Polymer Science Part B: Polymer Physics, 48 (2010) 1685-1718.

[17] F. Helfferich, Ion Exchange, McGraw-Hill Book Co., Inc., New York, 1962.

[18] J. Kamcev, E.-S. Jang, N. Yan, D.R. Paul, B.D. Freeman, Effect of ambient carbon dioxide on salt permeability and sorption measurements in ion-exchange membranes, Journal of Membrane Science, 479 (2015) 55-56.

[19] R.B. Bird, W.E. Stewart, E.N. Lightfoot, Transport phenomena, John Wiley & Sons, 2007.

[20] A.J. Bard, L.R. Faulkner, J. Leddy, C.G. Zoski, Electrochemical methods: fundamentals and applications, Wiley New York, 1980.

[21] A.L.I.a.V.S.M. G. E. Zaikov, Diffusion of electrolytes in polymers, Institute of Chemical Physics, Academy of Sciences of the USSR, Moscow, USSR, 1988.

[22] G.S. Manning, Limiting laws and counterion condensation in polyelectrolyte solutions I. Colligative properties, The Journal of Chemical Physics, 51 (1969) 924-933.

[23] J. Kamcev, D.R. Paul, G.S. Manning, B.D. Freeman, Accounting for frame of reference and thermodynamic non-idealities when calculating salt diffusion coefficients in ion exchange membranes, Journal of Membrane Science, 537 (2017) 396-406.

[24] N. Yan, D.R. Paul, B.D. Freeman, Water and ion sorption in a series of cross-linked AMPS/PEGDA hydrogel membranes, In preparation, (2017).

[25] J. Kamcev, R. Sujanani, E.-S. Jang, N. Yan, N. Moe, D. Paul, B. Freeman, Salt concentration dependence of ionic conductivity in ion exchange membranes, In preparation, (2017).

Bibliography

Aggour, Y. (1994). Thermal degradation of copolymers of 2-acrylamido-2-methylpropanesulphonic acid with acrylamide. *Polymer Degradation and Stability, 44*(1), 71-73.

Alexandratos, S. D. (2009). Ion-Exchange Resins: A Retrospective from Industrial and Engineering Chemistry Research. *Industrial & Engineering Chemistry Research, 48*(1), 388-398.

Alsvik, I. L., & Hägg, M. B. (2013). Pressure Retarded Osmosis and Forward Osmosis Membranes: Materials and Methods. *Polymers, 5*(1), 303-327.

ASTM. (2011). Standard test method for ash in the analysis sample of coal and coke from coal. *D3174-11*.

Bai, Z., Houtz, M. D., Mirau, P. A., & Dang, T. D. (2007). Structures and properties of highly sulfonated poly (arylenethioethersulfone) s as proton exchange membranes. *Polymer, 48*(22), 6598-6604.

Baker, R. W. (2004). *Membrane Technology and Applications*. England: John Wiley & Sons Ltd: West Sussex.

Bard, A. J., Faulkner, L. R., Leddy, J., & Zoski, C. G. (1980). *Electrochemical methods: fundamentals and applications* (Vol. 2). New York: Wiley

Basheer, R. A., Hopkins, A. R., & Rasmussen, P. G. (1999). Dependence of transition temperatures and enthalpies of fusion and crystallization on composition in polyaniline/nylon blends. *Macromolecules, 32*(14), 4706-4712.

Bauman, W., & Eichhorn, J. (1947). Fundamental properties of a synthetic cation exchange resin. *Journal of the American Chemical Society, 69*(11), 2830-2836.

Biesheuvel, P. M., & Van der Wal, A. (2010). Membrane capacitive deionization. *Journal of Membrane Science, 346*(2), 256-262.

Biesheuvel, P. M., Van Limpt, B., & Van der Wal, A. (2009). Dynamic adsorption/desorption process model for capacitive deionization. *The Journal of Physical Chemistry C, 113*(14), 5636-5640.

Bird, R. B., Stewart, W. E., & Lightfoot, E. N. (2007). *Transport phenomena*: John Wiley & Sons.

Bockris, J. O. M., Reddy, A. K. N., Gamboa-Aldeco, M. E., & NetLibrary, I. (2002). *Modern electrochemistry: Volume 1, Ionics* (2nd ed.). New York: Kluwer Academic.

Bonner, O. (1954). A selectivity scale for some monovalent cations on Dowex 50. *The Journal of Physical Chemistry, 58*(4), 318-320.

Aggour, Y. (1994). Thermal degradation of copolymers of 2-acrylamido-2-methylpropanesulphonic acid with acrylamide. *Polymer Degradation and Stability, 44*(1), 71-73.

Alexandratos, S. D. (2009). Ion-Exchange Resins: A Retrospective from Industrial and Engineering Chemistry Research. *Industrial & Engineering Chemistry Research, 48*(1), 388-398.

Alsvik, I. L., & Hägg, M. B. (2013). Pressure Retarded Osmosis and Forward Osmosis Membranes: Materials and Methods. *Polymers, 5*(1), 303-327.

ASTM. (2011). Standard test method for ash in the analysis sample of coal and coke from coal. *D3174-11*.

Bai, Z., Houtz, M. D., Mirau, P. A., & Dang, T. D. (2007). Structures and properties of highly sulfonated poly (arylenethioethersulfone) s as proton exchange membranes. *Polymer, 48*(22), 6598-6604.

Baker, R. W. (2004). *Membrane Technology and Applications*. England: John Wiley & Sons Ltd: West Sussex.

Bard, A. J., Faulkner, L. R., Leddy, J., & Zoski, C. G. (1980). *Electrochemical methods: fundamentals and applications* (Vol. 2). New York: Wiley

Basheer, R. A., Hopkins, A. R., & Rasmussen, P. G. (1999). Dependence of transition temperatures and enthalpies of fusion and crystallization on composition in polyaniline/nylon blends. *Macromolecules, 32*(14), 4706-4712.

Bauman, W., & Eichhorn, J. (1947). Fundamental properties of a synthetic cation exchange resin. *Journal of the American Chemical Society, 69*(11), 2830-2836.

Biesheuvel, P. M., & Van der Wal, A. (2010). Membrane capacitive deionization. *Journal of Membrane Science, 346*(2), 256-262.

Biesheuvel, P. M., Van Limpt, B., & Van der Wal, A. (2009). Dynamic adsorption/desorption process model for capacitive deionization. *The Journal of Physical Chemistry C, 113*(14), 5636-5640.

Bird, R. B., Stewart, W. E., & Lightfoot, E. N. (2007). *Transport phenomena*: John Wiley & Sons.

Bockris, J. O. M., Reddy, A. K. N., Gamboa-Aldeco, M. E., & NetLibrary, I. (2002). *Modern electrochemistry: Volume 1, Ionics* (2nd ed.). New York: Kluwer Academic.

Bonner, O. (1954). A selectivity scale for some monovalent cations on Dowex 50. *The Journal of Physical Chemistry, 58*(4), 318-320.

Boyd, G., & Bunzl, K. (1967). The Donnan equilibrium in cross-linked polystyrene cation and anion exchangers. *Journal of the American Chemical Society, 89*(8), 1776-1780.

Boyd, G., Schubert, J., & Adamson, A. (1947). The exchange adsorption of ions from aqueous solutions by organic zeolites. I. Ion-exchange equilibria. *Journal of the American Chemical Society, 69*(11), 2818-2829.

Brannon-Peppas, L., & Harland, R. S. (2012). *Absorbent polymer technology* (Vol. 8): Elsevier.

Calmon, C. (1952). Application of volume change characteristics of sulfonated low cross-linked styrene resin. *Analytical Chemistry, 24*(9), 1456-1458.

Calmon, C. (1953). Application of volume characteristics of sulfonated polystyrene resins as a tool in analytical chemistry. *Analytical Chemistry, 25*(3), 490-492.

Cath, T. Y., Childress, A. E., & Elimelech, M. (2006). Forward Osmosis: Principles, Applications, and Recent Development. *Journal of Membrane Science, 281*, 70-87.

Chen, C. C., Britt, H. I., Boston, J., & Evans, L. (1982). Local composition model for excess Gibbs energy of electrolyte systems. Part I: Single solvent, single completely dissociated electrolyte systems. *AICHE Journal, 28*(4), 588-596.

Chikh, L., Girard, S., Teyssie, D., & Fichet, O. (2008). Proton conducting PAMPS networks: From flexible to rigid materials. *Journal of Applied Polymer Science, 107*(6), 3672-3680.

Coşkun, R., Soykan, C., & Delibaş, A. (2006). Study of free-radical copolymerization of itaconic acid/2-acrylamido-2-methyl-1-propanesulfonic acid and their metal chelates. *European polymer journal, 42*(3), 625-637.

Davies, C., & Yeoman, G. (1953). Swelling equilibria with some cation exchange resins. *Transactions of the Faraday Society, 49*, 968-974.

Długołęcki, P., Anet, B., Metz, S. J., Nijmeijer, K., & Wessling, M. (2010). Transport limitations in ion exchange membranes at low salt concentrations. *Journal of Membrane Science, 346*(1), 163-171.

Długołęcki, P., Gambier, A., Nijmeijer, K., & Wessling, M. (2009). Practical potential of reverse electrodialysis as process for sustainable energy generation. *Environmental science & technology, 43*(17), 6888-6894.

Długołęcki, P., Nymeijer, K., Metz, S. J., & Wessling, M. (2008). Current status of ion exchange membranes for power generation from salinity gradients. *Journal of Membrane Science, 319*(1), 214-222.

Donnan, F. G. (1924). The theory of membrane equilibria. *Chemical Reviews, 1*(1), 73-90.

Donnan, F. G. (1995). Theory of membrane equilibria and membrane potentials in the presence of non-dialysing electrolytes. A contribution to physical-chemical physiology. *Journal of Membrane Science, 100*, 11.

Dorfner, K. (1972). *Ion exchangers: properties and applications*: Ann Arbor Science Publishers Inc.

Duncan, J. (1952a). A theoretical treatment of cation exchangers. II. Equilibria between an ion exchanger and an aqueous solution with a common cation. *214*(1118), 344-355.

Duncan, J. (1952b). *A theoretical treatment of cation exchangers. II. Equilibria between an ion exchanger and an aqueous solution with a common cation.* Paper presented at the Proceedings of the Royal Society of London A: Mathematical, Physical and Engineering Sciences.

Erdemi, H., Bozkurt, A., & Meyer, W. H. (2004). PAMPSA-IM based proton conducting polymer electrolytes. *Synthetic metals, 143*(1), 133-138.

Every, H., Forsyth, M., & MacFarlane, D. (1996). Plasticized single conductung polyelectrolytes based on poly (AMPS). *Ionics, 2*(1), 53-62.

Farmer, J. C., Fix, D. V., Mack, G. V., Pekala, R. W., & Poco, J. F. (1996). Capacitive deionization of NaCl and NaNO3 solutions with carbon aerogel electrodes. *Journal of the Electrochemical Society, 143*(1), 159-169.

Ferry, J. D. (1980). *Viscoelastic properties of polymers*: John Wiley & Sons.

Flory, P. J. (1953). *Principles of polymer chemistry*: Cornell University Press.

Freeman, D. H. (1960). Electrolyte uptake by ion-exchange resin. *The Journal of Physical Chemistry, 64*(8), 1048-1051.

Freeman, D. H., Patel, V. C., & Buchanan, T. M. (1965). Electrolyte uptake equilibria with low cross-linked ion-exchange resins. *The Journal of Physical Chemistry, 69*(5), 1477-1481.

Fried, J. R. (2014). *Polymer science and technology*: Pearson Education.

Fritzmann, C., Löwenberg, J., Wintgens, T., & Melin, T. (2007). State-of-the-art of reverse osmosis desalination. *Desalination, 216*, 1-76.

G. E. Zaikov, A. L. I. a. V. S. M. (1988). *Diffusion of electrolytes in polymers*: Institute of Chemical Physics, Academy of Sciences of the USSR, Moscow, USSR.

Gabbott, P. (2008). *Principles and applications of thermal analysis*: John Wiley & Sons.

Galama, A., Saakes, M., Bruning, H., Rijnaarts, H., & Post, J. (2014). Seawater predesalination with electrodialysis. *Desalination, 342*, 61-69.

Galizia, M., Benedetti, F. M., Paul, D. R., & Freeman, B. D. (2017). Monovalent and divalent ion sorption in a cation exchange membrane based on cross-linked poly (p-styrene sulfonate-co-divinylbenzene). *Journal of Membrane Science, 535*, 132-142.

Geise, G. M., Curtis, A. J., Hatzell, M. C., Hickner, M. A., & Logan, B. E. (2013). Salt concentration differences alter membrane resistance in reverse electrodialysis stacks. *Environmental Science & Technology Letters, 1*(1), 36-39.

Geise, G. M., Falcon, L. P., Freeman, B. D., & Paul, D. R. (2012). Sodium chloride sorption in sulfonated polymers for membrane applications. *Journal of Membrane Science, 423-424*, 195-208.

Geise, G. M., Freeman, B. D., & Paul, D. R. (2010). Characterization of a novel sulfonated pentablock copolymer for desalination applications. *Journal of Membrane Science, 24*(51), 5815-5822.

Geise, G. M., Freeman, B. D., & Paul, D. R. (2013). Sodium chloride diffusion in sulfonated polymers for membrane applications. *Journal of Membrane Science, 427*, 186-196.

Geise, G. M., H.B.Park, Sagle, A. C., Freeman, B. D., & McGrath, J. E. (2011). Water peameability and water/salt selectivity tradeoff in polymers for desalination. *Journal of Membrane Science, 369*, 130-138.

Geise, G. M., Hickner, M. A., & Logan, B. E. (2013). Ionic resistance and permselectivity tradeoffs in anion exchange membranes. *ACS applied materials & interfaces, 5*(20), 10294-10301.

Geise, G. M., Lee, H. S., Miller, D. J., Freeman, B. D., McGrath, J. E., & Paul, D. R. (2010). Water purification by membranes: The role of polymer science. *Journal of Polymer Science Part B: Polymer Physics, 48*, 1685-1718.

Geise, G. M., Paul, D. R., & Freeman, B. D. (2013). Fundamental water and salt transport properties of polymeric materials. *Progress in Polymer Science, 39*(1), 1-42.

Ghalloussi, R., Garcia-Vasquez, W., Bellakhal, N., Larchet, C., Dammak, L., Huguet, P., & Grande, D. (2011). Ageing of ion-exchange membranes used in electrodialysis: Investigation of static parameters, electrolyte permeability and tensile strength. *Separation and Purification Technology, 80*(2), 270-275.

Gibbs, J. W. (1878). On the equilibrium of heterogeneous substances. *American Journal of Science*(96), 441-458.

Glueckauf, E. (1952). A theoretical treatment of cation exchangers. I. The prediction of equilibrium constants from osmotic data. *Proceedings of the Royal Society of London. Series A. Mathematical and Physical Sciences, 214*(1117), 207-225.

Glueckauf, E., & Watts, R. (1961). Non-uniformity of cross-linking in ion-exchange polymers. *Nature, 191*, 904-905.

Glueckauf, E., & Watts, R. E. (1962). The Donnan law and its application to ion exchanger polymers. *Proceedings of the Royal Society of London. Series A. Mathematical and Physical Sciences, 268*(1334), 339-349.

Goh, S., Chan, H., & Ong, C. (1998). Miscible blends of conductive polyaniline with tertiary amide polymers. *Journal of Applied Polymer Science, 68*(11), 1839-1844.

Gottlieb, M. H., & Gregor, H. P. (1954). Studies on ion exchange resins. XI. Activity coefficients of diffusible ions in a strong base anion-exchange resin. *Journal of the American Chemical Society, 76*(18), 4639-4641.

Gray, G. T., McCutcheon, J. R., & Elimelech, M. (2006). Internal Concentration Polarization in Forward Osmosis: Role of Membrane Orientation. *Desalination, 197*, 8.

Gregor, H. P. (1948). A general thermodynamic theory of ion exchange processes. *Journal of the American Chemical Society, 70*(3), 1293-1293.

Gregor, H. P. (1951). Gibbs-Donnan equilibria in ion exchange resin systems. *Journal of the American Chemical Society, 73*(2), 642-650.

Gregor, H. P., & Gottlieb, M. H. (1953). Studies on ion exchange resins. VIII. Activity coefficients of diffusible ions in various cation-exchange resins. *Journal of the American Chemical Society, 75*(14), 3539-3543.

Gregor, H. P., Gutoff, F., & Bregman, J. (1951). Studies on ion-exchange resins. II. Volumes of various cation-exchange resin particles. *Journal of colloid science, 6*(3), 245-270.

Gude, V. G., Nirmalakhandan, N., & Deng, S. (2010). Renewable and sustainable approaches for desalination. *Renewable and Sustainable Energy Reviews, 14*(9), 2641-2654.

Gudipati, C. S., & MacDonald, R. J. (2015). Washington, DC: U.S. Patent and Trademark Office.

Güler, E., Elizen, R., Vermaas, D. A., Saakes, M., & Nijmeijer, K. (2013). Performance-determining membrane properties in reverse electrodialysis. *Journal of Membrane Science, 446*, 266-276.

Günday, S., Bozkurt, A., Meyer, W. H., & Wegner, G. (2006). Effects of different acid functional groups on proton conductivity of polymer-1, 2, 4-triazole blends. *Journal of Polymer Science Part B: Polymer Physics, 44*(23), 3315-3322.

Gustafson, R. L. (1966). Donnan equilibria in polystyrenesulfonate gels. *The Journal of Physical Chemistry, 70*(4), 957-961.

Haiqing Lin, E. V. W., John S. Swinnea, Benny D. Freeman, Steven J. Pas, Anita J. Hill, Sumod Kalakkunnath, Douglass S. Kalika. (2006). Transport and structural characteristics of crosslinked poly(ethylene oxide) rubbers. *Journal of Membrane Science, 276*, 17.

Helfferich, F. (1962). *Ion Exchange*. New York: McGraw-Hill Book Co., Inc.

Hernández-Luis, F., Amado-González, E., & Esteso, M. A. (2003). Activity coefficients of NaCl in trehalose–water and maltose–water mixtures at 298.15 K. *Carbohydrate research, 338*(13), 1415-1424.

Hernández-Luis, F., Galleguillos, H. R., Fernández-Mérida, L., & González-Díaz, O. (2009). Activity coefficients of NaCl in aqueous mixtures with ε-increasing co-solvent: Formamide–water mixtures at 298.15 K. *Fluid Phase Equilibria, 275*(2), 116-126.

Hiemenz, P. C., & Lodge, T. P. (2007). *Polymer chemistry*: CRC press.

Hills, G., Jacobs, P., & Lakshminarayanaiah, N. (1961). *Membrane potentials I. The theory of the emf of cells containing ion-exchange membranes.* Paper presented at the Proceedings of the Royal Society of London A: Mathematical, Physical and Engineering Sciences.

Huglin, M. B., Rego, J. M., & Gooda, S. R. (1990). Comments on thermal transitions in some polyelectrolyte complexes. *Macromolecules, 23*(26), 5359-5361.

Illescas, J., Ramírez-Fuentes, Y. S., Zaragoza-Galan, G., Porcu, P., Mariani, A., & Rivera, E. (2015). PEGDA-based luminescent polymers prepared by frontal polymerization. *Journal of Polymer Science Part A: Polymer Chemistry, 53*(24), 2890-2897.

Inc., P. E. (2001). *DMA - A beginner's guide* Roylance.

Jang, E.-S., Kamcev, J., Kobayashi, K., Yan, N., Galizia, M., Sunjai, R., . . . Freeman, B. D. (2017). Effect of water content on alkali metal chloride sorption in cross-linked poly(ethylene glycol diacrylate), In Preparation.

Jardat, M., Hribar-Lee, B., Dahirel, V., & Vlachy, V. (2012). Self-diffusion and activity coefficients of ions in charged disordered media. *The Journal of Chemical Physics, 137*(11), 114507.

Jardat, M., Hribar-Lee, B., & Vlachy, V. (2008). Self-diffusion coefficients of ions in the presence of charged obstacles. *Physical Chemistry Chemical Physics, 10*(3), 449-457.

Ju, H., McCloskey, B. D., Sagle, A. C., Kusuma, V. A., & Freeman, B. D. (2009). Preparation and characterization of crosslinked poly (ethylene glycol) diacrylate hydrogels as fouling-resistant membrane coating materials. *Journal of Membrane Science, 330*(1), 180-188.

Ju, H., Sagle, A. C., Freeman, B. D., Mardel, J. I., & Hill, A. J. (2010). Characterization of sodium chloride and water transport in crosslinked poly (ethylene oxide) hydrogels. *Journal of Membrane Science, 358*(1), 131-141.

Jung, H. H., Hwang, S. W., Hyun, S. H., Lee, K. H., & Kim, G. T. (2007). Capacitive deionization characteristics of nanostructured carbon aerogel electrodes synthesized via ambient drying. *Desalination, 216*(1), 377-385.

Kabiri, K., Mirzadeh, H., Zohuriaan-Mehr, M. J., & Daliri, M. (2009). Chitosan-modified nanoclay-poly (AMPS) nanocomposite hydrogels with improved gel strength. *Polymer international, 58*(11), 1252-1259.

Kalakkunnath, S., Kalika, D. S., Lin, H., Raharjo, R. D., & Freeman, B. D. (2007). Molecular relaxation in cross-linked poly (ethylene glycol) and poly (propylene glycol) diacrylate networks by dielectric spectroscopy. *Polymer, 48*(2), 579-589.

Kamcev, J., & Freeman, B. D. (2016). Charged polymer membranes for environmental/energy applications. *Annual review of chemical and biomolecular engineering, 7*, 111-133.

Kamcev, J., Galizia, M., Benedetti, F. M., Jang, E.-S., Paul, D. R., Freeman, B. D., & Manning, G. S. (2016). Partitioning of mobile ions between ion exchange polymers and aqueous salt solutions: importance of counter-ion condensation. *Physical Chemistry Chemical Physics, 18*(8), 6021-6031.

Kamcev, J., Jang, E.-S., Yan, N., Paul, D. R., & Freeman, B. D. (2015). Effect of ambient carbon dioxide on salt permeability and sorption measurements in ion-exchange membranes. *Journal of Membrane Science, 479*, 55-56.

Kamcev, J., Paul, D. R., & Freeman, B. D. (2015). Ion activity coefficients in ion exchange polymers: Applicability of Manning's counterion condensation theory. *Macromolecules, 48*(21), 8011-8024.

Kamcev, J., Paul, D. R., & Freeman, B. D. (2017a). Accounting for Frame of Reference and Thermodynamic Non-Idealities When Calculating Ion Diffusion Coefficients in Ion Exchange Membranes. *Journal of Membrane Science, 537*, 396-406.

Kamcev, J., Paul, D. R., & Freeman, B. D. (2017b). Effect of fixed charge group concentration on equilibrium ion sorption in ion exchange membranes. *Journal of Materials Chemistry A, 5*(9), 4638-4650.

Kamcev, J., Paul, D. R., Manning, G. S., & Freeman, B. D. (2017a). Accounting for frame of reference and thermodynamic non-idealities when calculating salt diffusion coefficients in ion exchange membranes. *Journal of Membrane Science, 537*, 396-406.

Kamcev, J., Paul, D. R., Manning, G. S., & Freeman, B. D. (2017b). Predicting salt permeability coefficients in highly swollen, highly charged ion exchange membranes. *ACS applied materials & interfaces, 9*(4), 4044-4056.

Kamcev, J., Sujanani, R., Jang, E.-S., Yan, N., Moe, N., Paul, D., & Freeman, B. (2017). Salt concentration dependence of ionic conductivity in ion exchange membranes, In preparation.

Khawaji, A. D., Kutubkhanah, I., & Wie, J. M. (2008). Advances in seawater desalination technologies. *Desalination, 221*(1), 47-69.

Klaysom, C., Cath, T. Y., Depuydt, T., & Vankelecom, I. F. J. (2013). Forward and pressure retarded osmosis: potential solutions for global challenges in energy and water supply. *Chemical Society Reviews, 42*, 6959-6989.

Kraus, K. A., & Moore, G. E. (1953). Anion exchange studies. V. Adsorption of hydrochloric acid by a strong base anion exchanger. *Journal of the American Chemical Society, 75*(6), 1457-1460.

Lakshminarayanaiah, N. (1963). Activity coefficients of small ions in ion-exchange resins. *Journal of Polymer Science Part A: General Papers, 1*(1), 139-149.

Lakshminarayanaisah, N. (1969). *Transport phenomena in membranes*. New York and London: Academic Press.

Lammertz, S., Grünfelder, T., Ninni, L., & Maurer, G. (2009). A model for the Gibbs energy of aqueous solutions of polyelectrolytes. *Fluid Phase Equilibria, 280*(1), 132-143.

Lee, J. B., Park, K. K., Eum, H. M., & Lee, C. W. (2006). Desalination of a thermal power plant wastewater by membrane capacitive deionization. *Desalination, 196*(1), 125-134.

Lee, Y. H., Lee, J. Y., & Lee, D. S. (2000). A novel conducting soluble polypyrrole composite with a polymeric co-dopant. *Synthetic metals, 114*(3), 347-353.

Li, Z., & Ruckenstein, E. (2003). Improved surface properties of polyaniline films by blending with Pluronic polymers without the modification of the other characteristics. *Journal of colloid and interface science, 264*(2), 362-369.

Lin, H., Freeman, B. D., Kalakkunnath, S., & Kalika, D. S. (2007). Effect of copolymer composition, temperature, and carbon dioxide fugacity on pure-and mixed-gas permeability in poly (ethylene glycol)-based materials: Free volume interpretation. *Journal of Membrane Science, 291*(1), 131-139.

Lin, H., Kai, T., Freeman, B. D., Kalakkunnath, S., & Kalika, D. S. (2005). The effect of cross-linking on gas permeability in cross-linked poly (ethylene glycol diacrylate). *Macromolecules, 38*(20), 8381-8393.

Lin, H., Wagner, E. V., Swinnea, J. S., Freeman, B. D., Pas, S. J., Hill, A. J., . . . Kalika, D. S. (2006). Transport and structural characteristics of crosslinked poly (ethylene oxide) rubbers. *Journal of Membrane Science, 276*(1), 145-161.

Lindenbaum, S., Jumper, C., & Boyd, G. (1959). Selectivity coefficient measurements with variable capacity cation and anion exchangers. *The Journal of Physical Chemistry, 63*(11), 1924-1929.

Liu, J. D., Sue, H.-J., Thompson, Z. J., Bates, F. S., Dettloff, M., Jacob, G., . . . Pham, H. (2009). Effect of crosslink density on fracture behavior of model epoxies containing block copolymer nanoparticles. *Polymer, 50*(19), 4683-4689.

Lonsdale, H. K., Merten, U., & Riley, R. L. (1965). Transport properties of cellulose acetate osmotic membranes. *Journal of Applied Polymer Science, 9*, 1341-1362.

Lonsdale, H. K., Merten, U., & Tagami, M. (1967). Phenol Transport in Cellulose Acetate Membranes. *Journal of Applied Polymer Science, 11*, 1807-1820.

Mackie, J., & Meares, P. (1955). *The diffusion of electrolytes in a cation-exchange resin membrane. II. Experimental.* Paper presented at the Proceedings of the Royal Society of London A: Mathematical, Physical and Engineering Sciences.

Mackie, J. S., & Meares, P. (1955a). The diffusion of electrolytes in a cation-exchange resin membrane. I. Theoretical. *Proceedings of the Royal Society of London A: Mathematical, Physical and Engineering Sciences, 232*(1191), 498-509.

Mackie, J. S., & Meares, P. (1955b). The sorption of electrolytes by a cation-exchange resin membrane. *Proceedings of the Royal Society of London. Series A. Mathematical and Physical Sciences, 232*(1191), 485-498.

Manning, G. S. (1969a). Limiting laws and counterion condensation in polyelectrolyte solutions I. Colligative properties. *The Journal of Chemical Physics, 51*(3), 924-933.

Manning, G. S. (1969b). Limiting laws and counterion condensation in polyelectrolyte solutions II. Self‐diffusion of the small ions. *The Journal of Chemical Physics, 51*(3), 934-938.

Manning, G. S. (1977). Limiting laws and counterion condensation in polyelectrolyte solutions: IV. The approach to the limit and the extraordinary stability of the charge fraction. *Biophysical Chemistry, 7*(2), 95-102.

Martinez-Felipe, A., Lu, Z., Henderson, P. A., Picken, S. J., Norder, B., Imrie, C. T., & Ribes-Greus, A. (2012). Synthesis and characterisation of side chain liquid crystal copolymers containing sulfonic acid groups. *Polymer, 53*(13), 2604-2612. doi: http://dx.doi.org/10.1016/j.polymer.2012.02.029

Maurya, S., Shin, S.-H., Kim, Y., & Moon, S.-H. (2015). A review on recent developments of anion exchange membranes for fuel cells and redox flow batteries. *RSC Advances, 5*(47), 37206-37230.

McCutcheon, J. R., & Elimelech, M. (2006). Influence of concentrative and dilutive internal concentration polarization on flux behavior in forward osmosis. *Journal of Membrane Science, 284*, 237-247.

McHardy, W., Meares, P., Sutton, A., & Thain, J. (1969). Electrical transport phenomena in a cation-exchange membrane II. Conductance and electroosmosis. *Journal of colloid and interface science, 29*(1), 116-128.

Meares, P. (1956). The conductivity of a cation-exchange resin. *Journal of Polymer Science, 20*(96), 507-514.

Meares, P. (1958). Self-diffusion coefficients of anions and cations in a cation-exchange resin. *The Journal of Chemical Physics, 55*, 273-279.

Meares, P. (1981). Coupling of ion and water fluxes in synthetic membranes*. *Journal of Membrane Science, 8*(3), 295-307.

Meares, P. (1983). Ion-exchange membranes *Mass Transfer and Kinetics of Ion Exchange* (pp. 329-366): Springer.

Meares, P. (1986). Ion exchange membranes: Principles, production and processes *Ion Exchange: Science and Technology* (pp. 529-558): Springer.

Meares, P., Dawson, D., Sutton, A., & Thain, J. (1967). Diffusion, conduction and convection in synthetic polymer membranes. *Berichte der Bunsengesellschaft für physikalische Chemie, 71*(8), 765-775.

Menard, K. P. (2008). *Dynamic mechanical analysis: a practical introduction*: CRC press.

Menczel, J. D., & Prime, R. B. (2014). *Thermal analysis of polymers: fundamentals and applications*: John Wiley & Sons.

Merten, U. (1963). Flow Relationships in Reverse Osmosis. *I & EC Fundamentals, 2*(3), 229-232.

Merten, U. (1966). *Desalination by Reverse Osmosis*: The M.I.T. Press.

Miller, J. E., & Evans, L. R. (2006). *Forward osmosis: a new approach to water purification and desalination*: Sandia Report.

Miyagawa, H., Misra, M., Drzal, L. T., & Mohanty, A. K. (2005). Fracture toughness and impact strength of anhydride-cured biobased epoxy. *Polymer Engineering & Science, 45*(4), 487-495.

Nagasawa, M., Izumi, M., & Kagawa, I. (1959). Colligative properties of polyelectrolyte solutions. V. Activity coefficients of counter-and by-ions. *Journal of Polymer Science, 37*(132), 375-383.

Nagasawa, M., & Kagawa, I. (1957). Colligative properties of polyelectrolyte solutions. IV. Activity coefficient of sodium ion. *Journal of Polymer Science, 25*(108), 61-76.

Nagvekar, M., Tihminlioglu, F., & Danner, R. P. (1998). Colligative properties of polyelectrolyte solutions. *Fluid Phase Equilibria, 145*(1), 15-41.

Nelson, F., & Kraus, K. A. (1958). Anion-exchange studies. XXIII. Activity coefficients of some electrolytes in the resin phase. *Journal of the American Chemical Society, 80*(16), 4154-4161.

Newman, J., & Thomas-Alyea, K. E. (2012). *Electrochemical systems*: John Wiley & Sons.

Oh, H. J., Freeman, B. D., McGrath, J. E., Lee, C. H., & Paul, D. R. (2014). Thermal analysis of disulfonated poly (arylene ether sulfone) plasticized with poly (ethylene glycol) for membrane formation. *Polymer, 55*(1), 235-247.

Oldham, K., Myland, J., & Bond, A. (2011). *Electrochemical science and technology: Fundamentals and applications*: John Wiley & Sons.

Othmer, K. *Ion Exchange*. Kirk-Othmer encyclopedia of chemical technology.

Pancratz, T. (2007). Membranes Provide Emergency Relief. *Water Desalination Report, 43*, 3-5.

Park, H. B., Freeman, B. D., Zhang, Z. B., Sankir, M., & McGrath, J. E. (2008). Highly chlorine-tolerant polymers for desalination. *Angewandte Chemie, 120*(32), 6108-6113.

Parthasarathy, R., Misra, A., Park, J., Ye, Q., & Spencer, P. (2012). Diffusion coefficients of water and leachables in methacrylate-based crosslinked polymers using absorption experiments. *Journal of Materials Science: Materials in Medicine, 23*(5), 1157-1172.

Paul, D. R. (1972). The Role of Membrane Pressure in Reverse Osmosis. *Journal of Applied Polymer Science, 16*, 771-852.

Paul, D. R. (2004). Reformulation of the solution-diffusion theory of reverse osmosis. *Journal of Membrane Science, 241*, 371-386.

Peppas, N. A., & Merrill, E. W. (1976). Poly (vinyl alcohol) hydrogels: Reinforcement of radiation-crosslinked networks by crystallization. *Journal of Polymer Science: Polymer Chemistry Edition, 14*(2), 441-457.

Pepper, K., Reichenberg, D., & Hale, D. (1952). Properties of ion-exchange resins in relation to their structure. Part IV. Swelling and shrinkage of sulphonated polystyrenes of different cross-linking. *Journal of the Chemical Society (Resumed)*, 3129-3136.

Pintauro, P. N., & Bennion, D. N. (1984). Mass transport of electrolytes in membranes. 1. Development of mathematical transport model. *Industrial & engineering chemistry fundamentals, 23*(2), 230-234.

Pitzer, K. S. (1973). Thermodynamics of electrolytes. I. Theoretical basis and general equations. *The Journal of Physical Chemistry, 77*(2), 268-277.

Pitzer, K. S. (1987). A thermodynamic model for aqueous solutions of liquid-like density. *Reviews in Mineralogy and Geochemistry, 17*, 46.

Pitzer, K. S., & Mayorga, G. (1973). Thermodynamics of electrolytes. II. Activity and osmotic coefficients for strong electrolytes with one or both ions univalent. *The Journal of Physical Chemistry, 77*(19), 2300-2308.

Porada, S., Zhao, R., Van Der Wal, A., Presser, V., & Biesheuvel, P. M. (2013). Review on the Science and Technology of Water Desalination by Capacitive Deionization. *Progress in Materials Science, 58*(8), 1388-1442.

Pusch, W. (1986). Measurement techniques of transport through membranes. *Desalination, 59*, 105-199.

Qiao, J., Hamaya, T., & Okada, T. (2005). Chemically modified poly (vinyl alcohol)-poly (2-acrylamido-2-methyl-1-propanesulfonic acid) as a novel proton-conducting fuel cell membrane. *Chemistry of materials, 17*(9), 2413-2421.

Raluy, G., Serra, L., & Uche, J. (2006). Life cycle assessment of MSF, MED and RO desalination technologies. *Energy, 31*(13), 2361-2372.

Reid, C. E., & Breton, E. J. (1959). Water and Ion Flow Across Cellulosic Membranes. *Journal of Applied Polymer Science, 1*(2), 133-143.

Reid, C. E., & Kuppers, J. R. (1959). Physical Characteristics of Osmotic Membranes of Organic Polymers. *Journal of Applied Polymer Science, 2*(6), 264-272.

Robinson, R. A., & Stokes, R. H. (2002). *Electrolyte solutions*: Courier Corporation.

Sagle, A. C., Ju, H., Freeman, B. D., & Sharma, M. M. (2009). PEG-based hydrogel membrane coatings. *Polymer, 50*, 756-766.

Sagle, A. C., Van Wagner, E. M., Ju, H., McCloskey, B. D., Freeman, B. D., & Sharma, M. M. (2009). PEG-coated reverse osmosis membranes: desalination properties and fouling resistance. *Journal of Membrane Science, 340*(1), 92-108.

Sata, T. (2004). *Ion exchange membranes: preparation, characterization, modification and application*: Royal Society of Chemistry.

Sen, U., Acar, O., Bozkurt, A., & Ata, A. (2011). Proton conducting polymer blends from poly (2, 5-benzimidazole) and poly (2-acrylamido-2-methyl-1-propanesulfonic acid). *Journal of Applied Polymer Science, 120*(2), 1193-1198.

Service, R. F. (2006). Desalination freshens up. *Science(Washington, D. C.), 313*(5790), 1088-1090.

Shannon, M. A., Bohn, P. W., Elimelech, M., Georgiadis, J. G., Marinas, B. J., & Mayes, A. M. (2008). Science and technology for water purification in the coming decades. *Nature, 452*(7185), 301-310.

Shen, Y., Xi, J., Qiu, X., & Zhu, W. (2007). A new proton conducting membrane based on copolymer of methyl methacrylate and 2-acrylamido-2-methyl-1-propanesulfonic acid for direct methanol fuel cells. *Electrochimica Acta, 52*(24), 6956-6961.

Soykan, C., Coşkun, R., Kirbağ, S., & Şahin, E. (2007). Synthesis, characterization and antimicrobial activity of poly (2-acrylamido-2-methyl-1-propanesulfonic acid-co-crotonic acid). *Journal of Macromolecular Science Part A: Pure and Applied Chemistry, 44*(1), 31-39.

Strathmann, H., Grabowski, A., & Eigenberger, G. (2013). Ion-Exchange Membranes in the Chemical Process Industry. *Industrial & Engineering Chemistry Research, 52*(31), 10364-10379.

Stumm, W., & Morgan, J. J. (2012). *Aquatic chemistry: chemical equilibria and rates in natural waters* (Vol. 126): John Wiley & Sons.

Sundheim, B. R., Waxman, M. H., & Gregor, H. P. (1953). Studies on ion exchange resins. VII. Water vapor sorption by cross-linked polystyrenesulfonic acid resins. *The Journal of Physical Chemistry, 57*(9), 974-978.

T.Sata. (2002). *Ion exchange membranes: Preparation, characterization, modification and application*. Tokuyama City, Japan: Tokuyama Research.

Tanaka, Y., Moon, S. H., Nikonenko, V. V., & Xu, T. (2012). Ion-Exchange Membranes. *International Journal of Chemical Engineering, 2012*, 1-3.

Tye, F. (1961). Absorption of electrolytes by ion-exchange materials. *Journal of the Chemical Society (Resumed)*, 4784-4789.

Veerman, J., De Jong, R. M., Saakes, M., Metz, S. J., & Harmsen, G. J. (2009). Reverse electrodialysis: Comparison of six commercial membrane pairs on the thermodynamic efficiency and power density. *Journal of Membrane Science, 343*(1), 7-15.

Wang, J. H., & Miller, S. (1952). Tracer-diffusion in Liquids. II. The Self-diffusion as Sodium Ion in Aqueous Sodium Chloride Solutions1. *Journal of the American Chemical Society, 74*(6), 1611-1612.

Wang, K., Guan, J., Mi, F., Chen, J., Yin, H., Wang, J., & Yu, Q. (2015). A novel method for preparation of cross-linked PEGDA microfibers by low-temperature photopolymerization. *Materials Letters, 161*, 317-320.

Webber, M. E. (2008). Energy versus water: solving both crises together. *Scientific American, 18*(4), 1-5.

Welgemoed, T. J., & Schutte, C. F. (2005). Capacitive deionization technology™: an alternative desalination solution. *Desalination, 183*(1), 327-340.

Wijmans, J. G., & Baker, R. W. (1995). The solution-diffusion model: a review. *Journal of Membrane Science, 107*, 1-21.

Wiśniewski, J., & Różańska, A. (2006). Donnan dialysis with anion-exchange membranes as a pretreatment step before electrodialytic desalination. *Desalination, 191*(1), 210-218.

Wu, Y.-H., Park, H. B., Kai, T., Freeman, B. D., & Kalika, D. S. (2010). Water uptake, transport and structure characterization in poly (ethylene glycol) diacrylate hydrogels. *Journal of Membrane Science, 347*(1), 197-208.

Xie, W., Cook, J., Freeman, B. D., Lee, C. H., & McGrath, J. E. (2011). Fundamental salt and water transport properties in directly copolymerized disulfonated poly(arylene ether sulfone) random copolymers. *Polymer, 52*, 12.

Xu, T. (2005). Ion Exchange Membranes: State of Their Development and Perspective. *Journal of Membrane Science, 263*, 1-29.

Xu, T. (2005). Ion exchange membranes: state of their development and perspective. *Journal of Membrane Science, 263*(1), 1-29.

Yan, N., Kamcev, J., Galizia, M., Jang, E.-S., Paul, D. R., & Freeman, B. D. (2017). Influence of fixed charge concentration and water uptake on ion sorption in AMPS/PEGDA membranes, In preparation.

Yan, N., Paul, D. R., & Freeman, B. D. (2017). Water and ion sorption in a series of cross-linked AMPS/PEGDA hydrogel membranes, In preparation.

Yasuda, H., Lamaze, C. E., & Ikenberry, L. D. (1968). Permeability of solutes through hydrated polymer membranes. Part I. Diffusion of sodium chloride. *Die Makromolekulare Chemie, 118*(1), 19-35.

Yuan-Hui, L., & Gregory, S. (1974). Diffusion of ions in sea water and in deep-sea sediments. *Geochimica et cosmochimica acta, 38*(5), 703-714.

Zagorodni, A. A. (2006). *Ion exchange materials: properties and applications*: Elsevier.

Zhang, C., & Easteal, A. J. (2003a). Study of free-radical copolymerization of N-isopropylacrylamide with 2-acrylamide-2-methyl-1-propanesulphonic acid. *Journal of Applied Polymer Science, 88*(11), 2563-2569.

Zhang, C., & Easteal, A. J. (2003b). Study of poly (acrylamide-co-2-acrylamido-2-methylpropane sulfonic acid) hydrogels made using gamma radiation initiation. *Journal of Applied Polymer Science, 89*(5), 1322-1330.